THE JOURNAL
OF
CHEMICAL PHYSICS

VOLUME 4 JANUARY, 1936 NUMBER 1

Raman Spectra of Amino Acids and Related Compounds
I. The Ionization of the Carboxyl Group

JOHN T. EDSALL, *Department of Physical Chemistry, Harvard Medical School, Boston, Massachusetts*

(Received October 10, 1935)

Raman spectra have been determined for four amino acids and their hydrochlorides; for three fatty acids and chloracetic acid, and their sodium salts; and for several related compounds. The influence of the solvent water on the Raman spectra of aqueous solutions is discussed. The "carbonyl" frequency, lying near 1670 cm^{-1} in the pure fatty acids, shifts to 1720 cm^{-1} when they are dissolved in water. No shift is found for the corresponding frequency in methyl acetate or acetone. The presence of a charged NH_3^+ group on the carbon α to the carboxyl increases this frequency by about 20 cm^{-1}. On ionization of the carboxyl group it is found that: (1) The "carbonyl" frequency vanishes in all cases investigated. The behavior of the amino acids in this respect is entirely consistent with their structure as zwitterions. (2) A group of lines in the region 1200–1420 cm^{-1} undergoes characteristic changes in position and intensity. (3) In most cases there is a powerful line in the region 750–930 cm^{-1} whose frequency increases by 20–40 cm^{-1} on ionization. The frequency of this line is decreased by about 50 cm^{-1} for each additional methyl group on the carbon atom adjoining the carboxyl. (4) Ionization markedly decreases the C–H frequency in formic acid, and also certain strong frequencies in methyl and ethyl amine.

INTRODUCTION

THE amino acids form an important class of compounds, containing a wide variety of organic radicals, but especially distinguished by the presence of electrically charged ammonium ($-NH_3^+$) and carboxylic (COO^-) groups, even when the molecule as a whole is electrically neutral. Because of this structure, the amino acids possess very large permanent electric moments, and in some properties they are closely akin to the inorganic salts, especially in their high melting points, relatively great solubility in water, and nearly complete insolubility in most organic solvents.[1]

With the aim of obtaining further insight into their structure, an extensive study of the Raman spectra of amino acids and related compounds has been undertaken in this laboratory. This first communication is concerned particularly with the changes in Raman spectrum accompanying ionization of the carboxyl group. For an amino acid cation ($^+H_3N \cdot R \cdot COOH$) the reaction may be written:

$$^+H_3N \cdot R \cdot COOH \rightleftharpoons {}^+H_3N \cdot R \cdot COO^- + H^+. \quad (1)^2$$

The study of the spectra of four amino acids, and their hydrochlorides, has provided a basis for the consideration of this reaction; four other carboxylic acids and their sodium salts have also been studied for comparison, as well as a number of related compounds. Since the salts studied are virtually completely dissociated in water, the sodium or chloride ions present do not contribute to the observed Raman spectrum.[3]

[1] Bjerrum, Zeits. f. physik. Chemie **104**, 147 (1923); Cohn, Ergeb. Physiol. **33**, 781 (1931); Ann. Rev. Biochem. **4**, 93 (1935).

[2] Edsall and Blanchard, J. Am. Chem. Soc. **55**, 2337 (1933).

[3] See Krishnamurti, Ind. J. Phys. **5**, 113 (1930); Kohlrausch, Naturwiss. **22**, 196 (1934).

Experimental Methods and Materials

The experimental arrangement for exciting the Raman spectra was based on that of Wood.[4] A cylindrical tube 30 mm in diameter, containing a filter solution, was interposed between the mercury arc and the Raman tube, and served as a combined lens and filter. The axes of the tubes and the arc were horizontal and parallel. Filter tube and Raman tube were supported in a wooden frame which rested on the housing of the mercury lamp. When desired, an additional filter in the form of a suitable type of glass plate could be introduced between the filter tube and the Raman tube. The mercury arc was cooled by a blast of compressed air directed horizontally across the aperture between the arc and the filter tube. An aluminum reflector was placed over the Raman tube to increase the light intensity.

The spectra were photographed with a Hilger E-439 glass spectrograph (aperture ratio of camera *f* 3, dispersion about 70A/mm at 4600A), and Eastman spectroscopic plates (generally the plates were type I−O; in special cases type I−H or I−J). The instrument was calibrated by using an argon lamp as the source of a standard spectrum. The slit width was generally 0.07 mm.

Filters

To remove the mercury *e* line[5] (4358A) and transmit the *k* line (4047A) Corning red purple ultra glass 2 mm thick[6] was found very satisfactory. Simultaneous elimination of the *o*, *p*, *q* triplet is accomplished by a dilute solution of sodium nitrite (2 to 4 cc of saturated solution in 125 cc of water) in the filter tube. We have found this combination preferable to the noviol-iodine filter used by Wood.

To transmit the *e*, *f* and *g* lines, removing all those of higher frequency, a solution of sodium nitrite (0.4 saturated) in the filter tube was employed.[7]

Glycine crystals were studied in the powder form, by using the method of complementary filters.[8] The details of the method, and of the filters used, will be reported in a subsequent communication.

In dilute aqueous solutions, such as those frequently employed in these investigations, there is great danger that the continuous background in the spectrum of the mercury arc may be so intense as to mask the Raman lines of the solute. The intensity of the continuous background was greatly diminished by two procedures: (1) The mercury arc was run at low intensity (40–50 volts) and cooled at the same time by a strong blast of compressed air. This low intensity (in combination with the filters used) made long exposures necessary (18 to 24 hours or more with the red purple ultra glass) but enormously decreased the continuous background. Such a procedure is only practicable with a spectrograph of high luminosity; otherwise the exposures would become intolerably long. (2) Solutions of the salts and amino acids, which could not be purified by distillation, were shaken with norit (highly purified charcoal) and heated for ten or fifteen minutes, with stirring, to 60° or 70°. They were then filtered through a fine-pore filter paper, the filtrate being collected and poured on to the filter again repeatedly for five or ten minutes, to wash out dust particles in the filter system. The filtrate was then allowed to flow directly into the Raman tube. This technique removed almost all the suspended particles in the liquid. It was particularly effective in the acid solutions, appreciably less so (although still valuable) when the solution was neutral. It proved unsuitable for alkaline solutions, as the norit then gave rise to a fluorescent impurity in the solution. Control experiments with norit in pure water and in 3 normal HCl showed no Raman lines or bands not found in pure distilled water.

The amino acid hydrochlorides studied (also chloracetic acid in water) contained an excess of hydrochloric acid (0.5 to 1 normal) to repress the ionization of the carboxyl group, and to make sure that the form R·COOH was alone present. As stated above, control experiments showed that HCl, even in concentrations higher than this, gives rise to no Raman lines (as would be

[4] R. W. Wood, *Physical Optics* (1934), third edition, Chapter XIV.

[5] The notation of the mercury lines is that of Kohlrausch, *Der Smekal-Raman-Effekt* (Berlin, 1931), p. 19.

[6] Murray and Andrews, J. Chem. Phys. **1**, 406 (1933).

[7] Pfund, Phys. Rev. **42**, 581 (1932).

[8] For references see Kohlrausch, *Der Smekal-Raman-Effekt*, p. 37.

expected, since it is virtually completely ionized at this concentration in water). The fatty acids in water did not require addition of HCl, since their dissociation constants are much lower than those of the carboxyl groups in the amino acids.

In preparing the salts of the fatty acids and of chloracetic acid, the *p*H was calculated (from the known dissociation constant of the acid) at which there would be 50 to 100 moles of salt present per mole of acid. Concentrated c.p. sodium hydroxide solution was then added (slowly and with cooling) to the concentrated aqueous solution of the acid, until the *p*H (tested by a suitable indicator)[9] had reached the desired value. In this way the amount of free acid present was made so small that it could scarcely contribute to the Raman spectrum, and the solutions were at the same time maintained slightly on the acid side of neutrality, thereby avoiding absorption of carbon dioxide and other complications.

Discussion

Since the great majority of the spectra here reported were obtained from aqueous solutions, it is important to differentiate the Raman lines (or bands) due to water from those due to the solute. The principal (double or triple) water band in the region 3250–3600 cm^{-1} is so intense and so characteristic that it is scarcely likely to be confused with anything else. It can, however, obscure the presence of other Raman lines lying in the same region of the spectrum, notably frequencies due to the N−H vibration, which lie in the region 3200–3400 cm^{-1}. Except in urea we have found no such frequencies in aqueous solutions which could be attributed to the solute, but the possibility that they exist cannot of course be excluded. In unfiltered light, some Raman lines of low frequency excited by the mercury *e* line will be obscured by the water band excited by the *k* and *i* lines, and some lines of low frequency excited by *k* or *i* are covered by the water band due to the *o*, *p*, *q* triplet. These complications are eliminated by the use of suitable filters, as described above under experimental methods.

Besides this very intense water band, a number of fainter bands have been reported by various authors. Notably Bolla[10] has reported bands at 60, 172, 510, 780, 1645, 2150 and 3990 cm^{-1}. We

[9] Clark, *The Determination of Hydrogen Ions* (Baltimore, 1928), third edition.

[10] Bolla, Nuovo cimento (N. S.) **9**, 290 (1932); **10**, 101 (1933).

Table I. *Frequencies in the range 1200–1750 cm^{-1}.* (The estimated intensity of each line is given in parenthesis following its frequency.)

Substance	Form	(1)	(2)	(3)	(4)	(5)
Formic acid	R COOH	1214 (2*b*)	1400 (3)			1727 (4*b*)
	R COO^-	—	1351 (6)			—
			1386 (1)			
Acetic acid	R COOH	1272 (1)	1370 (1)		1436 (2)	1720 (4*b*)
	R COO^-	—	1347 (2*b*)		1413 (6*b*)	—
Propionic acid	R COOH	1263 (½*b*)	—	1424 (3)	1459 (3)	1719 (2*b*)
	R COO^-	1257 (2)	1300 (2)	1417 (4)	1464 (2)	—
			1368 (1)			
Chloracetic acid	R COOH	—			1413 (4)	1729 (4*b*)
	R COO^-	1263 (1)			1404 (5)	—
Glycine	R COOH	1260 (1)	1315 (2)		1436 (3)	1743 (3*vb*)
	R COO^-	—	1331 (3)		1412 (3)	—
Alanine	R COOH	1240 (0)	1356 (0)	—	1460 (2*b*)	1738 (2*vb*)
	R COO^-	1310 (1)	1358 (2)	1416 (2)	1467 (2)	—
α-amino-*n*-butyric acid	R COOH	1316 (1)	1363 (1)	—	1450 (4*b*)	1746 (3*vb*)
	R COO^-	1258 (2)	1358 (4)	1413 (3)	1459 (3)	—
α-amino-isobutyric acid	R COOH	1273 (0)	1359 (0)	—	1452 (3*b*)	1729 (½*b*)
					1467 (2*b*)	
	R COO^-	1264 (1*vb*)	1374 (3*b*)	1411 (3)	1444 (2*b*)	—
					1465 (3*b*)	

All values tabulated are for the substances dissolved in water.

TABLE II. *The "sensitive frequency" (intensities given in parentheses).*

SUBSTANCE	R COOH	R COO⁻	Δ
Glycine	871 (4)	897 (3)	26
Alanine	823 (5)	846 (5)	23
Aminoisobutyric acid	765 (5*b*)	795 (6*b*)	30
Acetic acid	898 (5)	928 (7)	30
Propionic acid	845 (6)	886 (4)	41
Chloracetic acid	906 (3*b*)	928 (3)	22

have observed bands corresponding in position to the first two of these, lying very close to the exciting mercury line. They do not overlap, however, with any of the Raman lines with which we are here concerned, and need not be considered further.

The bands near 510 and 780 are very broad and extremely faint, and could not possibly be confused with the relatively very sharp Raman lines given by the solutes studied in this range. The bands at 2150 and 3990 were not observed in these studies. That at 1645, however, appeared in most of the aqueous solutions studied. Though broad, it is sharper than most of the water bands, and it might readily be confused with Raman lines due to the solute. Its distinctive breadth and appearance, however, render it easy to identify, and its probable origin is indicated in the spectra for which it is listed in Table IV.

Having examined the influence of the solvent, we may now consider the spectra of the amino acids and fatty acids themselves, with special reference to the ionization of the carboxyl group. The complete Raman spectra are listed in Table IV, at the end of the paper; sets of lines which appear particularly significant in connection with the problem of ionization are listed in Tables I and II. A number of systematic empirical correlations between Raman frequencies and chemical structure can be readily derived from the observed data.

(1) The "carbonyl" frequency in the fatty acids and their salts [Table I, column (5)]

A frequency in the range 1650–1800 cm^{-1} is known to be present in all compounds containing the C=O group (esters, aldehydes, ketones, carboxylic acids, urea, etc.).[11] In the pure fatty acids this line is broad and lies at the lower limit of this range (1650–1670), far below the typical values for the esters (1730), aldehydes (1720) or ketones (1710). However, when the three fatty acids here studied were dissolved in water, it was found that this frequency was increased by some 50 cm^{-1}, from about 1670 to about 1720 (see data in Table IV).[12] Pure anhydrous formic acid possesses two frequencies in this range, a powerful one at 1672 and a weak one near 1730. In aqueous solution the strong line has shifted to 1727, and the weaker line has vanished or is covered up. The "carbonyl" frequency in methyl acetate and in acetone, however, was found (within the limits of experimental error) to be the same in aqueous solution as in the pure liquid (Table IV, Nos. 26–29). This shift, therefore, appears to be characteristic of the carboxyl group, and is not found for the C=O frequency in an ester or ketone.

A shift of this magnitude in a Raman frequency strongly suggests the possibility of an actual chemical change in the structure of the substance concerned. It appears probable that most of the fatty acids (acetic acid may be taken as typical) exist largely as double molecules in the pure state. Smyth and Rogers[13] conclude from several lines of evidence that acetic acid in benzene solution exists mainly as double molecules. This is also probably true of the pure acid; while in ether both double and single molecules appear to be present. In aqueous solutions, freezing-point measurements indicate that the single molecules greatly predominate.[14] Correspondingly Dadieu and Kohlrausch[15] have found the C=O frequency for acetic acid in benzene (1656) to be very slightly lower than that for the pure acid. In ether solution the frequency splits into two (at 1664 and 1750) while our measurements in water indicate one high frequency at 1720. It appears at present a tenable hypothesis that the high frequency (near 1720) arises from single molecules,

[11] Kohlrausch and Pongratz, Zeits. f. physik. Chemie **B27**, 176 (1934).

[12] This is in accord with the finding of Krishnamurti, Ind. J. Phys. **6**, 401 (1931–32) on acetic acid in water.

[13] Smyth and Rogers, J. Am. Chem. Soc. **52**, 1824 (1930); also Smyth, *Dielectric Constant and Molecular Structure* (New York, 1931), p. 173; see also Pauling and Brockway, Proc. Nat. Acad. Sci. **20**, 336 (1934).

[14] See for instance Lewis and Randall, *Thermodynamics* (New York, 1923), p. 290.

[15] Dadieu and Kohlrausch, Physik. Zeits. **31**, 514 (1930).

and the low frequency (near 1670) from double molecules of the acid.[16]

When the fatty acids are ionized, the "carbonyl" frequency vanishes. No trace of it could be detected in the spectrum of sodium formate, acetate, propionate or chloroacetate. This effect of ionization has been reported by Ghosh and Kar[17] and by Krishnamurti[18] but the spectra reported here are considerably richer in lines than those given in either of the above-mentioned papers. In conjunction with the data on the amino acids (discussed below), these findings furnish very powerful additional evidence for the validity of the view originally put forward by Ghosh and Kar.

It cannot, of course, be proved that the "carbonyl" frequency vanishes completely in the ionized carboxyl group, but it must in any case be extremely weak. It might lie in the region covered by the water band near 1640 cm^{-1}, but the appearance of the spectra gave no indication of such overlapping.

(2) The "carbonyl" frequency in the amino acids and their hydrochlorides

In the amino acid cations ($^{+}H_3N \cdot R \cdot COOH$) this frequency (Table I, column 5) is strongly present. In the free amino acids, however, as in the sodium salts of the fatty acids, it vanishes. Therefore it is clear that when an amino acid cation is titrated with base, it is the carboxyl group which dissociates (Eq. (1)). This may be taken as the fundamental hypothesis of the theory that the neutral amino acids exist as zwitterions ($^{+}H_3N \cdot R \cdot COO^{-}$); and these findings from the Raman spectrum could be used (in the absence of other evidence) as virtually conclusive proof of the validity of that theory. They also suggest that the Raman spectrum might be used in the titration of a substance containing several dissociable groups, to determine which group was reacting at a given stage in the titration.

The "carbonyl" frequency in the amino acid cations appears to be appreciably higher than in the fatty acids. The average value for the four amino acid cations is 1739 cm^{-1}, that for acetic and propionic acids is 20 cm^{-1} lower. This effect is presumably due to the positively charged $-NH_3^{+}$ group attached to the α carbon atom. It is interesting to note that the effect of the uncharged $-NH_2$ group is in the opposite direction. Thus in ethyl formate ($H \cdot COOC_2H_5$)[19] the C=O frequency is 1715; in ethyl carbamate ($H_2N-COOC_2H_5$)[19] it decreases to 1692. In urea $CO(NH_2)_2$ (Table IV, No. 25) it is still lower, namely 1666. This effect is apparent only when the amino group is directly attached to the C=O group. An intervening CH_2 group virtually abolishes the effect; thus the C=O frequency in the amino acid esters (Table IV, Nos. 23 and 24) is virtually identical with the typical value for the fatty acid esters. Since the effect of the charged $-NH_3^{+}$ group is still appreciable when this group is separated by a CH_2 group from the carboxyl it may be concluded that its effect is more powerful than that due to the uncharged $-NH_2$ group.

(3) The lines in the range 1200–1420 cm^{-1}

A group of lines in this region (Table I, columns 1–3) appears to undergo characteristic changes when the form $R \cdot COOH$ is transformed into the form $R \cdot COO^{-}$. All the amino acids but glycine, in the form $R \cdot COO^{-}$, show strong lines near 1360 and near 1412. The former of these lines becomes extremely weak, and the latter vanishes completely, when these amino acids are converted into their hydrochlorides. The lines at 1300 and 1368 in the propionate ion, and that at 1263 in the chloracetate ion (none of which appear in the form $R \cdot COOH$) may be analogous. The relation of these lines to ionization is the converse of that of the carbonyl frequency.

In contrast, the strong frequency in the range 1450–1470 (Table I, column 4) remains essentially unaltered by ionization in all the substances in which it occurs. This probably represents a deformational frequency of the methylene or methyl group,[20] and its constancy indicates that this type of vibration is not measurably affected by ionization of the carboxyl group, unless the CH_2 or CH_3 group involved is directly attached

[16] Dadieu and Kohlrausch reported a frequency of only 1676 in an acetic acid-water solution, but in their experiment the mole ratio acid : water was 1 : 1, whereas in ours it was approximately 1 : 10. See also Krishnamurti, Ind. J. Phys. **6**, 401 (1931–32).

[17] Ghosh and Kar, J. Phys. Chem. **35**, 1735 (1931).

[18] Krishnamurti, Ind. J. Phys. **6**, 309 (1931–32).

[19] Kohlrausch, Köppl and Pongratz, Zeits. f. physik. Chemie **B22**, 359 (1933).

[20] Reference 8, pp. 190, 206.

to the carboxyl. If it is so attached, as in glycine or acetic acid, this characteristic frequency is lowered to 1436 in the form R·COOH, and is still further lowered to 1412 by the ionization of the carboxyl group. The line at 1413 in chloracetic acid, which shifts to 1404 on ionization, doubtless represents the same type of vibration. Certain other lines in this range are listed for consideration in Table I, although it seems premature as yet to attempt a discussion of them.

The close similarity of glycine and acetic acid is notable in Table I. They resemble each other in Raman spectrum far more closely than either one resembles its higher homologs.

(4) The "sensitive frequency" in the range 750–930 cm^{-1}

In this range all the acids investigated (except formic and α-amino n-butyric acids) show a powerful line, which always increases in frequency on ionization of the carboxyl group (Table II).

It is possible that the line at 708 in aqueous formic acid, shifting to 772 in the formate ion, is analogous to those listed in Table II; but this appears dubious, as formic acid contains no C−C bond.

Regarding this frequency, it may be noted that: (a) In all the substances listed in Table I except chloracetic acid, it is by far the most powerful Raman line in the range 600–1000 cm^{-1}. (b) It is unaltered by change of state, being the same for glycine crystals as for glycine in solution, the same for aqueous solutions of acetic and propionic acids as for the pure acids. (c) Its frequency invariably increases (by 20–40 cm^{-1}) on ionization of the carboxyl group (column headed Δ in Table II). (d) The substitution of a methyl group for a hydrogen atom, on the carbon α to the carboxyl group, decreases this frequency by approximately 50 cm^{-1}. (See the progressive decrease in the series glycine → alanine → aminoisobutyric acid, in Table II; also the shift from acetic to propionic acid.)

This last-mentioned characteristic suggests a close relationship between this frequency and a very strong Raman line found in certain aldehydes, ketones, fatty acids and amides, studied by Kohlrausch and his collaborators (Table III). In every substance (except acetaldehyde) listed in Table III, the indicated line is by far the most powerful in the spectrum, in the range 600–1000 cm^{-1}, and the decrease in frequency for each additional methyl group on the α carbon atom is similar to that shown in Table II. It seems a reasonable inference that all these lines belong to the same family and have their origin in a similar type of molecular vibration.[21]

Compounds containing extended hydrocarbon chains show no one outstandingly powerful frequency in this range, but a large number of relatively weak lines. (See for instance α-amino-n-butyric acid, Table IV, Nos. 6 and 7.)

TABLE III. *The "sensitive frequency" in the range 600–900 cm^{-1} for molecules of the form* $R\cdot C(=O)X$.

R	Aldehydes X = H	Acids X = OH	Amides X = NH_2	Ketones X = CH_3
CH_3^-	887 (1)	893 (9)	862 (7*b*)	787 (8)
$CH_3CH_2^-$	846 (6)	844 (7)	807 (8*b*)	763 (7)
$(CH_3)_2CH^-$	796 (6)	800 (10)		724 (8)
$(CH_3)_3C^-$	762 (7)	753 (10)		671 (10)
$(CH_3)_2(C_2H_5)C^-$	749 (4)	736 (8)		660 (6)

References: (1) Aldehydes and ketones: Kohlrausch and Köppl, Zeits. f. physik. Chemie **B24**, 370 (1934). (2) Acids: Kohlrausch, Köppl and Pongratz, ibid. **B21**, 242 (1933). (3) Amides: Kohlrausch and Köppl, ibid. **B27**, 176 (1934).

(5) Other effects of ionization

Just as the loss of a proton by the carboxyl group increases the frequency of the "sensitive line" discussed above, so the acquisition of a proton by the amino group in methyl or ethylamine decreases the frequency of a strong line in the same range. In methylamine[22] the shift is from 1038 in the free amine to 995 in its hydrochloride; in ethylamine[23] from 1092 to 1047. A systematic study of the ionization of the amino group is now being undertaken.

A striking effect of ionization is the decrease of the principal C−H vibrational frequency from 2947 in formic acid to 2823 in the formate ion. In this case, the shift may reasonably be taken as reflecting an actual change in the strength of the C−H bond, and a similar interpretation

[21] For similar sets of lines in other types of compounds, and their possible interpretation, see Dadieu, Pongratz and Kohlrausch, Ber. Wien Akad. (II a) **141**, 267 (1932); Kohlrausch and Köppl, Monatsch. f. Chem. **63**, 255 (1933).

[22] Reference 8, p. 311; and Table IV (this paper, No. 21).

[23] Reference 8, p. 312; and Table IV, No. 22.

might be offered of some of the other effects of ionization discussed above.

I am indebted to Mr. Joseph Shack for valuable assistance in the carrying out of the experimental work.

In the following list of spectra there is listed for each Raman line: first, its frequency in cm^{-1}; second, in parenthesis, its intensity as estimated by direct observation; third, in parenthesis, the mercury lines (Kohlrausch's notation) exciting it. The letter "*b*" following the number indicating the intensity, signifies a broad line (*vb* = very broad). In some cases an approximate numerical estimate of the breadth of the line (in cm^{-1}) is given. The band near 1630 cm^{-1} is marked "water" to indicate the probable origin (see discussion in text above). The principal water band, in the region 3200–3600 cm^{-1}, was observed in all aqueous solutions, but is not listed here. In general, the presentation in this table closely follows that of Kohlrausch.[24]

Reference may be made to the literature regarding substances previously studied.[25]

Since this paper was written, Wright and Lee[26] have reported Raman spectra for glycine and alanine (as also for the hydrochlorides of tyrosine and cystine). In general, their frequency values agree with ours within the limits of experimental error. They report a line at 1445 cm^{-1} in glycine, and one at 1715 in alanine, which we have not observed (although the hydrochlorides of these substances give rise to lines very close to these values). Conversely, several of the fainter lines in glycine and alanine, here reported, were not observed by Wright and Lee.

TABLE IV. *Complete list of observed Raman spectra.*

1. *Glycine*, $^{+}H_3N\cdot CH_2\cdot COO^{-}$ (Eastman product, three times recrystallized from water) (aqueous solution, 22 percent): 508 (2*b*) (*k, g, f, e*); 590 (1) (*e*); 665 (1) (*e*); 897 (3) (*k, g, f, e*); 1033 (1) (*k, e*); 1122 (1) (*k, e*); 1331 (3) (*k, e*); 1412 (3) (*k, e*); 1491 (0) (*e?*); 1630±60 (1*b*) (*e*) (water); 2978 (3*b*) (*k*); 3018 (1) (*k*).

2. *Glycine* (*crystalline*): 507 (½) (*e*); 589 (1) (*e*); 891 (2) (*k, e*); 1033 (1) (*e*); 1112 (½) (*e*); 1323 (3) (*k, e*); 1404 (1) (*k, e*); 2968 (3) (*k, e*); 3002 (1) (*k*).

3. *Glycine hydrochloride*, $Cl^{-}NH_3^{+}\cdot CH_2COOH$ (aqueous solution 20 percent, with added HCl): 504 (2*b*) (*k, e*); 559 (0) (*e?*); 654 (1) (*k, e*); 871 (4) (*k, e*); 1049 (2) (*k, e*); 1111 (1) (*k, e*); 1260 (1) (*k, e*); 1315 (2) (*k, e*); 1436 (3) (*k, e*); 1516 (0) (*e?*) 1630±45 (2) (*e*) (water); 1743±27 (3) (*e*); 2973 (4) (*q, p, k, e*); 3014 (1) (*q, k*).

4. *dl-Alanine*, $^{+}H_3N\cdot CH(CH_3)\,COO^{-}$ (Eastman product, twice recrystallized) (aqueous solution, 13 percent): 421 (1) (*e*); 533 (2*b*) (*f, e*); 846 (5) (*k, f, e*); 920 (1) (*k, e*); 1003 (1) (*k, e*); 1125 (2*b*) (*k, e*); 1310 (1) (*k, e*); 1358 (2) (*k, e*); 1416 (2) (*k, e*); 1467 (2) (*k, e*); 1636±40 (1) (*e*) (water); 2893 (1) (*k*); 2949 (4) (*k, i, e*); 3003 (1) (*k*).

5. *dl-Alanine hydrochloride*, $Cl^{-}\,^{+}H_3N\cdot CH(CH_3)COOH$ (aqueous solution containing 20 percent of alanine by weight, and excess HCl): 401 (1*b*) (*e*); 520 (1*b*) (*k, e*); 620 (0*b*) (*e*); 680 (00) (*e?*); 747 (1) (*k, e*); 823 (5) (*k, e*); 920 (1*b*) (*k, e*); 1008 (1*b*) (*k, e*); 1120 (1*b*) (*k, e*); 1240 (0) (*k, e*); 1356 (0) (*k, e*); 1460 (2*b*) (*k, e*); 1619±30 (1*vb*) (*e*) (water); 1738±18 (2) (*e*); 2893 (2*b*) (*k*); 2953 (5*b*) (*q, p, k*); 3007 (3*b*) (*q, k*).

6. *dl-α-Amino-n-butyric acid*, $^{+}H_3N\cdot CH(C_2H_5)COO^{-}$ (Eastman product, once recrystallized) (aqueous solution, 17 percent): 542 (2) (*e*); 772 (1) (*e*); 842 (1) (*e*); 872 (1) (*e*); 914 (2) (*k, e*); 980 (2) (*k, e*); 1043 (3) (*k, e*); 1120 (2) (*k, e*); 1258 (2) (*e*); 1358 (4) (*k, e*); 1413 (3) (*k, e*); 1459 (3) (*k, e*); 1637±40 (1) (*e*) (water); 2900 (3) (*k*); 2954 (6*b*) (*k, e*); 2995 (2*b*) (*k*).

7. *dl-α-Amino-n-butyric acid hydrochloride*, $^{-}Cl^{+}H_3N\cdot CH(C_2H_5)\cdot COOH$ (aqueous solution containing 25 percent of amino acid, and excess HCl): 365 (2) (*e*); 429 (½*vb*) (*e*); 538 (3) (*k, e*); 659 (1*b*) (*e*); 745 (1) (*k, e*); 790 (1) (*k, e*); 831 (2) (*k, e*); 859 (2) (*k, e*); 913 (2) (*k, e*); 993 (2) (*k, e*); 1043 (3*b*) (*k, e*); 1127 (2*b*) (*k, e*); 1194 (1*vb*) (*k?*); 1316 (1) (*k, e*); 1363 (1) (*k, e*); 1450 (4*b*) (*k, e*); 1634±30 (1) (*e*) (water); 1746±15 (3) (*e*); 2894 (1) (*k*); 2953 (3) (*q, k, i, e*); 2995 (1) (*q, k*).

8. *α-Aminoisobutyric acid*, $^{+}H_3N\cdot C(CH_3)_2COO^{-}$ (Eastman product, once recrystallized) (aqueous solution, 12 percent): 353 (0) (*e*); 400 (0) (*e*); 600 (4) (*k, f, e*); 795 (6*b*) (*k, g, f, e*); 886 (1) (*k, e*); 948 (2*b*) (*k, i, e*); 1066 (1*vb*) (*e*); 1193 (0*b*) (*k, e*); 1264 (1*vb*) (*k, e*); 1374 (3*b*) (*k, e*); 1411 (3) (*k, e*); 1444 (2*b*) (*k*); 1465 (3*b*) (*k, e*); 1630±40 (1) (*e*) (water); 2880 (1*b*) (*k*); 2937 (4*b*) (*q, k*); 2998 (4*b*) (*q, k*).

9. *α-Aminoisobutyric acid hydrochloride*, $Cl^{-}\,^{+}H_3N\cdot C(CH_3)_2COOH$ (aqueous solution containing 16 percent of amino acid and excess HCl): 258 (2) (*e*); 358 (1*b*) (*e*); 407 (1*b*) (*e*); 538 (1) (*e*); 594 (2*b*) (*k, e*); 765 (5*b*) (*k, i, e*); 880 (1) (*k, e*); 951 (3) (*k, i, e*); 1066 (0*b*) (*k, e*); 1195 (0) (*k, e*); 1273 (0) (*e*); 1359 (0) (*e*); 1452 (3*b*) (*k, e*); 1467 (2) (*k*); 1623±40 (0) (*e*) (water); 1729 (½*b*) (*e*); 2879 (1) (*k*); 2945 (6*vb*) (*q, k*); 2998 (6*vb*) (*q, k*).

10. *Formic acid*, $H\cdot COOH$ (Eastman b. p. 99.8–100.2° at 755 mm): 180±35 (1*vb*) (*e*); 678 (3) (*k, e*); 873 (½) (*k?*); 1065 (1) (*k, e*); 1204 (2*b*) (*k, e*); 1396 (5) (*k, i, e*); 1670±20 (3*b*) (*e*); 1731 (1*b*) (*e*); 2148 (½) (*k*); 2598 (½*vb*) (*k*); 2787 (1) (*k*); 2961 (6*b*) (*k, i, e*).

11. *Formic acid* (aqueous solution, 35 percent): 170±30 (*e*); 708 (1*b*) (*e*); 1065 (0*b*) (*k, e*); 1214 (2*b*) (*k, e*); 1400 (3) (*k, i, e*); 1727 (4*b*) (*e*); 2792 (½*b*) (*k*); 2947 (6*b*) (*k, i, e*).

12. *Sodium formate*, $H\cdot COO^{-}Na^{+}$ (aqueous solution containing 35 percent of formic acid, neutralized with c.p. sodium hydroxide): 159 (band) (*e*); 503 (0) (*k?*); 772 (1)

[24] Kohlrausch, Köppl and Pongratz, Zeits. f. physik. Chemie **B21**, 242 (1933) and later papers in Zeits. f. physik. Chemie and Monatsch. f. Chem.

[25] Formic, acetic, propionic and chloracetic acids: Kohlrausch, Köppl and Pongratz, reference 24. Also for acetic acid, pure and in water, Krishnamurti, Ind. J. Phys. **6**, 367, 401 (1931–32). Sodium formate, sodium acetate, sodium chloracetate: Ghosh and Kar, J. Phys. Chem. **35**, 1735 (1931). (For sodium acetate also Kohlrausch, reference 8, p. 317.) Methyl acetate: Kohlrausch, Köppl and Pongratz, Zeits. f. physik. Chemie **B22**, 359 (1933). Acetone: Kohlrausch and Köppl, Zeits. f. physik. Chemie **B24**, 370 (1934). Urea: Kohlrausch and Pongratz, Zeits. f. physik. Chemie **B27**, 176 (1934). All these papers give references to the earlier literature.

[26] Wright and Lee, Nature **136**, 300 (1935).

(*k, e*); 1072 (1) (*k, e*); 1351 (6) (*k, i, g, f, e*); 1386 (1) (*k*); 1611 (0*vb*) (*e*) (water); 2123 (1*b*) (*k*); 2734 (2*b*) (*k*); 2823 (6*b*) (*k, i*).

13. *Acetic acid*, CH_3COOH (Baker's Glacial): $\Delta\nu=452$ (3) (*k, e*); 563 (0) (*k*); 623 (4) (*k, e*); 895 (5) (*k, i, e, f, g*); 1015 ($\frac{1}{2}$) (*e*); 1150 ($\frac{1}{2}$) (*k*); 1291 ($\frac{1}{2}$) (*e*); 1366 (3) (*k, e*); 1433 (4) (*k, e*); 1670 (4) (*e*); 2858 (0) (*k*?); 2946 (6) (*k, e*); 3017 ($\frac{1}{2}$*vb*) (*k*).

14. *Acetic acid*, CH_3COOH (aqueous solution, 33 percent from Baker's Glacial c.p.): 470 (1*b*) (*e*); 630 (3*b*) (*e*); 898 (5) (*k, i, e*); 1026 (1) (*e*); 1272 (1) (*k, e*); 1370 (1) (*k, f, e*); 1436 (2) (*k, f, e*); 1720 (4*b*) (*e*); 2936 (6) (*q, p, k, i, e*); 2994 (0) (*k*); 3026 (0) (*k*).

15. *Sodium acetate*, $CH_3COO^-Na^+$ (saturated aqueous solution of Sterling's c.p., once recrystallized): 475 (2) (*k, e*); 613 (0) (*k*); 652 (3) (*k, e*); 928 (7) (*k, i, g, f,* $\pm e$); 1011 (0) (*e*); 1347 (2*b*) (*k, e*); 1413 (6*b*) (*k, e*); 1542 (00*b*) (*e*); 1648 (00*b*) (*e*) (water); 2851 (0) (*k*); 2930 (5*b*) (*k, e*).

16. *Propionic acid*, C_2H_5COOH (Eastman, once distilled b.p. 140.2°): 290 (1*b*) (*e*); 480 (3*b*) (*k, e*); 606 (2) (*k, e*); 844 (6) (*k, i, f, e*); 1005 (3*b*) (*k, e*); 1078 (5) (*k, e*); 1256 (2) (*k, e*); 1424 (5) (*k, e*); 1462 (4) (*k, e*); 1665±8 (3) (*e*); 2753 (3) (*k*); 2900 (6) (*q, k, e*); 2950 (6) (*q, k, i, e*); 2998 (6) (*k, i*).

17. *Propionic acid* (aqueous solution, 35 percent, Eastman product, once distilled): 268 (2*b*) (*e*); 492 (3*b*) (*k, e*); 603 (1*b*) (*e*); 845 (6) (*k, e*); 998 (1*b*) (*k, e*); 1079 (2) (*k, e*); 1219 (0) (*e*?); 1263 ($\frac{1}{2}$*b*) (*k, e*); 1424 (3) (*k, e*); 1459 (3) (*k, e*); 1719±12 (2*b*) (*e*); 2749 (1) (*k*); 2891 (1) (*k*); 2950 (5) (*q, k*); 2991 (2) (*q, k*).

18. *Sodium propionate*, $C_2H_5COO^-Na^+$ (aqueous solution containing 30 percent distilled propionic acid+a very slight excess of sodium hydroxide): 294 (1) (*e*); 512 (2*b*) (*k, e*); 630 (2*b*) (*k, e*); 886 (4) (*k, g, f, e*); 1014 (3) (*k, e*); 1078 (3) (*k, e*); 1257 (2) (*k, e*); 1300 (2) (*k, e*); 1368 (1) (*k, e*); 1417 (4) (*k, e*); 1464 (2) (*k, e*); 2888 (1) (*k*); 2950 (2) (*k, e*); 2984 (1) (*k*).

19. *Chloracetic acid*, $CH_2ClCOOH$ (aqueous solution, 40 percent, Eastman Product m.p. 62–64°): $\Delta\nu=244$ (3) (*k, e*); 430 (4*vb*) (*k,* $\pm e$); 573 (1*vb*) (*k, e*); 676 (1*vb*) (*k, e*); 794 (6) (*k, i,* $\pm e$); 906 (3*b*) (*k, i, e*); 1185 (2) (*k, i, e*); 1413 (4) (*k, e*); 1729±29 (4*b*) (*e*); 2964 (6) (*k, e*); 3009 (2) (*k*).

20. *Sodium chloracetate*, $CH_2Cl\cdot COO^-Na^+$ (aqueous solution containing 33 percent acid, and equivalent sodium hydroxide): $\Delta\nu=255$ (1) (*k, e*); 433 (5) (*k,* $\pm e$); 584 (1) (*e*); 690 (1) (*e*); 780 (5) (*k, i, e*); 928 (3) (*k, e*); 1186 (1) (*k, e*); 1263 (1) (*k, e*); 1404 (5) (*k, i, e*); 1624±40 (1*b*) (*e*) (water); 2969 (5) (*k, e*); 3021 (1) (*k*).

21. *Methylamine hydrochloride*, $CH_3NH_3^+Cl^-$ (aqueous solution, 50 percent, containing excess HCl. Eastman product, once recrystallized from alcohol): $\Delta\nu=995$ (6) (*k, i, f, e*); 1268 (1) (*k, e*); 1466 (3) (*k, e*); 2833 (2) (*k*); 2914 (2) (*k, i*); 2975 (6) (*k, i, e*); 3032 (3) (*k, e*).

22. *Ethylamine hydrochloride*, $C_2H_5NH_3^+Cl^-$ (aqueous solution, 50 percent, with excess HCl. Eastman product, once recrystallized from alcohol): $\Delta\nu=411$ (2) (*k, e*); 873 (5) (*k, f, e*); 1047 (4) (*k, f, e*); 1205 (2) (*k, e*); 1335 (3) (*k, e*); 1458 (5) (*k, f, e*); 2883 (2) (*k, e*); 2946 (3) (*q, k, e*); 2986 (3) (*q, k, e*).

23. *dl-Alanine ethyl ester*, $H_2N\cdot CH(CH_3)\cdot COOC_2H_5$ (prepared from *dl*-alanine by the method of Fischer[27] twice distilled, b.p. 48.0° to 48.4° at 11–12 mm): $\Delta\nu=353$ (2) (*e*); 501 (2) (*k, e*); 628 (0) (*k, e*); 670 (0) (*k, e*); 757 ($\frac{1}{2}$) (*k, e*); 794 (1) (*k, e*); 860 (5*b*) (*k, g, f, e*); 934 (2) (*k, e*); 1021 (3) (*k, e*); 1107 (3) (*k, e*); 1268 (1) (*e*); 1319 (1) (*k, e*); 1456 (5) (*k, e*); 1740 (3) (*e*); 2880 (1) (*k, i*); 2937 (6) (*k, i, e*); 2987 (6) (*k, i*); 3003 (6) (*k, e*); 3318 (3) (*k, e*); 3395 (2) (*k*).

24. *dl-a-Amino-n-butyric acid ethyl ester*, $H_2NCH(C_2H_5)COOC_2H_5$ (prepared from *dl-a*-amino-*n*-butyric acid by method of Fischer; twice distilled, b.p. 66.5° at 17 mm): $\Delta\nu=334$ (5*b*) (*e*±); 512 (3*b*) (*e*±); 646±25 ($\frac{1}{2}$) (*e*); 788 (0) (*e*); 867 (6*b*) (*k, e, g*); 934 (1*b*) (*e*); 1003 (2) (*e*); 1034 (2) (*e*); 1111 (3*b*) (*e*); 1276 (1) (*e*); 1309 (1) (*e*); 1454 (6*b*) (*k, e*); 1740 (3) (*e*); 2876 (3) (*k*); 2932 (6) (*k*); 2982 (3) (*k*); 3324 (3*b*) (*k*); 3389 (2) (*k*).

25. *Urea*, H_2NCONH_2 (aqueous solution—saturated, about 60 percent urea): $\Delta\nu=521$ (1) (*e*); 584 (1) (*e*); 1000 (6) (*k, e*); 1170 (1*vb*) (*k, e*); 1468 (0) (*k*); 1580 (0) (*k, e*); 1666 (1*b*) (*e*); 1768 (*e*?) (*e*); 3230 (1) (*k*); 3380 (3*b*) (*k*); 3489 (1*b*) (*k*).

The very broad line at 3380 is probably due, at least in part, to water; but the two lines at 3230 and 3489 are sharply distinct from this central band, and appear very differently from the bands in pure water. The line at 1666 is probably due to urea, not to water, since even the strong water bands appear relatively weak in the spectrum of this solution.

This spectrum is in good agreement with those reported by Kohlrausch and Pongratz,[25] and by Schneider (see reference 25).

26. *Methyl acetate*, (CH_3COOCH_3) (Eastman, b.p. 56.3°) anhydrous: $\Delta\nu=304$ (3) ($\pm e$); 433 (5) (*k,* $\pm e$); 639 (6) (*k, g, f,* $\pm e$); 843 (6) (*k, g, f,* $\pm e$); 983 (1) (*e*?); 1042 (4) (*k, f, e*); 1191 (1*b*) (*e*); 1254 ($\frac{1}{2}$*b*) (*e*); 1374 (1) (*e*); 1451 (5*vb*) (*k, e*); 1741 (5) (*e*); 2850 (3) (*k, e*); 2948 (6*b*) (*k, i, f, e*); 3023 (4*vb*) (*k*).

27. *Methyl acetate*, (20 percent in water): $\Delta\nu=303$ (1) (*e*); 436 (2) (*k, e*); 640 (3) (*k, e*); 855 (4) (*k, e*); 1046 (1*b*) (*k, e*); 1453 (1*b*) (*k, e*); 1730 (2*b*) (*e*); 2863 (2) (*k*); 2956 (5) (*k, e*); 3039 (2*vb*) (*k*).

28. *Acetone*, (CH_3COCH_3) (Eastman, from bisulfite compound b.p. 56.2°) anhydrous: $\Delta\nu=385$ (3) (*e*); 488 (1) (*k, e*); 527 (4) (*k, i, e*); 783 (7*b*) (*k, i, g, f,* $\pm e$); 903 (1*b*) (*k, e*); 1061 (3) (*k, e*); 1217 (4) (*k, e*); 1356 (1) (*k, e*); 1426 (6*vb*) (*k, i, e*); 1703 (5) (*e*); 2698 (2) (*k*); 2846 (1) (*k*); 2921 (6*vb*) (*k*); 3011 (3*b*) (*k, i*).

29. Acetone in water (30 percent): $\Delta\nu=399$ (2) (*e*); 499 ($\frac{1}{2}$) (*k, e*); 542 (3) (*k, e*); 797 (6*b*) (*k, i, e*); 1068 (2) (*k, e*); 1236 (3) (*k, e*); 1363 (2) (*k, e*); 1425 (5*b*) (*k, e*); 1702 (6*b*) (*e*); 2860 (1) (*k*); 2934 (7*vb*) (*q, p, i, e*); 2975 (3) (*q, k*); 3018 (3) (*q, k*).

Several frequencies appear to be 10 to 20 cm^{-1} higher in aqueous acetone than in the anhydrous liquid. The line at 1703, however, is unchanged in frequency.

[27] Fischer, Sitzungsber. Preuss. Akad. Wiss. 1062 (1900).

Resonance Fluorescence of Benzene. II

G. R. CUTHBERTSON[1] AND G. B. KISTIAKOWSKY, *Division of Chemistry, Harvard University*

(Received October 23, 1935)

Further study of the resonance fluorescence of benzene with an improved technique is described and the analysis of the spectrum given some time ago by Kistiakowsky and Nelles is amplified and corrected. The new assignment shows that, upon absorption of the 2536A mercury line, only the changes of the quantum number of one (ν_1; $\omega = 990$ cm^{-1}) vibration of the nonexcited benzene molecule are unrestricted in fluorescence. In other vibrations the changes of the quantum numbers are not larger than unity (or two when required by selection rules). This interpretation of the resonance spectrum accounts for most of the line groups measured on the new plates. Five frequencies, besides ν_1, or their multiples can be tentatively identified; they are: 432; 791; 1542; 2557 and 3174 cm^{-1}. The fluorescence of hexadeuterobenzene has also been studied and the spectrum interpreted in the same manner but not as completely as that of benzene. The frequencies observed are: 944 ($\Delta\nu$ unrestricted); 2460. The quenching of the resonance fluorescence of benzene has been investigated with five different gases. This fluorescence is quenched by being changed into high pressure fluorescence. There is very little, if any, loss of electronic excitation energy by benzene molecules on collisions. The quenching action is quite unspecific and appears to increase as the kinetic cross section of the foreign gas molecules. Some new high pressure fluorescence bands have been observed in benzene in the presence of foreign gases. These bands support V. Henri's analysis of the absorption spectrum as consisting of two close electronic levels of the excited molecule. Attempts to excite resonance fluorescence of benzene derivatives have, on the whole, been unsuccessful. Fluorobenzene and toluene, even at 0.01 mm pressure, emit spectra which, by using a spectrograph with a resolving power of better than 25,000, appear nearly continuous. Other derivatives tried have too little fluorescence to study it at low pressures.

Introduction and Experimental Details

SOME time ago, Kistiakowsky and Nelles[2] described experiments dealing with the fluorescence of benzene vapor excited by the monochromatic radiation of the 2536A wave-length. In agreement with the earlier and more qualitative observations of Pringsheim and Reimann,[3] it was found that a lowering of the vapor pressure of benzene produced changes of the spectrum emitted, its structure at low pressures resembling in many ways resonance fluorescence known from studies on diatomic molecules. Although some effort was made in the paper of Kistiakowsky and Nelles (henceforth denoted as I) to give an assignment of the line groups observed, the results were inconclusive and better measurements of the spectrum were clearly needed.

The measurements now presented have been obtained with a technique essentially the same as described previously. In details, however, many improvements were made. The most important of these was the use of the resonance lamp made in one piece out of fused quartz,[4] but otherwise similar to that described in I. The new lamp made it possible to use a much higher current (25–30 amp.) and to maintain better vacuum with a corresponding increase in intensity of the mercury resonance line. In consequence, it became possible to use an efficient system of light blends and to reduce the amount of direct light reaching the spectrograph so far that even after the longest exposures the mercury lines were not very much overexposed and no continuum from the lamp was to be observed on the plates. To get an idea of the efficiency of the optical arrangement chosen, it was found that a strong Raman spectrum excited by the 2536A line was obtained after five minutes' exposure when the resonance tube was filled with liquid water. The exposure time for low pressures of benzene was varied from thirty-five minutes to forty-eight hours and for high pressures from one to thirty minutes depending on the intensity desired.

Two procedures have been used in the study of the quenching of the resonance fluorescence. The one consisted in circulating the quenching gas by means of a high pressure mercury diffusion pump. From the pump the gas passed cold traps for purification, then traps maintained at constant temperature and containing solid benzene for saturation, then the resonance tube and

[1] Loomis Foundation Fellow.
[2] Kistiakowsky and Nelles, Phys. Rev. **41**, 595 (1932).
[3] Pringsheim and Reimann, Zeits. f. Physik **29**, 115 (1924).
[4] We are greatly indebted to Professor H. S. Taylor of Princeton University for lending us this lamp.

finally, it reentered the pump. In the other procedure, benzene vapor and the other gas were admitted into the resonance tube through fine capillaries from containers maintained at constant pressure. Another narrow tube leading to the pump controlled the total pressure in the resonance tube. The capillaries had been calibrated for gas flow with the substances studied under conditions obtained in the quenching experiments. The total pressure in the resonance tube was also closely followed by means of a heated McLeod gauge. In these and in all previously mentioned experiments the rate of flow was chosen such that only an insignificant fraction of benzene was decomposed during a single passage through the resonance tube.

The same procedure, as in the work on benzene, was employed in the study of the fluorescence of hexadeuterobenzene. The latter has been presented to us, very generously, by Professor H. S. Taylor of Princeton University. Because of the limited amount of substance available, only two plates—one at higher and one at low pressure—have been obtained.

The spectrograph used was a thermostated Hilger E-1 instrument.

The Results and Interpretation

The pressure range in which the high pressure type of fluorescence begins to give place to the resonance type was reinvestigated. It was found that in I it was estimated as too low. Actually, already at 0.2 mm pressure there are no visible traces of the high pressure fluorescence on the plates and from this pressure down to 0.005 mm no change in intensity distribution of the spectrum emitted can be observed. The use of water or of strong acetic acid as the cooling jacket around the resonance tube produces no changes in the low pressure spectrum and thus it may be safely concluded that it is due to resonance type of fluorescence of benzene molecules excited by the 2536A line. Even the rather improbable supposition that the life of excited benzene molecules is long enough for them to collide with the walls of the resonance tube before emitting fluorescence, is eliminated by the experiments on quenching. An admixture of 0.5 mm of helium to 0.1 mm of benzene, for instance, produces no visible changes in the intensity distribution of the spectrum, but it increases considerably the diffusion time of the average benzene molecule to the walls.

The plates obtained showed no continuous background and it was possible, therefore, by extending the exposure time, to obtain many more lines and to follow the spectrum further towards the visible. In all, some 450 lines have been measured on the resonance fluorescence plates. In many instances these "lines" are considerably broader and more diffuse than the mercury lines registered on the same plates, although one could expect the reverse to be true. It is therefore very probable that some of the "lines" measured are in reality unresolved rotational line groups and that therefore the wave numbers obtained have little intrinsic significance. This consideration prompted us to abstain from publishing the complete records of the measurements but they may be found in the thesis submitted by one of us (G. R. C.) to Harvard University. It suffices to state here that the new measurements are found to agree with the old (reported in I) to about ± 1 cm^{-1} or better, wherever the comparison is possible. The lines, as the microphotometer tracing published in I will show, are grouped into more or less distinct groups. Each group is to be interpreted as representing one vibrational transition coupled with several rotational transitions. The structure of the latter could be readily predicted if it was not for the fact that the mercury resonance line consists of several hyperfine components and that each of these may be sufficiently broad to cover more than one absorption line in the benzene absorption spectrum. By disregarding the rotational structure for the time being, the vibrational structure of the spectrum can be rather fully interpreted, but the interpretation deviates in several particulars from that presented tentatively in I. In fact, only one progression, termed *A* in I, could be extended on the new plates. Table I gives the mean of the wave numbers of the two prominent lines in each group (the center of the doublet); the separation of the groups and the separation of the doublet components. Two more members were visually observed but were too weak to measure.

While the figures leave no doubt as to the reality of the progression, the frequency of the

TABLE I. *Resonance series A of benzene.*

	2536A line													
ν cm^{-1}	39,412.0		38,424.0		37,434.8		36,448.4		35,463.4		34,479.8		33,495.8	32,515.4
$\Delta\nu$ cm^{-1}		988.0		989.2		986.4		985.0		983.6		984.0	980.4	
Doublet separation			5.7		9.7		12.9		15.5		16.6		19.5	20.2

TABLE II. *Resonance series A of deuterobenzene.*

	2536A line								
ν cm^{-1}	39,412.0		38,469.0		37,525.0		36,583.0		34,708.0
$\Delta\nu$ cm^{-1}		943		942		938		937	

vibration of the normal benzene molecule involved in it can be established, because of the width of the line group, only to a few wave numbers and the magnitude of the anharmonic term only estimated as being quite small.

The benzene-d_6 yielded a similar progression, given in Table II. The "doublet" structure of the groups is not noticeable, one line being prominent in each group. The progression is much shorter because the plate obtained gave a strong continuous background and the groups could be measured only with difficulty. This vibration, as stated in I, can undoubtedly be identified with the Raman frequencies 991 of benzene and 945[5] of deuterobenzene, ν_1 in the notation of Wilson.[6]

In the first publication the attempt was made to look for doublet structure in other line groups and to find progressions involving other frequencies than the above 990 cm^{-1}. The new plates, however, yielded no extension of the previously suggested regularities comparable to that of the *A* progression. Furthermore, the existence of the doublets in these other line groups appeared at least very doubtful, their structure varying greatly.

One obtains a more satisfactory representation of the spectrum by assuming that the same frequency of 990 cm^{-1} is involved in other progressions also. Their shift with respect to progression *A* is to be interpreted then as showing that these progressions are due to combination transitions, involving, besides an arbitrary change in the quantum number of the ν_1 vibration, a change of one or two in the quantum numbers of one of the other vibrations in the normal benzene. That this interpretation is qualitatively right is demonstrated best by Fig. 1 which shows a microphotometer record of

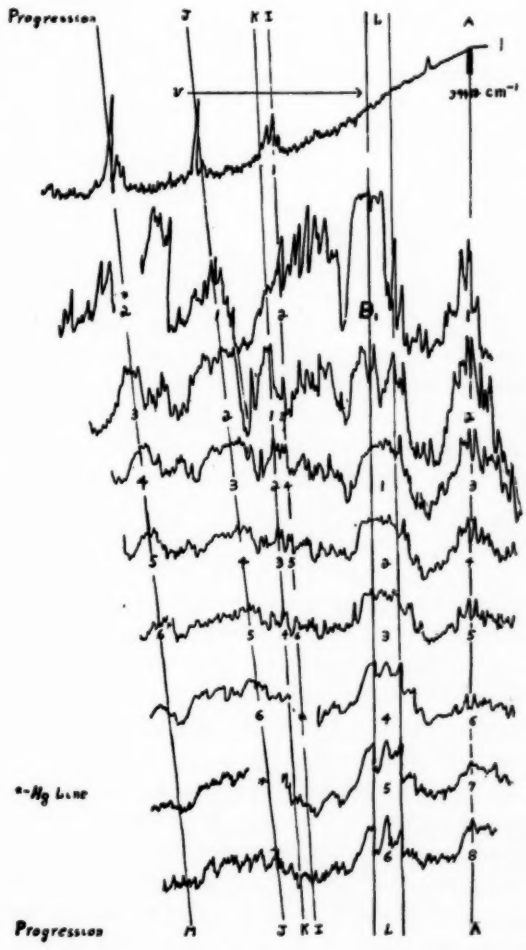

FIG. 1.

[5] Wood, J. Chem. Phys. **3**, 444 (1935).
[6] Wilson, Phys. Rev. **45**, 706 (1934).

TABLE III. *Combination progressions of benzene.*

						Series *I*								
	2536A line													
ν cm^{-1}	39,412		38,979		37,991		37,003		36,014		35,027		34,039	
$\Delta\nu$ cm^{-1}		432		988		988		989		987		988		
						Series *J*								
	2536A line													
ν cm^{-1}	39,412		37,870		36,876		35,886		34,898		33,910		32,925	
$\Delta\nu$ cm^{-1}		1542		994		990		988		988		985		
						Series *K*								
	2536A line													
ν cm^{-1}	39,412			36,965			35,970			34,977			33,985	
$\Delta\nu$ cm^{-1}		2557			995			993			992			
						Series *L*								
	2536A line													
ν cm^{-1}	39,412		36,237		35,238		34,244		33,251		32,259		31,274*	30,289*
$\Delta\nu$ cm^{-1}		3174		999		994		993		992		985	985	
						Series *M*								
	2536A line													
ν cm^{-1}	39,412		38,621		37,628		36,638		35,653		34,667		33,684	
$\Delta\nu$ cm^{-1}		791		993		990		985		986		983		

* Very weak.

the spectrum after it had been cut into sections covering about 990 cm^{-1} each and these placed one below the other. The structures of all these sections show great similarity, although some new progressions appear on sections further away from the exciting line and others disappear. The new interpretation has another point in its favor, namely, that groups of similar fine structure are now found to belong to the same progressions, while groups belonging to different progressions show, in general, quite different appearances. The complete repetition of the fine structure in succeeding groups is the main guide in selecting progressions given in Table III. Some others could perhaps be added, but in general we find the selection not altogether easy and free from arbitrariness. Concerning series *L* it should be remarked that although the microphotometer tracing indicates the possibility of extending this progression nearer to the exciting frequency, the two line groups in question have quite a different structure and no 990 cm^{-1} intervals can be found. Furthermore, in benzene-d_6 these groups are considerably displaced, having even no superficial connection to the *L* series.

It is quite easy to select corresponding lines in groups belonging to one progression, but the decision, as to which of the several possible lines to use for comparison, is quite arbitrary. Therefore the 990 cm^{-1} frequency is determined in the above progressions with a reasonable degree of accuracy, while the other frequencies may be in error by as much as 20 cm^{-1}. No attempt was made, in selecting progressions of Table III, to choose only frequencies known from Raman spectra because the symmetry character of excited benzene molecules is unknown and thus uncertainty exists concerning selection rules in resonance fluorescence. Actually, the agreement of the frequencies of Table III with Raman data is not perfect but it is probably premature to draw from this conclusions concerning the approximate shape of the excited molecule.

In the spectrum of deuterobenzene only one combination progression could be identified with some certainty, and is given in Table IV.

TABLE IV. *Combination progression of benzene-d_6.*

			Series *L*		
	2536A line				
ν cm^{-1}	39,412	36,944	35,996	35,052	
$\Delta\nu$ cm^{-1}	2468	948	944		

While the progression is quite short, its reality is well established, the groups being the most prominent in the spectrum. Their fine structure is quite similar to those of the *L* progression in benzene and therefore we regard both as involving the same vibration. These groups consist of five strong and approximately equidistant lines with 10–11 cm^{-1} separation. The middle lines of the groups have been given in the tables. The spectrum of benzene-d_6 contains several other diffuse and indistinct groups which can be arranged into 940–950 cm^{-1} progressions. How-

ever, the origins of these progressions are quite uncertain and the number of members in each is short. It is therefore of little value to give them here.

The benzene-d_6 resonance spectrum, contrary to findings with benzene, shows a rather diffuse anti-Stokes group, with the most prominent lines at 40,163, 40,149 and 40,139 cm^{-1}; thus an absorption band originating from a vibrating state of the normal molecule with about 720–750 cm^{-1} energy must overlap the mercury resonance line.

The most prominent group in the benzene spectrum, denoted as B_1 in the first communication, could not be fitted into any of the progressions. This same group appears also in the spectrum of benzene-d_6, although it has lost here its particular prominence. The separation from the exciting line has been changed from 1187–1216 to 1121–1158 cm^{-1}. This eliminates the possibility of identifying this group with the Raman frequency 1178, since the latter is supposed to be changed in benzene-d_6 to 873 cm^{-1}.[4]

The rotational structure of the resonance spectrum remains quite uncertain. Because progression A of benzene-d_6 and all other progressions of both isotopic modifications do not show a doublet structure, we believe now that undue importance was attached to such appearance of the groups in the first communication. Rather, the "doublets" are due to a more or less "accidental" grouping of rotational lines; however, only photographs taken with a much better resolving power spectrograph than that used here can settle the question.

The quenching of benzene resonance fluorescence has been studied with helium, hydrogen, nitrogen, carbon dioxide and cyclohexane as quenching gases. On raising the pressure of the foreign gas, while that of benzene is kept constant, no appreciable weakening of the total amount of fluorescence emitted has been noticed but instead only a gradual transition to the high pressure type of spectrum. Apparently, as remarked already by Pringsheim, the electronic excitation energy is very seldom lost by benzene molecules on collision and only the rotational and vibrational energies suffer losses and changes. The line groups typical of the resonance fluorescence disappear as such and instead fully developed high pressure bands appear. Thus no evidence of preferential rotational or of vibrational quenching could be obtained. Because of many experimental difficulties only crude visual observations of the quantitative amount of quenching were made by comparing the intensities of the resonance groups and of the high pressure bands on the same plate and taking several exposures at different pressures of the foreign gas. Different parts of the spectrum seemed to be quenched about equally efficiently. Selecting, for instance, the second (most intense) member of the A resonance progression and the first head of the high pressure bands (O_0 in notation adopted in I) equal intensities were obtained in the presence of helium, hydrogen and nitrogen at *ca.* 12 mm each, with carbon dioxide at 8 mm and with cyclohexane (and benzene itself) at 5 mm pressure. A choice of other groups and bands would give, of course, different numerical results but they all are of the same order of magnitude. There is thus little selective action in quenching resonance fluorescence of benzene and the effectiveness of molecules increases roughly as their kinetic cross sections. At the same time the total efficiency is quite low, if one attributes to the excited benzene molecule a mean life of the order of 10^{-8} to 10^{-7} second.

One result of the quenching studies, which is of some interest, is the finding of several new high pressure bands. These are located near the exciting line, in a region where benzene shows very strong absorption. Their reabsorption is of course the reason why they have not been noticed when, as usual in earlier work, higher pressures of benzene vapor were used, rather than a mixture of very little (0.1 mm) benzene vapor with much foreign gas. The first head of the new bands is at 38,609 cm^{-1} and is followed by other band heads of decreasing intensity in 160 cm^{-1} intervals. Another progression of identical spacing but lower intensity starts at 83 cm^{-1} to the red from the first one. The whole band group thus has an appearance identical with that of the well-known absorption and fluorescence groups of benzene. As the latter, the new band group is repeated to the red in 990 cm^{-1} intervals by other band groups of identical structure. These are mixed with the more intense bands of the main emission spectrum of benzene and only the first

head of the second group can be observed in the microphotometer tracing of the first communication at 135 cm^{-1} to the violet from the O_0 head. The disentanglement of these two progressions clarifies somewhat the high pressure fluorescence spectrum of benzene and shows it to consist of two progressions, each with the 990 interval, one starting at 38,609, the other at 37,481 cm^{-1}. Each member of the progression has the structure as described above and no other bands can be observed in fluorescence excited by the 2536A mercury line. One can interpret the entire spectrum as being due to emission by nonvibrating molecules from two excited electronic levels. This attitude is in conformity with the views of Henri who has interpreted the absorption spectrum with the help of two electronic levels, one at 37,483, the other at 38,612 cm^{-1}, thus with energies identical with those needed to explain the fluorescence spectrum. The difference in intensities of the two band-group progressions in emission one can attribute to the circumstance that the 2536A line coincides with a band belonging to the 37,483 electronic state. On the other hand, Pringsheim has reported that the appearance of the fluorescence spectrum is not affected by a change in the exciting wave-length and this is rather against the outlined interpretation. One way is to regard the upper of the two initial levels as belonging to the same electronic state but with one quantum of vibrational energy of a 1129 cm^{-1} frequency of the excited molecule. It is then necessary to assume that the energy of this vibration is much less readily lost in inelastic collisions than that of the other vibrations of the excited molecule which are known from the absorption spectrum. Neither interpretation is altogether satisfactory.

With benzene-d_6 a spectrum is obtained which is quite similar to that of ordinary benzene. The origin of the strong progression (now with a 945 cm^{-1} interval) is at 37,710 cm^{-1} and that of the faint system at 38,790 cm^{-1}.[7] Both origins are, thus, displaced to the violet, because of a larger zero-point energy of the benzene and benzene-d_6 molecules in their normal, rather than in the excited states. The 160 cm^{-1} frequency of the ordinary benzene appearing within each band group is changed in benzene-d_6 to 143 (± 1 cm^{-1}) and the weaker of the two such progressions is now displaced to the red by 80 cm^{-1} from the other one.

Although, thus, the two molecules show very similar structure in the band groups, a detailed interpretation of it in terms of molecular vibrations appears to us at present impossible. Assuming tentatively that the entire structure of the band groups is produced by transitions from the same initial level to different levels of the normal molecule, one has to use at least two low frequency vibrations to account for it. Several choices are possible. Thus, for the light benzene, one can use any one of the following pairs: 160 and 83; 80 and 83; 83 and 77, etc. However, as Dr. Wilson has kindly pointed out to us, it is extremely unlikely that there are two vibrations in benzene of quite such low frequency. Furthermore, the selection rules for vibrations ν_4 and ν_{16} of his interpretation, which should have the lowest frequencies of all, are such that, notwithstanding several attempts, it has not been possible to explain the observed structure. It seems more likely at present that only one (160 or $\frac{1}{2}160$ cm^{-1}) frequency of the normal molecule is involved and that the appearance of two progressions is due to electronic multiplicity or the presence of low frequencies in the upper state.

Four benzene derivatives have now been studied in an attempt to produce resonance fluorescence. Fluorobenzene and toluene at ordinary pressures and with illumination by the 2536A line emit a strong fluorescence consisting mainly of a continuum (see a tracing in the earlier communication) with a few faint and indistinct bands. Upon lowering the pressure to about 0.01 mm the appearance of the spectrum hardly changes at all and, if anything, the bands become even fainter.

This behavior seems very hard to understand because, using instruments of about the same resolving power as the spectrograph here used, Henri[8] and others have obtained well-developed banded absorption spectra It is possible, of course, that from the levels reached upon absorption of the 2536A line, transitions to more

[7] This was obtained by adding 945 wave numbers to the frequency of the first head of the *second* group of this progression.

[8] Henri, J. de phys. et rad. **9**, 249 (1928).

numerous vibrational levels of the normal molecule are consistent with the Franck-Condon rule than is the case in absorption by the nonvibrating molecule. Even allowing this, one does not see why sharp band heads typical of absorption should not be visible in fluorescence.

The fluorescence of chlorobenzene and ethyl benzene was too faint to be followed into the region of low pressures.

In conclusion, it is a pleasant duty to thank Dr. E. B. Wilson for many valuable suggestions and criticisms.

JANUARY, 1936 JOURNAL OF CHEMICAL PHYSICS VOLUME 4

Raman Effect of Acetylenes

II. Diiodoacetylene, Liquid Acetylene and Deuteroacetylenes[1]

GEORGE GLOCKLER AND CHARLES E. MORRELL,[2] *Department of Chemistry, University of Minnesota*

(Received August 30, 1935)

An apparatus consisting of eight discharge tubes for Raman work has been designed which is more convenient than the usual helical design of these light sources. It is possible to arrange these eight tubes concentrically around a Raman tube of any diameter. Cylindrical filters of any dimensions can be interposed with great convenience. The vibration Raman spectra of C_2I_2: 191.3, 310.2, 627.0 688.2 and 2109.4; liquid C_2H_2: 381.6, 618, 631, 1762, 1959 and 3338; gaseous C_2H_2: 1973.8 and 3373.7; gaseous C_2HD: 1851.2 and 3334.8; gaseous C_2D_2: 1762.4 and 2700.5 cm^{-1} have been observed and are interpreted in the usual manner on the basis of symmetry considerations. Striking differences in the spectra of liquid and gaseous acetylene (C_2H_2) indicate a serious distortion of the molecules in the liquid state. The extent of this disturbance seems to change completely the symmetry of the molecules of the liquid which are no longer linear as in the gaseous state. Certain Raman lines are accompanied by faint satellites which fit a rotation formula and may be due to rotation effects. The free energies of C_2HD and C_2D_2 were calculated and the free energy change of the reaction $C_2H_2+C_2D_2 \rightleftarrows 2C_2HD$ has been evaluated and the equilibrium constant determined for a series of temperatures.

I. Introduction

OUR study of acetylenes has been continued with still further improvements in technique. The compounds used are C_2I_2 in alcohol and acetone solution; gaseous and liquefied C_2H_2 (at $-80°C$); gaseous deuteroacetylenes: C_2D_2 and C_2HD.[3]

II. Experimental Procedure

A new set of Ne-Hg discharge tubes

The helical tubes used as light sources in our former researches[4] were inconvenient in respect to the possibility of inserting into the helix, Raman tubes of various diameters. Obviously the internal diameter of the helix determines the maximum thickness of the Raman tubes and the various filters needed at times. The new arrangement shown in Fig. 1 admits any size Raman tube and any number or thickness of cylindrical filters. The greater number of discharge tubes adds to the intensity of illumination. Two such tubes are fed by a 200/7000-volt 3-kva transformer. The whole set-up is sufficiently flexible to have motion in all directions. A cylindrical reflector is used.

---

[1] Part of this work was reported at the Cleveland meeting of the A. C. S., September 1934.

[2] This article is based upon a thesis presented to the faculty of the Graduate School of the University of Minnesota by Charles E. Morrell in partial fulfillment of the requirements of the degree of Doctor of Philosophy.

[3] We are greatly indebted to Professor H. S. Taylor for a generous supply of C_2D_2 prepared under his direction at Princeton University by Dr. J. C. Jungers, C. R. B. fellow from Louvain. The liquid acetylene was prepared from a sample of very pure calcium carbide obtained through the courtesy of Mr. E. C. MacQuigg from the Union Carbide and Carbon Chemicals Corp. to whom we express our thanks. The gas C_2HD was loaned us kindly by Professor L. H. Reyerson of the School of Chemistry of the University of Minnesota.

[4] Glockler and Davis, J. Chem. Phys. **2**, 881 (1934) and Phys. Rev. **46**, 535 (1934); Glockler and Morrell, Phys. Rev. **46**, 233 (1934) and **47**, 569 (1935).

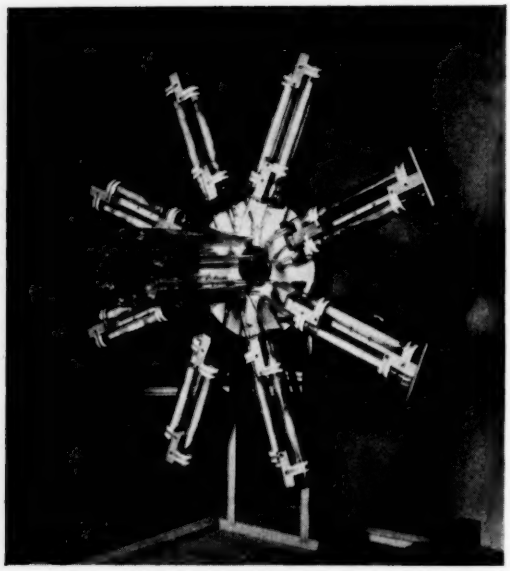

FIG. 1. Neon-mercury discharge tubes.

Preparation and source of compounds C_2I_2

This substance was prepared both according to the method of Biltz[5] and according to Dehn.[6] The latter method was found to give a purer and more stable product and was used in the preparation of samples which gave satisfactory Raman spectra. The product, recrystallized twice from petroleum ether, was pure white in color but slowly developed a yellow color when allowed to stand in a desiccator in the presence of air. The solid was used in solution in acetone and absolute alcohol. The former solvent was carefully purified by the sodium iodide method of Shipsey and Werner.[7] The solutions in acetone, although thoroughly pumped with an oil pump to rid them of dissolved air and sealed into the Raman tubes in vacuum, became yellow in color after a few hours exposure. This objectionable change in color was probably due not only to photochemical decomposition but also to the action of residual oxygen on the diiodoacetylene, producing carbon monoxide and free iodine. The latter may unite with the diiodoacetylene producing lemon yellow tetraiodoethylene. The yellow color which developed during exposure was undesirable because it produced a strong background between $\lambda=4358$A and $\lambda=4916$A and also greatly weakened the intensity of scattered radiation by absorption within the solution. It was noted that samples not washed entirely free of alkali during preparation showed less tendency to become discolored. For such alkaline solutions, absolute alcohol prepared by the distillation of sodium ethylate, was chosen as solvent. They were prepared by dissolving 8.5–11.0 grams of C_2I_2 in 20–21 cc of the alcohol and adding 8–10 drops of a solution of 3.2 grams of carbonate-free potassium hydroxide solution in 50 cc of the alcohol. These solutions were placed in flat-end Raman tubes of about 20 cc capacity, pumped with alternate freezing and thawing and sealed under vacuum. One such solution was exposed 48 hours with satisfactory results. The Raman frequency of potassium hydroxide $\Delta\nu=3600$ cm^{-1} was not found on any of the plates and it is extremely doubtful that any of the observed Raman lines are due to the comparatively small amounts of potassium hydroxide.

Acetylene, C_2H_2

This gas was prepared by the usual method from previously outgassed calcium carbide and purified by passing through alkaline sodium plumbite, chromic acid, concentrated sodium hydroxide, solid calcium chloride, and phosphorus pentoxide in the order named. It was solidified at liquid-air temperature and outgassed until no pressure could be read on a McLeod gauge. It was kept liquid in the Raman tube at -82°C at a pressure of about 895 mm in a specially constructed unsilvered Dewar flask shown in Fig. 2.

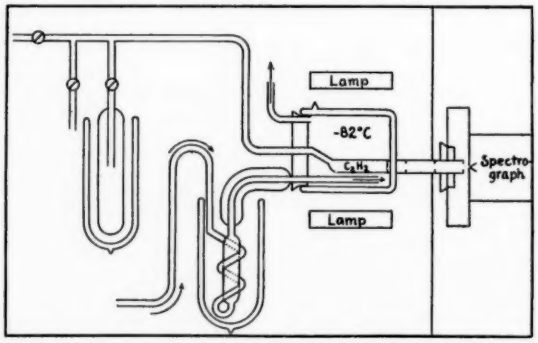

FIG. 2. Experimental arrangements for liquid acetylene.

[5] Biltz, Ber. **37**, 4415 (1904).
[6] Dehn, J. Am. Chem. Soc. **33**, 1598 (1911).
[7] Shipsey and Werner, J. Chem. Soc. **103**, 1255 (1913).

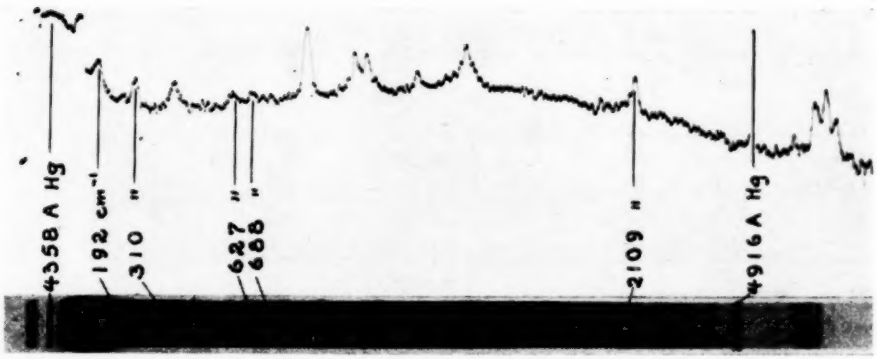

FIG. 3. Raman spectrum of diiodoacetylene.

Dideuteroacetylene

This substance was obtained from Professor Taylor of Princeton University.[3] Its exact purity was unknown but was undoubtedly quite high. No lines were found which could not readily be attributed to the C_2D_2 molecule. The gas was confined and exposed in a 280-cc tube at 763 mm pressure.

Monodeuteroacetylene

The spectra of gaseous C_2H_2 and C_2HD molecules were obtained from a mixture of the two substances confined at a total pressure of 2.8 atmospheres. The mixture was supplied by Dr. L. H. Reyerson[3] and was prepared from ordinary acetylene and 19 percent heavy water. It contained about 12–15 percent of monodeuteroacetylene at a partial pressure of about 0.4 atmosphere.

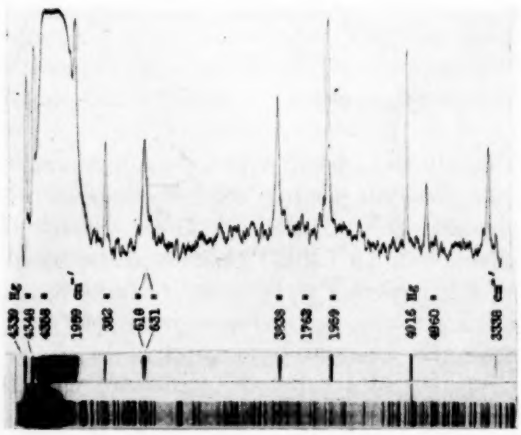

FIG. 4. Raman spectrum of liquid acetylene (C_2H_2) excited by 4046 Hg and 4358 Hg.

III. EXPERIMENTAL RESULTS

The Raman frequencies of the substances investigated are given in Tables I–III and shown in Figs. 3 and 4.

TABLE I. *Diiodoacetylene (alcohol solution).* Twenty-four hours exposure; sodium nitrite filter. Exciting line: 4358A Hg.

$\Delta\nu(cm^{-1})$	INTENSITY	NATURE
191.3	7	broad, diffuse
310.2	5	sharp
627.0	3	very diffuse
688.2	2	diffuse
2109.4	10	sharp

TABLE II. *Liquid acetylene; ten hours exposure.* No filter, exciting lines: 4047 and 4358A Hg.

$\Delta\nu(cm^{-1})$	INTENSITY	NATURE
1931.4*	1.5	sharp
1959.5*	10	sharp
381.6	5	sharp
618.0	2	diffuse
630.7	5	sharp
3338.0*	7	diffuse
1761.9	1	diffuse
1813.7	0.1	very faint
1855.8	0.1	very faint
1877.8	0.1	very faint
1903.2	1	slightly diffuse
1929.9	1	slightly diffuse
1958.0	10	sharp
3336.8	5	diffuse

* Excited by 4047A Hg.

TABLE III. *Gaseous acetylenes; valency vibrations.* Seventy hours to one week exposure; no filter. Exciting lines: 4047 and 4358A Hg.

	C_2H_2		C_2HD		C_2D_2	
TRIAL	P1	P2	P1	P2	P1	P2
1	1974.2	3374.2	1851.1	3334.8	1762.3	2700.9
2	1973.3	3373.1	1851.3		1762.6	2699.2
3	1974.4	3373.8			1762.2	
4	1973.3					
5	1973.8					
Ave.	1973.8	3373.7	1851.2	3334.8	1762.4	2700.5

TABLE IV. *Application of Placzek's selection and polarization rules to the spectra of a number of different space configurations of the molecule C_2X_2 ($X=I$ or H).*

	Configuration		Type of freq.	s	a	Total No. of freq.	Raman effect	ρ	Allowed No. of freq.
				I. Linear forms					
a	$D_{\infty h}$	X–C–C–X	A_1	C_∞ σ_v i		2	$c_{ik}=0$	0–$\frac{3}{4}$	
			A_2	C_∞ σ_v	i	1	forbidden	—	
			B_1	σ_v i	C_∞	1	only $c_{xz}=c_{yz}\neq 0$	$\frac{3}{4}$	
			B_2	σ_v	C_∞ i	1	forbidden	—	3
				II. Planar forms					
b	C_{1h}	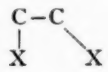	A	σ		5	$c_{xz}=c_{yz}=0$	0–$\frac{3}{4}$	
			B		σ	1	$c_{ii}=c_{xy}=0$	$\frac{3}{4}$	6
c	C_{2h}	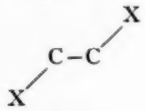	A_1	C_2 σ_h		3	$c_{xz}=c_{yz}=0$	0–$\frac{3}{4}$	
			A_2	C_2	σ_h	1	forbidden	—	
			B_1	σ_h	C_2	2	forbidden	—	
			B_2		C_2 σ_h	0	$c_{ii}=c_{xy}=0$	$\frac{3}{4}$	3
d	C_{2v}	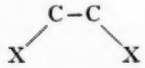	A_1	C_2 σ_x σ_y		3	$c_{ik}=0$	0–$\frac{3}{4}$	
			A_2	C_2	σ_x σ_y	0	only $c_{xy}\neq 0$	$\frac{3}{4}$	
			B_1	σ_y	C_2 σ_x	2	only $c_{xz}\neq 0$	$\frac{3}{4}$	
			B_2	σ_x	C_2 σ_y	1	only $c_{yz}\neq 0$	$\frac{3}{4}$	6
e	C_{2v}	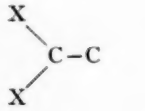	A_1	C_2 σ_x σ_y		3	$c_{ik}=0$	0–$\frac{3}{4}$	
			A_2	C_2	σ_x σ_y	0	only $c_{xy}\neq 0$	$\frac{3}{4}$	
			B_1	σ_y	C_2 σ_x	2	only $c_{xz}\neq 0$	$\frac{3}{4}$	
			B_2	σ_x	C_2 σ_y	1	only $c_{yz}\neq 0$	$\frac{3}{4}$	6
f	D_{3h}		A	σ_x σ_y σ_z		3	$c_{ik}=0$	0–$\frac{3}{4}$	
			B_1	σ_x σ_y	σ_z	1	forbidden	—	
			B_2	σ_z σ_x	σ_y	1	forbidden	—	
			B_3	σ_y σ_z	σ_x	1	forbidden	—	3
				III. Nonplanar forms					
g	C_{1h}	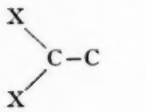	A	σ		4	$c_{xz}=c_{yz}=0$	0–$\frac{3}{4}$	
			B		σ	2	$c_{ii}=c_{xy}=0$	$\frac{3}{4}$	6
h	C_2		A	C_2		4	$c_{xz}=c_{yz}=0$	0–$\frac{3}{4}$	
			B		C_2	2	$c_{ii}=c_{xy}=0$	$\frac{3}{4}$	6
i	C_{2v}		A_1	C_2 σ_x σ_y		3	$c_{ik}=0$	0–$\frac{3}{4}$	
			A_2	C_2	σ_x σ_y	1	only $c_{xy}\neq 0$	$\frac{3}{4}$	
			B_1	σ_y	C_2 σ_x	1	only $c_{xz}\neq 0$	$\frac{3}{4}$	
			B_2	σ_x	C_2 σ_y	1	only $c_{yz}\neq 0$	$\frac{3}{4}$	6

IV. Discussion of Results

Symmetry considerations

For the discussion of these spectra it will be convenient to determine the symmetry classes possible for molecules of the type studied and to ascertain the number of possible Raman vibration frequencies from Placzek's theory and his selection rules.[8] These molecules must possess for purely dynamical reasons, six fundamental frequencies. All possible configurations of these molecules will be considered: linear, planar, and space models. In Table IV are listed the Schoenflies designations for the class of symmetry, the configuration pictorially represented, the types of frequencies denoted by capital A or B with appropriate subscripts, the symmetry elements to which the type of frequency is symmetric (s) or antisymmetric (a), the number of distinct fundamental frequencies belonging to a given

[8] Placzek, *Handbuch der Radiologie* (Leipzig, 1934), Vol. II, p. 205.

type, the selection rules for the Raman effect stated in terms of the magnitudes of the components of the scattering tensor c, the degree of depolarization ρ and the number of allowed Raman frequencies. If all the components of the scattering tensor are zero for a given type of vibration, then this vibration cannot be active in the Raman effect. The letters C, σ, i represent, respectively, an axis of rotational symmetry, a plane of symmetry and a center of symmetry. The term σ_v represents a plane of symmetry passing through an axis of symmetry. C_{1h}, C_2, and C_{2v} represent systems containing a single plane, a twofold axis and a twofold axis with a σ_v plane of symmetry. The system D_{3h} contains $3C_2$ axes and $3C_v$ planes. The system C_{2h} contains a center of symmetry, a twofold axis of symmetry and a plane of symmetry perpendicular to this axis. In cases where the symmetry planes are designated by the rectangular coordinates x, y, and z, the z axis is taken as the axis of symmetry. The letter X in the first column represents either hydrogen or iodine.

The gaseous acetylenes

From Table III it is seen that only two types of Raman frequencies have been observed. Most previous studies[9–14] show the same results. However from the selection rules (Table IV) these molecules should show three frequencies if they are linear. The two frequencies found are the valency vibrations ν_1 and ν_2 of Mecke's[15] assignment. The deformation frequency δ_2, Raman-allowed by Placzek's selection rule has never been found. It must mean that the components of the polarization tensor are very weak and the intensity of this line is very small. However δ_2 can be deduced from the infrared combination bands (Table VI). There is a great deal of evidence that gaseous acetylene (C_2H_2) is linear. The rotational structure of the bands is similar to that of a diatomic molecule. The individual rotation lines have alternating intensity showing that the molecule has a center of symmetry. Recently monodeuteroacetylene (C_2HD) has been investigated in the near infrared by McKellar and Bradley[16] and Herzberg, Spinks and Patat.[17] The parallel bands observed show a rotational structure which must be attributed to a linear oscillator. Dideuteroacetylene is most likely also linear in the gaseous state. It may then be said that *in the gaseous state acetylene molecules are linear.*

Liquid acetylene (C_2H_2)

The failure to find the deformation frequency δ_2 at 614 cm^{-1} (predicted from the infrared) in the gas lead to an investigation of the liquid. A frequency was indeed found at 618 cm^{-1} (Table II) but it has a companion at 631 cm^{-1}. Moreover a very low frequency is shown on our plates at 382 cm^{-1} and a very weak line at 1762 cm^{-1}. These four frequencies are excited by 4358A Hg and not by 4047A Hg, for if the latter were the exciting line, then their frequencies would be 2149 (382), 2385 (618), 2398 (631), and 3629 (1762). It would be expected that 4358A Hg would excite the lines 2149, 2385, 2398, and 3629 cm^{-1}. They are not found and hence it is certain that 4358A Hg is the exciting line. *In liquid acetylene six lines are found instead of three* as expected from Placzek's rules! The possibility must be considered that these selection rules are not valid for the closely crowded molecules of the liquid. Then the frequencies expected would be the ones of the gaseous molecule as given by Mecke[15] and summarized in Table V. But the new lines found are not the fundamentals of ordinary acetylene. They might be due to an impurity. However from the preparation and purification this possibility seems most unlikely. Moreover any sensible impurity would have a more complicated spectrum which should show in its entirety. Furthermore the lines 382, 618, and 631 are much too

TABLE V. *Fundamental frequencies of acetylene (C_2H_2).*

ν_1	H→	C→	←C	←H	1975 cm^{-1}
ν_2	H→	←C	C→	←H	3370
ν_3	H→	←C	←C	H→	3277
δ_1	H↓	C↑	C↑	H↓	729
δ_2	H↓	C↑	C↓	H↑	614

[9] Daure, Ann. de physique **12**, 375 (1929).
[10] Segrè, Rend. Linc. **12**, 226 (1930).
[11] Venkatesachar and Sibaiya, Ind. J. Phys. **5**, 319 (1931).
[12] Bhagavantam, Nature **127**, 817 (1931) and Ind. J. Phys. **6**, 319 (1931).
[13] Daure and Kastler, Comptes rendus **192**, 1721 (1931).
[14] Lewis and Houston, Phys. Rev. **44**, 903 (1933).
[15] Mecke, Zeits. f. physik. Chemie **B17**, 1 (1931).
[16] McKellar and Bradley, Phys. Rev. **46**, 664 (1934).
[17] Herzberg, Spinks and Patat, Zeits. f. Physik **92**, 87 (1934).

strong to be ascribed to an impurity. These new lines might be due to some strange reflections produced in the set-up due to improper alignment. However if such were the case then it would be expected that a great deal of general background would show on the photographic plates. However the photographs are remarkably free from such background.

A possible explanation of the appearance of these six Raman lines is the assumption that the acetylene molecules are not linear in the liquid state. Then six fundamental frequencies would be expected. They are: 381.6, 618, 631, 1762, 1959 and 2338 cm^{-1}. The lines 1813.7 to 1929.9 cm^{-1} are thought to be due to a rotation phenomenon and will be discussed below. Referring to Table IV it is seen that models *a*, *c* and *f* need not be considered because only three frequencies should appear in the Raman effect. Models *b*, *d*, *e*, *g* and *h* may perhaps be excluded because these structures would have an appreciable dipole moment. Liquid acetylene has most likely only a small dipole moment although no experimental evidence exists. The dipole moment of gaseous acetylene is zero. Model *i* can be thought of as a plane formed by two carbon atoms and one hydrogen atom with the other hydrogen atom not in this plane. Only slight displacements of the hydrogen atoms need to occur in the usual linear structure to remove them from the figure axis determined by the carbon atoms. Such distortions may conceivably occur in the liquid state due to the close interactions of the liquid molecules. Model *i* would quite possibly have only a small dipole moment. The important result of our findings is the suggestion that the molecules of a liquid may suffer deformations which affect their symmetry properties.

The possibility of association in the liquid state must also be considered but it does not seem possible to explain the present results on this basis. If a definite polymer were formed, more lines are expected than are actually found. For example $(C_2H_2)_2$ as a four-membered ring would be a polymer belonging to the point-group D_{4h} with seven Raman allowed frequencies and if the same polymer were of a linear configuration with methylene groups at the ends (D_{2h}) then nine frequencies should be observed in the Raman effect. As only six lines are found it might be said that the others are of low intensity and they might be discovered on longer exposure. While this possibility exists it must be said that other physical properties of liquid acetylene speak against association. Substances which do polymerize have large dipole moments, they do not behave like normal liquids regarding their surface-tension variation with temperature. Such molecules as water and ammonia have broad Raman bands. Liquid acetylene has probably only a small dipole moment, the constant *K* in the Ramsey-Shields-Eötvös equation has the value of a normal liquid and the Raman lines are sharp, i.e., not bands. However, some sort of special interaction between the acetylene molecules in the liquid state appears to take place for it should be noted that nitrogen and acetylene although isoelectronic boil about 100°C apart and C_2H_2 boils at a higher temperature.

These results indicate that a difference may exist in the structure of acetylene molecules depending on the state of aggregation. It appears that similar differences may be found with many other substances. For in many cases the number of Raman lines expected on the basis of Placzek's selection rules is not in agreement with published data.

Diiodoacetylene

From Table I it is seen that five Raman lines are found whereas only three would be expected if the molecule is linear, i.e., if the selection rules hold. Again it appears that the molecule may be nonlinear in solution, the interaction due to the solvent molecules causing the deformation. Consideration as made in the case of liquid acetylene would indicate model *i* of Table IV. There should be found a sixth frequency for this molecule. The fact that these molecules are conceivably nonlinear recalls to mind the arguments of organic chemists who have often put forward the idea that the symmetrical structures given these compounds do not explain all their reaction possibilities.[18]

[18] E. H. Ingold, J. Chem. Soc. **125**, 1528 (1924); and **127**, 1199 (1925); Nieuwland *et al.*, J. Am. Chem. Soc. **53**, 4197 (1931); Nef, Ann. **296**, 332 (1897); Ber. **34**, 2718 (1901), etc.

Calculated frequencies of the acetylenes

Both Mecke[19] and Olson and Kramers[20] have derived expressions for the fundamental frequencies of acetylene in terms of the masses of the atoms and Hooke's law constants on the theory of small vibrations. The calculated values are compared with the experimental frequencies in Table VI from various sources.[1, 16]

TABLE VI. *The fundamental frequencies of the acetylenes:* $k_{C-H}=k_{C-D}=5.868\times10^5$; $K_{C\equiv C}=15.49\times10^5$ dynes/cm.

	Type of Vibration	C_2H_2 calc.	C_2H_2 obs.	C_2HD calc.	C_2HD obs.	C_2D_2 calc.	C_2D_2 obs.
ν_1	H→ C→←C ←H	(1974)	1974	1846	1851	1757	1762
ν_2	H→←C C→←H	(3374)	3374	3326	3335	2678	2700
ν_3	←H C→ C→←H	3281	3277	2556	2570	2410	—
δ_1	H↓ C↑ C↑ H↓	—	729	—	679	—	520
δ_2	H↓ C↑ C↓ H↑	614	—	—	541	392	—

Free energies of C_2H_2, C_2HD, and C_2D_2

The possibility of calculating the thermodynamic properties of the simpler gaseous substances from spectrographic data was suggested by Urey[21] and Tolman and Badger.[22] The fundamental equations for such computations have been adequately outlined by Giauque.[23] For ordinary acetylene (C_2H_2) Kassel[24] has derived some simple expressions which have been used to calculate the free energy of the deutero-acetylenes. The fundamental frequencies are shown in Table VI. The moments of inertia (I) of these molecules are taken as: $I(C_2H_2)=23.509\times10^{-40}$, $I(C_2HD)=27.412\times10^{-40}$, and $I(C_2D_2)=31.616\times10^{-40}$.[16, 17] The effect of the spin terms in the acetylene molecules can be taken care of at higher temperatures by adding to the free energy the quantity $-RT\ln\mu$ where μ has the value

$$\mu=(2i+1)^2/2$$

for the symmetrical molecules C_2H_2 and C_2D_2 and the value

$$\mu=(2i_1+1)\times(2i_2+1)$$

for the asymmetrical molecule C_2HD.[25] The quantities i_1 and i_2 are the spin numbers of the hydrogen and deuterium nuclei. The spin of the deuterium nucleus is assumed to be unity. The carbon atoms have no spin. Although the values of the free energy (F°) of both C_2HD and C_2D_2 depend on the spin, the values of any equilibrium constants calculated for reactions into which these molecules enter, does not depend on the spin chosen. This independence is due to the very general fact that the nuclear spins are unchanged during chemical reactions at temperatures considerably removed from absolute zero. The quantity E_0° is the energy content of a species of molecules at standard condition at absolute zero.

From the values of Table VII equilibrium constants for the reaction

$$C_2H_2+C_2D_2\rightleftarrows2C_2HD$$

can readily be calculated by the following equation:

$$\Delta F^\circ=-RT\ln K=\Delta(F^\circ-E_0^\circ)+\Delta E_0^\circ.$$

On account of the great similarity of all the molecules taking part in the reaction the quantity ΔE_0° can be considered as the difference between the zero-point vibrational energies of the product and the reactants. With the frequencies given in Table VI $\Delta E_0^\circ=519.01$ cal.

The above values for the equilibrium constant are undoubtedly more accurate than the free

TABLE VII. *Values of* $-(F^\circ-E_0^\circ)/T$ *for the acetylene gases at one atmosphere pressure.* (Calories/degree/mole.)

Temp. (°K)	C_2H_2	C_2HD	C_2D_2
273.18	42.034	44.790	45.017
298.18	42.728	45.493	45.811
373.18	44.597	47.426	47.951
500.00	47.270	50.195	51.003
600.00	49.083	52.074	53.039
700.00	50.710	53.756	54.874

TABLE VIII. *Free energy changes and equilibrium constants for the reaction:* $C_2H_2+C_2D_2\rightleftarrows2C_2HD$.

Temp. (°K)	$-\Delta(F^\circ-E_0^\circ)$ (cal.)	$-\Delta F^\circ$ (cal.)	K
273.18	690.87	171.86	1.373
298.18	729.65	210.64	1.427
373.18	860.18	341.17	1.584
500.00	1058.50	539.49	1.722
600.00	1215.60	696.59	1.794
700.00	1349.60	834.09	1.822

[19] Mecke, Zeits. f. Physik **64**, 173 (1930).
[20] Olson and Kramers, J. Am. Chem. Soc. **54**, 136 (1932).
[21] Urey, J. Am. Chem. Soc. **45**, 1445 (1923).
[22] Tolman and Badger, J. Am. Chem. Soc. **45**, 2277 (1923).
[23] Giauque, J. Am. Chem. Soc. **52**, 4808 (1930).
[24] Kassel, J. Am. Chem. Soc. **55**, 1351 (1933).
[25] Urey and Rittenberg, J. Chem. Phys. **1**, 137 (1933).

energy values. The errors in the quantities $(F^\circ - E_0^\circ)$ arise not only from inaccuracies in the values of the fundamental frequencies but also from the failure to consider the stretching and anharmonicity terms in the formation of the Q sums. The values of ΔF° and K are not so much affected because errors which arise from these sources cancel out during the process of subtracting the individual free energy values. The curve obtained by plotting K as a function of temperature has the same general shape as that obtained by Urey and Rittenberg[25] for the reaction

$$H_2 + D_2 \leftrightarrows 2HD.$$

Rotation effects in liquid acetylene

A series of faint lines was observed on the short wave-length side of 1959 cm^{-1}. Similar lines have been observed previously in pinene[26] and in dimethylacetylene[27] and have been interpreted as the members of a P branch of a rotation-vibration band. The individual lines are so spaced that their displacements (cm^{-1}) from 1959 cm^{-1} can be represented quite accurately by means of the following equation:

$$\Delta\nu = 6.99(4m+4) - 0.014 \times 16(\tfrac{1}{2}m^3 + \tfrac{3}{2}m^2 + 2m + 1)$$
$$m = 0, 1, 2, \cdots.$$

This equation may be regarded as the difference between the $(m+2)$th and mth term of

$$E_m/(hc) = 6.99m^2 - 0.014m^4$$
$$m = 0, 1, 2, \cdots$$

of a nonrigid rotator with fixed axis. In Table IX are recorded the measured and calculated values of the displacements $\Delta\nu = 1959$ cm^{-1}. The constant 6.99 must be equal to $h/(8\pi^2 I_0 c)$, where I_0 is the moment of inertia of the assumed rotator. The calculated value is 3.96×10^{-40} g cm^2. The only conceivable type of rotation involving such a small moment of inertia is a spinning of the nonlinear molecule about the line of the carbon atoms.

TABLE IX. *The faint companion lines as displacements from* $\Delta\nu = 1959$ cm^{-1}.

TRANSITION	m	ν(calc.) (cm^{-1})	ν(obs.) (cm^{-1})
2→0	0	27.8	28.1
3→1	1	54.8	54.9
4→2	2	80.5	80.2
5→3	3	(104.2)	104.2
6→4	4	125.2	—
7→5	5	(142.9)	142.9

The lines appear from visual observation, to show alternating intensity, the ones corresponding to odd values, being stronger. In spite of the good agreement between the measured and the calculated displacements of Table IX, there are a number of important objections to the interpretation as a rotation effect. It is difficult to understand why the nonlinear acetylene molecule should not act as a space rotator rather than as a plane rotator even in the liquid state. The complete absence of a corresponding R branch is also at variance with the expectations of theory.

In the case of diiodoacetylene we also find a companion to the Raman line $\Delta\nu = 2109$ cm^{-1}. While the line is quite easily visible on a magnified spectrogram we have been unable to measure its position. The displacement appears to be about 20 cm^{-1}. It apparently has the same origin as the faint lines in acetylene. On account of the large masses of the iodine atoms, the possibility of this line being a member of a P branch seems difficult to understand.

[26] Bonino, Nature **126**, 915 (1930).
[27] Glockler and Davis, J. Chem. Phys. **2**, 881 (1932).

Predissociation of the Oxygen Molecule*

PAUL J. FLORY, *DuPont Experimental Station, Wilmington, Deleware*

(Received August 25, 1935)

In the emission spectrum of the oxygen molecule no bands in the Runge system, $^3\Sigma_u^- \rightarrow {}^3\Sigma_g^-$, having $v' > 2$ have ever been observed. The absence of these emission bands as well as evidence of broadened rotation lines in the $v' > 2$ absorption bands suggests that in the $^3\Sigma_u^-$ state vibration levels above the second undergo predissociation. Rassetti's observations of the fluorescence spectrum of oxygen as well as recent photochemical results support this conclusion. Although it cannot be said that any one of these lines of evidence provides rigorous proof that the oxygen molecule predissociates, collectively they present a convincing argument for the occurrence of predissociation. Radiationless transition from the $^3\Sigma_u^-$ state is doubtless to the $^3\Pi_u$ state formed from normal atoms. On the basis of the present interpretation the initial process in the photochemical reactions of oxygen caused by light in the region of Schumann-Runge band absorption is the formation of normal ^3P atoms as a result of the predissociation, rather than the reaction of an optically excited molecule with a normal molecule as heretofore has been supposed.

INTRODUCTION

IN studies of the photochemical reactions of oxygen, other than those carried out at high pressures, it has been customary to distinguish between the effects of light absorption in two different spectral regions. The first region is that of the Schumann-Runge absorption bands which extend from about 2000A down to their convergence limit at 1751A. The second region lies below the convergence limit and consists of strong continuous absorption. Differences in the photochemical effects of radiations falling in these two regions have been attributed to the difference in the reactivity of an optically excited oxygen molecule produced by band absorption and the reactivity of the oxygen atoms resulting from the continuous absorption. For instance, Smith and Kistiakowsky[1] have found that the relative yields of ozone and hydrogen peroxide in hydrogen-oxygen mixtures differ when the 1854–1862A lines and when the 1719–1725A lines of aluminum are used. It is the purpose of this paper to show, on the basis of data already in the literature, that predissociation occurs in the region of band absorption. The predissociation results in the production of two unexcited ^3P oxygen atoms whereas the continuous absorption produces one ^3P and one excited ^1D atom. Consequently, differences in the photochemical effects of light in the two spectral regions are due to the difference in the states of the atomic dissociation products.

THE OXYGEN SPECTRUM AND PREDISSOCIATION

The Schumann-Runge band system, $^3\Sigma_u^- \leftrightarrow {}^3\Sigma_g^-$, is responsible for the only absorption of oxygen in the visible and ultraviolet regions down to about 1000A, except for weak absorption due to forbidden transitions which is only observed with large optical densities. The (0, 0) band at 2026A is extremely weak. Proceeding to shorter wave-lengths the intensity of the successive absorption bands increases rapidly. The bands converge at 1751A, and the continuous absorption below this point continues to increase in intensity until a maximum is reached at about 1450A.[2]

Runge[3] photographed the same system of bands in emission in the second and third orders from a 6.5-meter grating. His source was a high potential d.c. arc operated in a quartz tube through which oxygen was streaming. Lochte-Holtgreven and Dieke,[4] using Runge's plates, analyzed the rotation structure of the bands indicated in Fig. 1. In the region from 3050 to 4450A they classified *all lines*, except weak and sporadically occurring ones, into these nineteen bands. Nine of the bands belong to the $v' = 0$ progression, five to the $v' = 1$, five to the $v' = 2$, and none to higher progressions. No evidence of emission from excited levels having $v' > 2$ was found. On

* Presented before the Division of Physical and Inorganic Chemistry of the American Chemical Society at the New York Meeting, April 23, 1935.

[1] Smith and Kistiakowsky, J. Am. Chem. Soc. **57**, 835 (1935).

[2] Ladenburg and Van Voorhis, Phys. Rev. **43**, 315 (1933).

[3] Runge, Physica **1**, 254 (1921).

[4] Lochte-Holtgreven and Dieke, Ann. d. Physik **3**, 937 (1929).

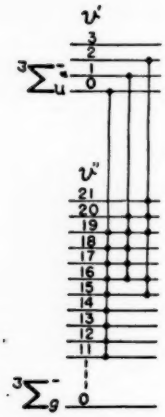

FIG. 1.

the basis of the Franck-Condon principle a number of such bands should have been observed in this spectral region. For example, the (3,15), (3,16), (3,20), (3,21), and (3,22) bands, all of which would fall within the spectral region investigated, lie close to the Condon curve of maximum intensities. Although the failure to observe these bands may have been the result of some experimental peculiarity, it appears to be much more probable that they are inherently absent, or greatly reduced in intensity, in the emission spectrum of oxygen. If this is the case, the absence of $v'>2$ progressions must be due to some process which destroys or deactivates molecules in vibration levels above $v'=2$ before they can emit radiation.

In a number of cases a breaking off in the emission spectrum such as occurs here has been associated with predissociation of the levels from which emission is absent. That is, if the probability of predissociation is much greater than the probability of emission (fluorescence), then the emission will be so weak as to escape observation. In fact, this has been used frequently as a criterion for predissociation. Predissociation of the $^3\Sigma_u^-$ state of oxygen for $v'>2$ levels would plausibly explain the absence of emission from such levels. In what follows this explanation will be shown to be in agreement with other lines of evidence.

Predissociation is most commonly recognized by the diffuse rotation lines of the absorption bands. In many instances rotation structure is entirely lost. The degree of broadening in any case is simply dependent upon the mean life of the excited state prior to predissociation. Recently Curry and Herzberg[5] have carefully analyzed the (1,0), (2,0), (3,0), (4,0), (5,0), (4,1), (5,1), (6,1), and (7,1) absorption bands of oxygen obtained with air in their grating spectrograph. Although they measured the rotation lines at a dispersion of 1.7A per mm, they do not mention predissociation. However, they point out that their most accurate measurements were made on the (2,0) band. Here the error in their measurements was about ± 0.2 cm^{-1}, whereas the errors in the seven bands of higher v' ran as high as ± 0.8 cm^{-1}. (Curry and Herzberg attribute the error to the characteristics of the line, i.e., intensity, overlapping, and breadth). Also, in the photograph which they publish the lines in the (2,0) band appear to be sharper than those in the neighboring (5,1) band, and in the (3,0) (6,1), and (4,0) bands. These observations, though in themselves inclusive, are indicative of an actual line broadening in $v'>2$ bands.

The absence of fluorescence from levels which predissociate has frequently been used as a sensitive test for predissociation. Rasetti[6] photographed an extremely weak fluorescence spectrum when he irradiated oxygen at atmospheric pressure with an intense mercury arc. The strong mercury 1849 line excited the oxygen molecules into the $^3\Sigma_u^-$, $v'=8$, $J=12$ and $J=8$ levels. In the fluorescence spectrum eighteen lines, all from these two upper levels, were found. In order to photograph the fluorescence it was necessary to run the exposures from fifty to eighty hours. Such a weak emission must mean that only a very few of the optically excited molecules dispose of their energy by fluorescing, a conclusion in agreement with the characteristics of the oxygen emission and absorption spectra discussed above.

Rasetti presumed that the low intensity of fluorescence was due to quenching of the excited molecules by collisions with other molecules. He was surprised, therefore, to find that on lowering the pressure to 8 mm so as to reduce the number of quenching collisions he could no longer obtain the fluorescence spectrum at all.

---

[5] Curry and Herzberg, Ann. d. Physik **19**, 800 (1934). Recently Knauss and Ballard (Phys. Rev. **48**, 796 (1935)), have reported measurements and analyses of the $v'=7$ to 15 absorption bands in the $v''=0$ progression. Their dispersion was not sufficiently high to show predissociation broadening.

[6] Rassetti, Proc. Nat. Acad. Sci. **15**, 411 (1929).

It was Rasetti's expectation, presumably, that inasmuch as the absorption was almost complete at atmospheric pressure, a hundred-fold decrease in pressure would reduce the amount of light absorbed much less than it would reduce the collision rate, and the net result would be an increase in fluorescence intensity. The failure to observe any fluorescence at the lower pressure is not surprising if, alternatively, the destruction of the excited molecules is not dependent upon collisions, in other words, if it is due to predissociation. Thus, predissociation of oxygen in the $^3\Sigma_u^-$ state not only accounts for the low intensity of the fluorescence observed by Rasetti, but it also explains his failure to observe fluorescence at the lower pressure.

Photochemical Evidence of Predissociation

Neujmin and Popov[7] in conjunction with their investigation of the photochemical reaction of oxygen and hydrogen observed photochemical effects produced in oxygen alone at pressures of about 0.1 mm. When the oxygen was subjected to light from a hydrogen discharge tube in the region of its continuous absorption from 1751A (the convergence limit of the Runge bands) down to about 1300A, the pressure decreased due to the reaction of the photochemically produced atomic oxygen with the picein or shellac used to attach the cell windows. The atomic oxygen was also shown to react with impurities on the cell walls unless these had been carefully cleaned by baking at red heat under vacuum. These experiments suggest that such a decrease in pressure due to reaction with impurities might serve as a criterion for the presence of oxygen atoms at low pressures.

When Neujmin and Popov, by interposing air in the light path, limited the exciting radiation to that lying above 1751A where only band absorption can occur, no pressure decrease similar to that mentioned above was observed. They considered that only excited molecules resulted from the band absorption. Since at 0.1 mm the time between collisions (about 10^{-6} sec.) is much greater than the life of an excited molecule with respect to fluorescence (10^{-9} to 10^{-8} sec.) they attributed their failure to observe evidence of reaction to the predominating disposal of excitation energy by fluorescence. These results might be interpreted to demonstrate the absence of oxygen atoms when oxygen is irradiated with light in this region. This interpretation is, of course, incompatible with the occurrence of predissociation.

In connection with their investigation of the photochemical decomposition of nitric oxide, Flory and Johnston[8] have obtained results which show that such an interpretation must be incorrect. In view of the important bearing of these results on the present problem it will be well to consider them in detail here. The reaction system, essentially the same as that used by Neujmin and Popov, was entirely of Pyrex and quartz and pressures were measured on a McLeod gauge. Although the reaction system was frequently "flamed out" under vacuum, it was never baked out intensively as Neujmin and Popov have shown to be necessary in order to eliminate the reaction of atomic oxygen with impurities. The 1775, 1832, and 1849 lines and some continuous radiation in the region of oxygen band absorption were present in the mercury arc source of illumination. The absence of light below the convergence limit was assured by the presence of about a centimeter of air between the arc and the cell window. The pressure decreased steadily from 0.1280 to 0.0963 mm in $7\frac{1}{2}$ hours and remained constant after discontinuing the illumination.

The results of this single experiment are substantiated quantitatively by the results of a number of others in which nitric oxide was first completely decomposed into nitrogen and oxygen. A subsequent pressure decrease, obviously due to a photo-reaction of the oxygen since nitrogen is transparent in this spectral region, was found to occur on further illumination. The fractional decrease per hour in the pressure of oxygen was about the same as that observed in the experiment with pure oxygen under the same conditions of illumination.

A bimolecular collision of an optically excited molecule with a normal molecule, as Neujmin and Popov point out, is much less probable at pressures around 0.1 mm than fluorescence of the excited molecule. If the reaction proceeds by

[7] Neujmin and Popov, Zeits. f. physik. Chemie **B27**, 15 (1934).

[8] Flory and Johnston, J. Am. Chem. Soc. **57**, December (1935).

such a bimolecular process as an initial step, even under the optimum conditions of a collision efficiency of unity, the quantum yield must be less than 0.01, assuming no chain mechanism.[9] It is very doubtful that such a low quantum yield could give rise to the rate of pressure decrease observed by Flory and Johnston. On the other hand, if one considers the reaction to depend on predissociation as the initial process this difficulty is overcome because for each quantum absorbed two oxygen atoms are produced. It is quite conceivable that subsequent reactions of these oxygen atoms cause the pressure decrease at the rate which has been observed. Thus, although this work does not elucidate the nature of secondary processes which occur when oxygen is irradiated under the conditions of the experiments, it does provide photochemical evidence which confirms the occurrence of predissociation independent of collisions.

These results in no way conflict with the view that the pressure decrease was due to a reaction of atomic oxygen kindred to that observed by Neujmin and Popov. Their failure to obtain any evidence of photochemical reaction caused by band absorption must have been due to the very much weaker absorption of oxygen in the banded region than in the continuum. Ladenburg and Van Voorhis[2] measured the absorption coefficient of oxygen in the continuum from 1700 to 1300A. By extrapolating their data to wave-lengths above 1750A one can see that at low pressures, where only a fraction of the total radiation at any wave-length is absorbed, the total absorption by the bands must be less than 1/50 of the total absorption in the continuum. This placed the rate of the photo-reaction at $\lambda > 1751$ below the limit of observation in the experiments reported by Neujmin and Popov. In the work of Flory and Johnston the use of a more intense source, the mercury arc, permitted the observation of the reaction in spite of weak absorption.

The Predissociation Process

It is the implication of the above lines of evidence that oxygen molecules in $v' > 2$ levels of the $^3\Sigma_u^-$ state are destroyed at a rate much greater than the rate of fluorescence. Furthermore, this destruction process must be independent of collisions with other molecules if it is to explain satisfactorily Rasetti's observations on the fluorescence spectrum, the photochemical results just cited, and the absence of $v' > 2$ emission bands.[10] Hence it must be a predissociation (independent of collisions; not a collision-dependent "induced predissociation"), and the transition to the repulsive electronic state responsible for it must obey Kronig's selection rules.[11]

Before discussing the radiationless transition to the repulsive state which is responsible for the predissociation, it will be desirable to mention the predissociations which have been observed in molecules analogous to oxygen, i.e., other molecules formed from atoms in the sixth group of the periodic table. Bands analogous to the Schumann-Runge bands have been found in the spectra of the molecules S_2, Se_2, Te_2, and SO. In each the transition is $^3\Sigma_u^- \leftrightarrow {}^3\Sigma_g^-$ (in SO it is $^3\Sigma^- \leftrightarrow {}^3\Sigma^-$, of course), the latter state being the normal state of the molecule. In each of these molecules except Se_2 a predissociation of the excited $^3\Sigma$ state has been found.[12] Hirschlaff[13] has predicted that a similar predissociation of Se_2 occurs close to the convergence limit where its observation would be difficult.

The predissociations of the $^3\Sigma_u^-$ states of S_2 and Te_2 (and of Se_2 also according to Hirschlaff's

[9] It is conceivable that the optically excited molecules might be dissociated by wall collision. However, at 0.1 mm pressure wall collisions occur much less frequently than bimolecular collisions. This mechanism would lead to a quantum efficiency less than 0.001.

[10] Runge does not state the pressure of the gas in the arc from which he photographed the emission spectrum, but unless it was much above 0.01 atmosphere, which is not likely, collision quenching could not prevent observation of these bands. On the other hand, Curry and Herzberg obtained their absorption spectrum at atmospheric pressure where the collision frequency is about 10^{10} per second. If a large fraction of the collisions of the activated molecules were effective in quenching them, it is conceivable that this quenching process would account for the broadened absorption lines.

[11] Jevons, *Report on Band-Spectra of Diatomic Molecules*, The Physical Society (London, 1932), p. 201. The selection rules for a radiationless transition derived by Kronig are, $\Delta\Lambda = \pm 1$ or 0, $\Delta\Sigma = 0$, $\Delta J = 0$, $+ \rightarrow +$ or $- \rightarrow -$, and $g \rightarrow g$ or $u \rightarrow u$.

[12] Predissociation of S_2, Christy and Naudé, Phys. Rev. **37**, 903 (1931); Te_2, Hirschlaff, Zeits. f. Physik **75**, 315 (1932); SO, Martin, Phys. Rev. **41**, 167 (1932). In addition to these, induced predissociations of Se_2 and Te_2 (Heil, Zeits. f. Physik **74**, 18 (1932); Kondratjew and Lauris, Zeits. f. Physik **92**, 741 (1934)) have been found. The thresholds come at very low vibration levels, much below the thresholds for the ordinary predissociations.

[13] Hirschlaff, Zeits. f. Physik **75**, 315 (1932).

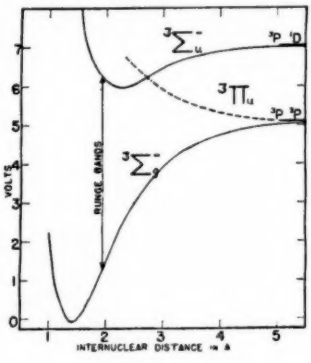

FIG. 2.

prediction) have been attributed to radiationless transitions to repulsive $^3\Pi_u$ states. This assignment was made on the basis of Kronig's rules[11] as follows. There are eighteen states which can be derived from two ^3P atoms, one of which is the $^3\Sigma_g^-$ ground state. Radiationless transitions from a $^3\Sigma_u^-$ state to all of the remaining seventeen states except the $^3\Pi_u$ are forbidden. Therefore, the transition must be $^3\Sigma_u^- \rightarrow {}^3\Pi_u$. (In SO the transition is $^3\Sigma^- \rightarrow {}^3\Pi$.) For identical reasons the repulsive state reponsible for the predissociation in oxygen must be $^3\Pi_u$ also. In Fig. 2 the $^3\Sigma_u^-$ and $^3\Sigma_g^-$ states are shown together with the repuslive $^3\Pi_u$ curve drawn to intersect the $^3\Sigma_u^-$ state at an energy between the second and third vibration levels. The relative positions of the three curves are similar to the analogs of O_2 discussed above.

In explaining the absence of bands in $v' > 2$ progressions in the emission spectrum and the low intensity of fluorescence in Rasetti's experiments it was shown that the probability of predissociation is much greater than the probability of fluorescence. The mean life of an excited molecule prior to fluorescence in the absence of predissociation is known to lie between 10^{-8} and 10^{-9} sec., and so the mean life of the excited state prior to predissociation must be $<10^{-9}$ sec.

A crude estimate of this lifetime is possible if it be assumed that Curry and Herzberg's error ($0.8\ cm^{-1}$) in measurement of the rotation lines in predissociation bands represents a satisfactory approximation of the line breadth. The lifetime, 10^{-11} to 10^{-10} sec., deduced in this manner is of the order of magnitude to be expected for a predissociation of this kind.

PHOTOCHEMICAL REACTIONS OF OXYGEN

Predissociation of oxygen in the region from about 1950A down to the convergence limit, 1751A, must release two unexcited ^3P atoms, each with kinetic energy given by:

$$\text{K.E.} = 1/2(\bar{\nu} - 41{,}260) \times 1.234 \times 10^{-4} \text{ volts}$$

where $\bar{\nu}$ is the frequency of the quantum absorbed in wave numbers. Below 1751A one ^3P and one ^1D atom are the dissociation products, the kinetic energy of each atom being,

$$\text{K.E.} = 1/2(\bar{\nu} - 57{,}110) \times 1.234 \times 10^{-4} \text{ volts.}$$

Differences between the photochemical reactions of oxygen caused by light above and below the convergence limit must be due either to a difference in kinetic energy or to the difference in the reactivities of a ^1D and a ^3P oxygen atom. Certainly the latter difference is likely to be the more apparent.

Heretofore reactions of oxygen initiated by band absorption have been explained by postulating a collision of the optically excited molecule with a normal molecule as the first step. In view of the occurrence of predissociation the primary process must be the formation of atoms. For instance, in the formation of ozone which takes place with light above 1751A the reaction

$$O_2^* + O_2 = O_2 + O \qquad (1)$$

(where O_2^* is an optically excited molecule) has been proposed.[14] According to the present interpretation (1) must be replaced by the reactions:

$$O_2^* \rightarrow O + O \qquad (2)$$

$$O + O_2 + M \rightarrow O_3 + M, \qquad (3)$$

where M is a third body necessary to stabilize the combination.[15] Eq. (3) has been used previously in explanations of oxygen-ozone photokinetics.

[14] This has been discussed by Noyes, Rev. Mod. Phys. **5**, 280 (1933).

[15] Professor G. B. Kistiakowsky has pointed out in a private communication that (1) is not necessarily ruled out if the rate of predissociation is less than the rate of collision. However, from the estimate of the life of the excited state prior to predissociation presented in the preceding section, the rate of predissociation can be no less than the rate of collisions at atmospheric pressure. Even if (1) occurs at every collision, which in itself is not likely, at atmospheric pressure (1) and (2) would be competing processes. At slightly lower pressures (2) would certainly predominate.

Exchange Reactions with Deuterium

I. Deuterium and Hydrogen Chloride

PAUL C. CROSS AND PHILIP A. LEIGHTON, *Department of Chemistry, Stanford University*

(Received October 27, 1935)

An apparatus for measuring exchange equilibria and rates of exchange of molecular deuterium with hydrogen containing compounds is described. The gas density balance is used to analyze the hydrogen-deuterium mixtures. Results on the equilibria $H_2+2DCl=D_2+2HCl$, $H_2+DCl=HD+HCl$ are reported which check the theoretical values to within the limits of the experimental errors.

ONE of the most important consequences of the discovery and separation of the heavy hydrogen isotope will undoubtedly be its use in the determination of the mechanisms of chemical and photochemical reactions. This use will generally be concerned with the reactions of substances in which deuterium has been substituted for hydrogen at certain places in the molecules and will involve determination of the distribution of deuterium in the products. In this connection, it is important to know the circumstances under which deuterium and hydrogen exchanges take place and the extent of the exchange in order to avoid misinterpretation of the cause of the deuterium-hydrogen distributions that are observed. As part of a program of this laboratory involving the use of deuterium in the study of photochemical mechanisms, the apparatus described here has been assembled to study thermal exchanges in systems which will later be studied photochemically. By way of checking the precision of the method, the equilibria $H_2+2DCl=D_2+2HCl$ and $H_2+DCl=HD+HCl$ have been measured and compared with the theoretical values.

A diagram of the apparatus is shown in Fig. 1. The experimental procedure was briefly (1) analysis of the deuterium-hydrogen mixture before exchange; (2) introduction of measured quantities, 200 to 300 mm, of deuterium-hydrogen mixture and HCl into the reaction vessel; (3) reaction at desired temperature accompanied by several mixings of gases in the dead space outside of the heated cell with the gases in the cell; (4) withdrawal, freezing out HCl−DCl mixture, and analyzing the final deuterium-hydrogen mixture.

Quite reliable analyses were obtained by the tedious process of making about ten separate determinations of the relative positions of the

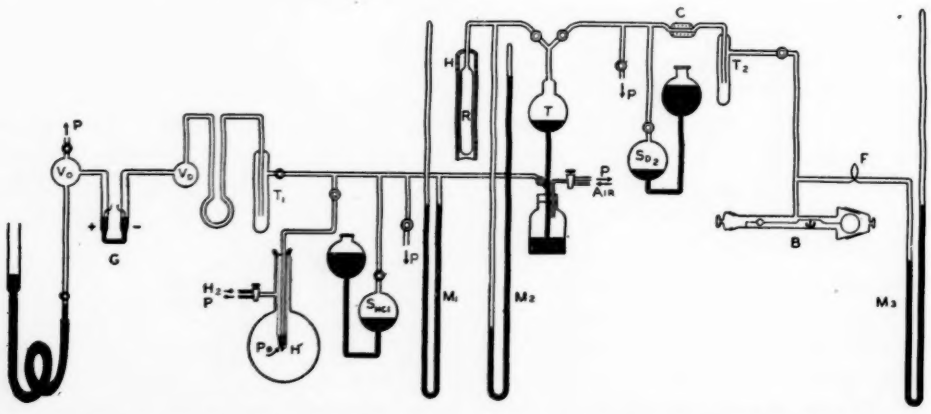

FIG. 1. Exchange apparatus. *B*, gas density balance; *C*, copper catalyst to remove O_2; *F*, flexible glass connection; *G*, electrolytic generator; *H*, heater for reaction cell; *H'*, heater for palladium thimble; M_1, M_2, M_3, manometers; $\rightarrow p$, to pumps; *Pd*, palladium thimble for H_2 purification; *R*, reaction vessel, about 75 cc capacity; S_{HCl}, S_{D_2}, reservoirs for HCl and D_2, respectively; *T*, Toepler pump; T_1, T_2, liquid-air traps; V_O, reservoir for O_2 from generator, adjustable to $V_O=V_D/2$; V_D, reservoir for D_2 from generator.

movable and stationary balance pointers against the gas pressure to obtain an average pressure corresponding to coincidence of the pointers. The statistical accuracy of this procedure was surprisingly good, the probable error usually being <0.1 mm of gas. Nearly all analyses were followed by standardization of the balance on H_2 purified by passing through palladium. These standardizations fluctuated over a range of about one percent of the total H_2 pressure, 154 mm, supposedly due to disturbances of the balance by vibrations between the determinations. No data were taken which give information concerning the absolute accuracy of the balance, but the agreement of the results reported here with the theoretical values is sufficient to warrant further use of the balance as is in the study of exchanges. The authors believe, and the results show, that with care, analyses of deuterium-hydrogen mixtures can be made to within ±0.2 percent.

Exchanges above 700°K were made in a quartz reaction vessel. Those below that temperature were made in a Pyrex cell containing platinum black as a catalyst. The uncatalyzed reaction at 768°K in quartz and the catalyzed reaction at 390°K in glass each required approximately a day to reach equilibrium to within the accuracy of the analyses.

The following molecular equilibria are established in the reaction vessel:

$$H_2+Cl_2=2HCl \quad (1)$$

$$D_2+Cl_2=2DCl \quad (2)$$

$$HD+Cl_2=HCl+DCl \quad (3)$$

$$H_2+2DCl=D_2+2HCl \quad (4)$$

$$H_2+DCl=HD+HCl \quad (5)$$

$$D_2+HCl=HD+DCl \quad (6)$$

$$H_2+D_2=2HD. \quad (7)$$

Reactions (1), (2), and (3) may be assumed to be completely to the right for the purposes of this investigation. The equilibrium (7) is undoubtedly established, through the mechanism of the other reactions if not directly. The theoretical constants of this equilibrium[1] were assumed in order to calculate the equilibria (4), (5) and (6). Furthermore $K_6=K_5/K_4=K_7/K_5$.

[1] H. C. Urey and D. Rittenberg, J. Chem. Phys. **1**, 137 (1933).

TABLE I.

EXP.	T	K_4	K_5	K_6	$\Delta E_0°(4)$	$\Delta E_0°(5)$
1	876	0.96	1.93	2.01	543	342
2	944	0.97	1.94	2.00	544	348
3	768	0.90	1.86	2.07	591	368
4	691	0.83	1.78	2.14	650	400
5	599	0.80	1.73	2.15	611	384
6	496	0.54	1.40	2.59	900*	527*
7	390	0.60	1.44	2.42	625	392
8	604	0.85	1.78	2.09	545	354
9	689	0.77	1.71	2.22	753*	448*
10	478	0.68	1.57	2.30	661	398
11	388	0.61	1.46	2.40	615	380
* Average, omitting Nos. 6 and 9					598±15	374±7
Theoretical $\Delta E_0°$:						
Urey and Rittenberg[1]			I		591.1	373.3
" " "			II		579.1	367.4
Farkas[3]					579.0	366.9

The results are summarized in Table I. Urey and Rittenberg's[1] calculations on reaction (4) were extended to 1000°K where $K_4=0.96$. Likewise K_5 (1000°K) = 1.93 (calculations are for the Cl^{35} isotope). The agreement of the observed equilibrium constants with the theoretical are shown in Figs. 2 and 3 where $\Delta F°/T=-R\ln K$ is plotted against $1/T$ for reactions (4) and (5). Also in the two final columns of Table I there are given the values of $\Delta E_0°$ calculated from the experimental measurements. $\Delta[(F°-E_0°)/T]$ values were obtained from Farkas[2] and Urey and Rittenberg[1] and the value $(F°-E_0°)/T$ for DCl at 1000°K = 47.58_5.

The results shown in Figs. 2 and 3 (runs 6 and 9 excluded) all agree with the theoretical values of $-R\ln K$ to within an amount corresponding approximately to an accuracy of ±0.3 percent in the analysis of hydrogen-deuterium mixtures. The sensitivity of $-R\ln K$ to small errors in analysis may be illustrated by the data of run 4. The final percentage of hydrogen was 53.8, $-R\ln K_4$ being 0.37. The theoretical value of $-R\ln K_4$, 0.27, would be obtained from the data on the reaction if the final percentage hydrogen were 53.6.

Experiments Nos. 6 and 9 show deviations from the mean which are so much larger than the other deviations that they may be disregarded in taking the average value for $\Delta E_0°$. These poor results were probably due to a disturbance of the balance, either during the

[2] A. Farkas, *Light and Heavy Hydrogen* (Cambridge, 1935), p. 166.

[3] Reference 2, pp. 155, 179.

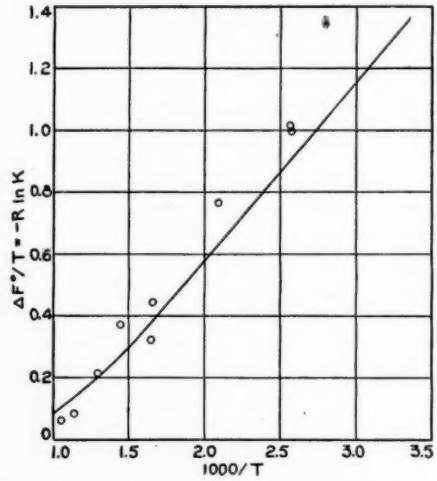

FIG. 2. $H_2+2DCl=D_2+2HCl$. —, theoretical curve; o, experimental points.

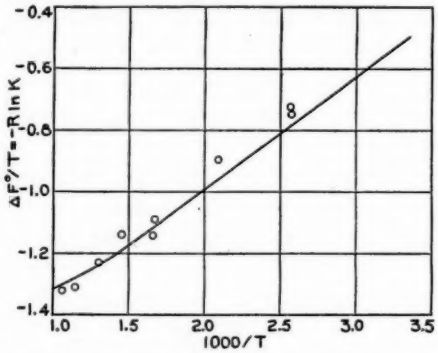

FIG. 3. $H_2+DCl=HD+HCl$. —, theoretical curve; o, experimental points.

process of analysis, or between the measurements on the mixture and the hydrogen standard.

The average values of $\Delta E_0°$, shown in Table I, are higher than the values obtained from band spectra. This might be taken as evidence in favor of Urey and Rittenberg's choice I of the hydrogen constants. However, the authors feel that there may be slight systematic errors in the use of the balance which could account for this discrepancy and too much confidence must not be placed in the accuracy as determined from chance distribution of results.

We are indebted to the Carnegie Institution of Washington for a grant in support of this research, and to Mr. A. I. Rambo for much of the preliminary work in connection with the construction of the balance and apparatus.

JANUARY, 1936 JOURNAL OF CHEMICAL PHYSICS VOLUME 4

The Viscosity of Deuterium Oxide and Its Mixtures with Water at 25°C

GRINNELL JONES AND HOLMES J. FORNWALT, *Mallinckrodt Chemical Laboratory, Harvard University*

(Received October 25, 1935)

The viscosity, η, of 97.6 percent deuterium oxide and six more dilute mixtures with water, as well as that of nearly pure protium oxide, has been determined by comparison with ordinary water, and found to be almost but not quite a linear function of the specific gravity. The relative fluidity, ϕ, has been related to the density by an equation of the type $\phi=1/\eta=1+A(\Delta s)+B(\Delta s)^2$, where (Δs) is the increase in the specific gravity over ordinary water. This equation has been found valid to 0.006 percent over the entire concentration range. Bingham's equation concerning the law of additive fluidities in binary systems, and containing but one arbitrary constant, has been tested and found valid to 0.01 percent.

A SCIENTIFIC problem of great interest and importance is the precise determination of the physical and chemical properties of deuterium oxide and its mixtures with water. Professor Harold C. Urey, who kindly supplied us with liberal amounts of nearly pure deuterium oxide and five other mixtures with water, has made it possible for us to measure the viscosity of these samples. Although the viscosity has been measured before, the viscometric apparatus available in this laboratory should enable us to obtain more precise results than are now extant.

The first measurements on the viscosity of deuterium oxide were made by Selwood and Frost.[1] Lewis and MacDonald,[2] using but a fraction of a cc of liquid, measured the viscosity of 70 and 90 percent samples at various tempera-

[1] P. W. Selwood and A. A. Frost, J. Am. Chem. Soc. **55**, 4335 (1933).

[2] G. N. Lewis and R. T. MacDonald, J. Am. Chem. Soc. **55**, 4730 (1933).

tures. Extrapolating from these values on the assumption that the viscosity-density curve is linear, they estimated the relative viscosity of 100 percent deuterium oxide at 20° to be 1.249, and at 25° to be 1.232. The 20° value did not agree with that previously reported by Selwood and Frost at the same temperature, but it was consistent with the other values on Lewis and MacDonald's viscosity-temperature curve. This suggested that the value of Selwood and Frost was in error. Taylor and Selwood[3] found that the value of Selwood and Frost was vitiated by a calibration error, and have confirmed that of Lewis and MacDonald, for 20°C. Baker and La Mer[4] have measured the viscosity of six mixtures of deuterium oxide, using an instrument having a volume of efflux of 5 cc, and a period of 75 seconds. They have covered the entire concentration range, up to 98 percent, and by extrapolation to 100 percent deuterium oxide estimate the relative viscosity at 25° to be 1.232, which agrees with Lewis and MacDonald.

So far as we know, the viscosity of pure protium oxide has not been measured. Through the kindness of Dr. C. H. Greene and R. J. Voskuyl, we were also able to measure the viscosity of a sample of water from which all or nearly all of the deuterium oxide had been removed by two electrolyses. This sample had a density ($d_{25°}^{25°}$) of 0.99998_2. Greene and Voskuyl will later publish a description of the preparation of this sample and a more precise determination of its density, and further tests as to the amount of deuterium oxide remaining. It seems probable that the deuterium oxide remaining in this sample is so small that its effect on the viscosity would be much less than the limit of error in our viscometric measurements, and therefore the result obtained can be regarded as the viscosity of pure protium oxide.

Experimental

To avoid loss by evaporation or contamination by atmospheric moisture, all samples were transferred from the Pyrex bulbs in which they were received, by distillation in a vacuum line equipped with standard ground glass joints for connecting the pycnometer and viscometer. These joints were mercury-sealed. The pycnometer was furnished with a stopcock, so that the volume could be obtained automatically by closing this stopcock when the contents of the pycnometer were at the proper temperature. A given sample was distilled without ebullition into the pycnometer (capacity 57 cc) by warming the container and chilling the pycnometer sufficiently to effect rapid condensation without freezing the liquid. When filled to a point slightly above the stopcock, distillation was stopped and the pycnometer and contents were allowed to come to the thermostat temperature of 25.00°C. The stopcock was then closed to fix the volume, and the excess liquid was distilled back into the original container, which was then sealed off before the next operation. The pycnometer was detached from the line and weighed. In four calibration runs with water, with the same procedure, the vacuum weights of water contained were 57.2325, 57.2339, 57.2332, 57.2336 g.

After the determination of the density, the filled pycnometer was again attached to the vacuum line and the contents distilled into the viscometer. This operation served to fix the amount of liquid delivered to the viscometer. Any vapors that might have been lost during the pumping out of the line were caught in a trap surrounded by solid carbon dioxide and ether, and this recovered material was also distilled into the viscometer. The viscometer was then removed, placed in the 25° thermostat, and after coming to temperature the viscosity was determined. This was done by the method and apparatus devised by Jones and Talley,[5] and used by them and others in this laboratory for precision measurements on the relative viscosity of electrolytic solutions. Before each run as described above, the viscometer was calibrated with pure, distilled water, using an amount as near as possible to that delivered by the pycnometer. Corrections were applied for any deviation in these volumes. The viscometer, of the Ostwald type and constructed entirely of quartz, had a water time of 533.7 seconds at 25°, an efflux volume of 10 cc, and a working volume of 57 cc.

[3] H. S. Taylor and P. W. Selwood, J. Am. Chem. Soc. **56**, 998 (1934).

[4] W. N. Baker and V. K. La Mer, J. Chem. Phys. **3**, 406 (1935).

[5] Grinnell Jones and S. K. Talley, J. Am. Chem. Soc. **55**, 624, 4124 (1933); Physics **4**, 215 (1933).

TABLE I.

$d_{25°}^{25°}$	d_c/d_0	t_c	t_0	$t_c d_c/t_0 d_0$	K.E.	η obs.
0.99998_2	0.99998_2	539.00	539.01	0.99996	0.00000	0.99996
1.00061	1.00061	533.88	533.50	1.00132	.00000	1.00132
1.02368	1.02371	547.12	533.73	1.04939	.00029	1.04968
1.04591	1.04597	559.46	533.70	1.09647	.00056	1.09703
1.05783	1.05790	566.26	533.99	1.12184	.00071	1.12255
1.07556	1.07565	575.33	533.56	1.15986	.00092	1.16078
1.08903	1.08913	582.23	533.50	1.18860	.00109	1.18969
1.10495	1.10508	590.35	533.63	1.22253	.00127	1.22380
(1.10790)		(extrapolated value)				(1.22996)

RESULTS

The fundamental data are shown in Table I. The column headings have the following significance: $d_{25°}^{25°}$ the relative density in vacuum or the specific gravity; d_c/d_0 the relative density in air based on water at 25° as 1.00000; t_c the average period of flow in seconds for the heavy (or light) water; t_0 the corresponding period of flow for ordinary water; $t_c d_c/t_0 d_0$ the relative viscosity without the kinetic energy correction; K.E. the kinetic energy correction; η the observed relative viscosity. The periods given for heavy water, t_c, and the corresponding values for ordinary water, t_0, are comparable, having been determined on the same day with all conditions maintained as nearly uniform as possible. The exceptionally high value for t_0 for the first experiment listed is due to the use of a larger working volume. The differences in the values of t_0 in successive experiments were due to necessary adjustments in the optical and timing systems.

DISCUSSION

The deuterium oxide-water mixtures whose viscosity we have measured are best defined in terms of the specific gravity in vacuum at 25°C. The specific gravity can be easily determined with precision and, except for the slight vagueness as to the relative proportions of the isotopes of oxygen, characterizes the mixture definitely. This is to be preferred to the use of the mole fraction because the estimation of the mole fraction of deuterium oxide in our mixtures would in any case have to be based on an experimental determination of the specific gravity interpreted with the aid of a formula giving the relationship between the mole fraction and the specific gravity. The best formula available for this purpose at the present time is less reliable and precise than our experimental data. Selwood *et al.*[6] have reported the density ($d_{25°}^{25°}$) of 100 percent deuterium oxide as 1.10790 ± 0.00005. Luten[7] has given a formula relating the mole fraction to the specific gravity, based on the early value of 1.1056 for the density of pure deuterium oxide by G. N. Lewis. La Mer and Baker[8] have revised Luten's equation, using Selwood's value. However, La Mer and Baker did not allow for the 0.02 percent of deuterium oxide present in ordinary water. If their formula is modified to allow for this it becomes,

$$N_{D_2O} = 0.0002 + 9.375\Delta s - 1.03(\Delta s)^2 + 0.2(\Delta s)^3,$$

where N_{D_2O} is the mole fraction of D_2O and $\Delta s = d_{25°}^{25°} - 1$.

The use of specific gravity as a means of identifying any particular deuterium oxide-water mixture is independent of any future revision of the figure chosen for the density of pure deuterium oxide and of the formula expressing the composition as a function of the density.

A plot of the relative viscosity *vs.* the specific gravity showed this relation to be approximately linear, but there appear to be systematic deviations greater than the probable experimental error. Test of linearity by actual computation showed that the curve deviated systematically from a straight line, giving a bow-shaped curve whose maximum deviation from linearity was 8 parts in 10,000 in the 50 percent region. This is at least 8 times the experimental error. These deviations were exaggerated considerably by plotting the relative fluidity *vs.* the specific gravity. A plot of $(\eta - 1)/\Delta s$ *vs.* Δs gave a smooth curve but indicated that the relationship between the viscosity and the density would not be a simple one. However, it was found that a plot of $(\phi - 1)/\Delta s$ *vs.* Δs (where $\phi = 1/\eta$ is the relative fluidity) gave a straight line as is shown by the points in circles in Fig. 1. This proves that the desired relationship is

$$\phi = 1/\eta = 1 + A(\Delta s) + B(\Delta s)^2.$$

The data were fitted to this equation by the method of least squares to determine the best values of the constants A and B. The final equation becomes

$$\phi = 1/\eta = 1 - 2.06855(\Delta s) + 3.1122(\Delta s)^2.$$

This equation is tested in Table II. The average

[6] P. W. Selwood, H. S. Taylor, J. A. Hipple and W. Bleakney, J. Am. Chem. Soc. **57**, 642 (1935).

[7] D. B. Luten, Jr., Phys. Rev. **45**, 161 (1934).

[8] V. K. La Mer and W. N. Baker, J. Am. Chem. Soc. **56**, 2641 (1934).

TABLE II.

N_{D_2O}	Δs	ϕ OBS.	ϕ CALC.	$\Delta\phi \times 10^5$
0.0000	−0.00002	1.00004	1.00004	0
.0059	+ .00061	.99868	.99874	−6
.2216	.02368	.95267	.95276	−9
.4285	.04591	.91155	.91159	−4
.5390	.05783	.89083	.89078	+5
.7028	.07556	.86149	.86146	+3
.8268	.08903	.84056	.84051	+5
.9730	.10495	.81713	.81718	−5
1.0000	(.10790)		(.81304)	

deviation of the calculated from the observed is 0.006 percent.

In a private communication Baker and La Mer have given us the specific gravities of their samples whose viscosity they measured. We find that their data are represented by the above equation to 0.1 percent, which is probably the magnitude of their experimental error. Baker and La Mer's data are shown by the crosses on Fig. 1. This private communication also disclosed a typographical error in their published paper. Their figure for viscosity of the sample having a mole fraction of 0.980 should read 1.226 instead of 1.228 as printed.

The following extrapolated values for pure deuterium oxide at 25°C are obtained from our data, based on 1.10790 as the specific gravity of 100 percent deuterium oxide: relative fluidity $\phi=0.81304$; relative viscosity $\eta=1.22996$; absolute fluidity = 90.987 rhes; absolute viscosity = 1.0992 centipoises, based on water as 0.8937 cp., by Bingham.[9]

APPLICATION TO BINGHAM'S LAW OF ADDITIVE FLUIDITIES IN BINARY MIXTURES

Bingham[10] has proposed the following formula for binary mixtures which give no volume change on mixing or which approach this ideal: $\phi=a\phi_A+b\phi_B-K(a-m)(v_A-v_B)$, where ϕ is the absolute fluidity of a mixture, a and b the volume fractions of the components A and B, ϕ_A and ϕ_B the absolute fluidities, v_A and v_B the specific volumes, and m and n the weight fractions. When the single arbitrary constant K is determined, the fluidity of any mixture may be calculated. In applying this formula to the system: protium oxide-deuterium oxide, the following data were used: protium oxide, $\phi_A=111.91_4$ rhes, $v_A=1.00296$ cc/g, molecular weight = 18.016; for

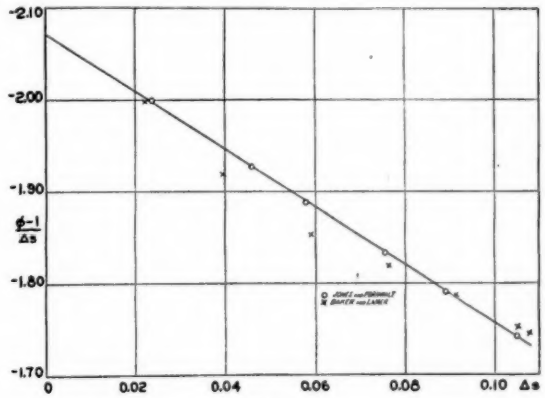

FIG. 1

deuterium oxide, $\phi_B=90.98_7$ rhes, $v_B=0.90526$, mol. wt. = 20.027. The revised Luten equation was used to calculate the mole fractions which in turn were converted to weight and volume fractions. The data were fitted to the Bingham equation by the method of least squares and K was found to be +373.98. If A and B are protium oxide and deuterium oxide, respectively, the equation becomes $\phi=111.914a+90.987b-373.98(a-m)(0.09770)$. Since $a=1-b$ and $m=1-n$, $\phi=111.914+15.611b-36.538n$, where b and n are the volume and weight fractions of deuterium oxide, respectively. Table III shows the test of this equation.

TABLE III.

b	n	ϕ CALC.	ϕ OBS.	% DEV.
0.0000	0.0000	111.914	111.914	0
.0002	.0002	111.910	111.910	0
.0059	.0065	111.769	111.762	−0.006
.2222	.2405	106.596	106.613	+.016
.4293	.4546	102.006	102.012	+.006
.5398	.5652	99.690	99.693	+.003
.7035	.7245	96.424	96.409	−.015
.8273	.8415	94.082	94.067	−.016
.9731	.9757	91.455	91.445	−.011
1.0000	1.0000	90.987	90.987	0

The average deviation of 0.01 percent is very satisfactory in view of average errors as high as 0.7 percent upon the application of this same formula to other binary liquid systems, as illustrated by Bingham. Whether the large deviations observed in the study of other binary systems are due to experimental error or mutual interaction between the components is not clear. However, in this case, there is great chemical similarity between the components and the data are more accurate, so that the Bingham equation describes this system with high precision.

[9] E. C. Bingham, *Fluidity and Plasticity* (McGraw-Hill, 1922), p. 340.
[10] Reference 9, p. 165.

Determination of the Thorium Content of Rocks*

WM. D. URRY,[1] *Massachusetts Institute of Technology*

(Received July 1, 1935)

A new method for the determination of thorium in quantities of the order of 10^{-5} to 10^{-6} g is employed to complete the data necessary for the calculation of the age of geological material. The alpha-particle activity of thoron in a streaming gas is measured with a counter, a procedure which is shown to be superior to the usual ionization measurements on the thoron deposit. Simultaneously, the Pa/Ra ratio in common rocks can be determined.

WHILE the determination of radium in ordinary rocks has received considerable attention,[2] the related problem of thorium determination has been almost neglected.[3] From his valuable treatment of the natural alpha-particles ejected from solids, R. D. Evans has developed a method of measuring the total alpha-particle emission from the surface of solids.[4] By deducting the emission due to the uranium and actinium series, determined by a separate radium measurement, the contribution from the thorium series can be computed and the amount of thorium determined. This differential method has given reliable results with granites. The present interest in the accurate determination of thorium is in connection with the calculation of the age of rocks by the helium method which has been found to yield reliable results with certain types of material. A detailed account of the method has been published elsewhere.[5] To illustrate the necessary determinations, the equation for the age of a rock in terms of He (cc), Ra and Th (grams per gram) is given.

$$\text{Age (in years)} = 1.515\times10^{10}\log_{10}\left[1+\frac{4.518\times10^{-10}\text{He}}{\text{Ra}+9.17\times10^{-8}\text{Th}}\right]. \quad (1)$$

Although the thorium series usually contributes much less to the helium content than the uranium series, the thorium series in certain cases may become the chief contributor with a high Th/U ratio. Methods must be devised so that all the necessary determinations can be made on the same sample even in a small hand specimen.

In all but the most recent rocks the radioactive series have long since reached equilibrium, hence it is possible to measure any member of a given series and calculate the amount of any other member present or substitute the measured member in Eq. (1) by using the appropriate constants. The most convenient member of either the uranium or thorium series to measure is the emanation. Because of the short half-life (54.5 sec.) of thoron a constant streaming method is employed by renewing the ionization chamber with fresh thoron from a solution containing its parent Th X. The thoron disintegration in the chamber may be measured directly, or the thoron active deposit measured after an appropriate streaming time. The latter process employed by most investigators is very inefficient as is shown later. Previous measurements have always been made on the total ionization with some type of electrometer, but an alpha-particle counter of the type used here has certain advantages over the total ionization method especially when applied to a streaming gas. Although the total ionization is affected by the various stopping powers of the carrier gases the alpha-particle count is not and HCl and water vapor absorbers can be dispensed with under certain conditions of operation. The alpha-particle counter can be built to register only alphas, passing by the usual sources of background ionization. Since the volume and hence the surface of the chamber can be much smaller than in ionization measurements the

* This research was supported by a grant from the Penrose Fund of the American Philosophical Society.

[1] Contribution No. 355 from the Research Laboratory of Physical Chemistry.

[2] See Urry, "Determination of the Radium Content of Rocks," following article.

[3] Joly, Phil. Mag. **18**, 146 (1909); Poole, Phil. Mag. **3**, 1246 (1927). Other papers by these authors are mainly results obtained by the method outlined in the above references. Mache and Bamberger, Akad. Wiss. Wien **123** (2A), 325 (1914); Hirschi, Vierteljahrsschrift d. Naturf. (Ges. Zürich) **65**, 545 (1920); Gräven and Kirsch, Akad. d. Wiss. Wien **141** (2A), 8, 521 (1932). This method has been justly criticised by R. D. Evans, Phys. Rev. **45**, 38 (1934).

[4] Evans, Phys. Rev. **45**, 29, 38 (1934).

[5] Urry, Chem. Rev. **13**, 2 (1933).

background alpha-particle count can be greatly reduced. The following consideration is important in the construction of the apparatus.

Fraction of thoron atoms disintegrating in the count chamber

The solution to be measured (reduced to as small a bulk as possible, see E in Fig. 2) contains the parent of the thoron—Th X separated from its parent radiothorium. The volume of the solution is kept constant and its temperature roughly controlled. Let f be the fraction of thoron atoms leaving the solution in a given time. Both rock and standard solutions are kept at approximately the same salt and HCl concentration but this may be varied appreciably without affecting f. Let A_0 be the number of Tn atoms leaving the solution surface, then the number entering the chamber

$$A = A_0 e^{-\lambda_{Tn}\tau} \qquad (2)$$

and the number leaving the chamber

$$A_1 = A_0 e^{-\lambda_{Tn}T} \qquad (3)$$

where τ sec. is the time to reach the chamber from the solution surface and T sec. is the time in the chamber. Then the fraction of Tn atoms disintegrating in the chamber is given by:

$$(A - A_1)/A_0 = e^{-\lambda_{Tn}\tau} \cdot (1 - e^{-\lambda_{Tn}T}) = \alpha. \qquad (4)$$

Fig. 1 gives the curves of this function α against T which is inversely proportional to the rate of streaming for a given apparatus. For each value of τ/T = the ratio of the dead space volume to the volume of the chamber, there is a maximum for α at some given streaming rate which rises

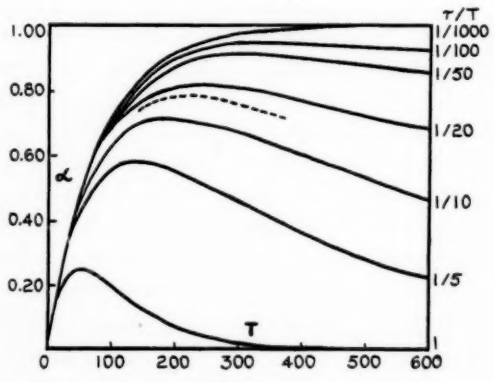

FIG. 1.

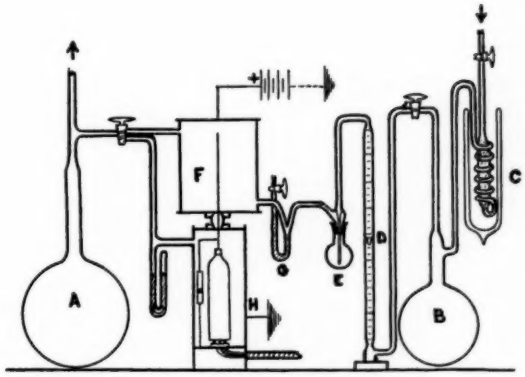

FIG. 2.

with decreasing value of τ/T. Since the count will be $f \cdot \alpha \cdot Q$ where Q is the theoretical count, it is important to construct the apparatus according to these curves and other considerations mentioned later. The dotted curve in Fig. 1 was experimentally determined for a particular apparatus with a solution equivalent to 2×10^{-5} g Th.

APPARATUS

The apparatus is shown in Fig. 2. The Pliotron FP-54 vacuum tube circuit is described by DuBridge.[6] The galvanometer alpha-particle deflections are photographically recorded over a period of several hours (usually about ten) for the measurements and an equal period for the background count. With ion collecting conditions of atmospheric pressure and 45 to 200 volts the deflection is proportional to the original ions produced (collision ionization negligible) and only alpha-particles and rare larger cosmic-ray bursts will be recorded. The large volumes A and B smooth out any streaming fluctuations. The air, drawn from outside the laboratory, passes through a drying train, a spiral and a charcoal immersed in liquid air C, which effectively removes any emanation in the air at even higher velocities than were employed. It then passes through a sensitive rotameter flowmeter, through the solution to be measured in the glass bulb E, whose volume is maintained as small as possible (30 cc), and into the ionization chamber F whence it is pumped away through A. Since the volume above the surface of the solution in

[6] DuBridge, Rev. Sci. Inst. **4**, 532 (1933).

E up to the entrance to F is the determining factor in τ (Eq. (4)) it should be kept as small as possible. The upper quarter of the ground glass joint of the container E is lubricated with P_2O_5 since grease is not permitted because of the large adsorption of the emanations. G is a mercury seal to close off the chamber during background counts. The ionization chamber F is insulated from the evacuated housing H of the FP-54 by a $1\frac{1}{2}$-inch round hard rubber block, coned into the steel base of F and the steel head of H, which carries a grounded brass guard ring, a coned amber plug and the electrode made from the same piece of brass as was the guard ring to avoid battery currents across the amber surface. The housing H is maintained at a pressure of 5 mm or less to prevent ionization by alpha-particle contamination in H. Since alpha-particles having a residual range of 1 cm or less can be detected, a large ionization chamber is unnecessary and the increased surface only tends to increase the background count, but a lower limit is set by the fact that decreasing the volume of F decreases T and hence increases τ/T which is the controlling factor in the constant α. It is inadvisable to increase τ/T much more than $1/20$ and hence the chamber has volume of 600 cc. The present chamber is constructed of steel having regard to Bearden's[7] extensive tests on the contamination of various materials. All inside faces were machined, carefully sand-papered and immediately put together giving a background count of 3–4 alpha-particles per hour per 100 cm², in good agreement with Bearden's result. Brass chambers have also been built giving a somewhat higher count but by coating all the metal surfaces with a thick layer of carbon by direct deposition from a yellow gas flame, the background count could be suppressed to that of steel. Such a coating has the added advantage of protecting the metal from corrosion due to acid vapors from the solution. The chamber parts were machined to fit tight, not soldered, but sealed with beeswax externally. In soldering it was found impossible to prevent a marked increase in the background caused by exposure of traces of solder to the interior.

[7] Bearden, Rev. Sci. Inst. **4**, 271 (1933).

Chemical Procedure

In determining the helium content a carbonate flux containing about 5 g of the original rock is left. This flux is treated as follows:

(1) The rock flux to which barium carbonate was originally added is dissolved in a minimum of warm water to maintain a concentrated solution but not boiled. Under these conditions the radiothorium carbonate is retained in solution.

(2) The carbonate solution is filtered from the residue which is washed with 15 percent Na_2CO_3 solution. The residue contains in particular barium (carrier), Th X, radium and Ac X.

(3) The residue is dissolved in HCl and dried to render the silica insoluble, dilute HCl is again added and the silica filtered off with a thorough washing with dilute HCl and finally hot water. The resulting clear solution is evaporated to convenient bulk maintaining sufficient acidity to prevent precipitation of radium and its isotopes on the walls as sulphate and is ready for measurement.

(4) The silica from (3) is added to the carbonate solution from (2) and dissolved by prolonged boiling. Barium chloride is added and any Ra, Th X or Ac X carbonate filtered off, dissoved in HCl and measured. In all cases so tested no Th X or Ra was found. It is important that the final solutions be free from suspended silica or other material to avoid adsorption of the emanations.

The addition of standard solutions of Th X and Ra to known rock solutions in the initial stages of the chemical work increased the amount of Th and Ra found by the amount of the standard added to within an accuracy of 3 percent. This is additional evidence of no adsorption losses in the chemical processes. After the thorium measurement the solution is transferred to a suitable container and the radon measured in the same solution.

Theoretical

Distribution of the thorium series below Th X at any given time

Suppose the solution to contain X_0 atoms of Th X separated from its parent Ra Th. By applying the equations constituting Case I in Rutherford, Chadwick and Ellis[8] the relative number of Th X, Tn, Th A, Th B, Th C, and Th D (stable) atoms at any given time can be determined. With the very short half-life of Th A (0.145 sec.) the number of Th A atoms will be practically zero except when considering intervals of a fraction of a second. For the same reason the terms in Th A and Tn may be omitted from the equations

[8] Rutherford, Chadwick and Ellis, *Radiations from Radioactive Substances* (The Macmillan Co., New York, 1930), p. 11.

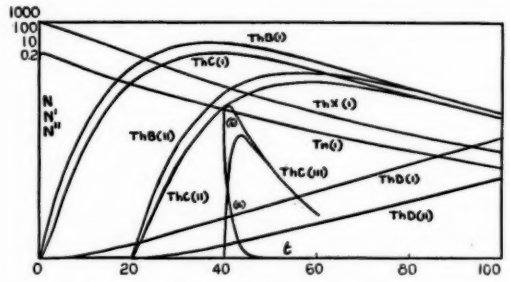

FIG. 3. Ordinate scale: 1000 atoms for Th X and Th D, 100 for Th B, 10 for Th C and 0.2 for Tn. t in hours.

giving $N_{\text{Th B}}$ and $N_{\text{Th C}}$. Using Rutherford's values of λ sec.$^{-1}$ we obtain the following equations (t in sec.):

$$N_{\text{Th X}}=X_0e^{-2.20\times10^{-6}t}, \quad (5)$$

$$N_{\text{Tn}}=X_0 1.732\times10^{-4}(e^{-2.20\times10^{-6}t}-e^{-1.27\times10^{-2}t}), \quad (6)$$

$$N_{\text{Th B}}=X_0 0.1375(e^{-2.20\times10^{-6}t}-e^{-1.82\times10^{-5}t}), \quad (7)$$

$$N_{\text{Th C}}=X_0(0.01324e^{-2.20\times10^{-6}t}-0.1448e^{-1.82\times10^{-5}t}+0.001226e^{-1.91\times10^{-4}t}), \quad (8)$$

$$N_{\text{Th D}}=X_0-(N_{\text{Th X}}+N_{\text{Tn}}+N_{\text{Th B}}+N_{\text{Th C}}). \quad (9)$$

In Fig. 3, curves I show the number of atoms of each member present at any time t after the separation of 1000 atoms of Th X from its parent.

The preparation of the solution for measurement however requires at least five hours after the separation of the Th X from the Ra Th. By substituting $N_{\text{Th X}}$ for the moment of commencing streaming, for example at $t=20$ hours, in place of $X_0=1000$ in Eqs. (7), (8) and (9) we obtain curves II, Fig. 3, for $N'_{\text{Th B}}$, $N'_{\text{Th C}}$ and $N'_{\text{Th D}}$ accumulating in the chamber. These equations need not be given but will be referred to as Eqs. (7a), (8a) and (9a).

Theoretical alpha-particle count

The alpha-rayers in the chamber will be Tn, Th A, and Th C or Th C'. Whether the disintegration proceeds via Th C' or Th C'' is immaterial on account of the very short half-life of Th C' (*ca.* 10^{-11} sec.). Let a be the fraction of Th A atoms disintegrating before reaching the electrode, then the number of alpha-particles from the thoron and Th A disintegrating in the gas space will be

$$\lambda_{\text{Tn}}N_{\text{Tn}}(1+a). \quad (10)$$

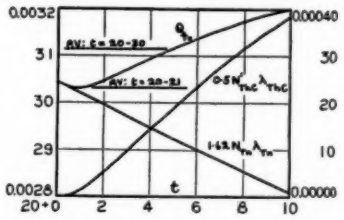

FIG. 4. Ordinate scale in alpha-particles per sec. per 1000 atoms of Th X at $t=0$; left, Q_{Tn} and $1.62\,N_{\text{Tn}}\lambda_{\text{Tn}}$; right, $0.5\,N'_{\text{Th C}}\lambda_{\text{Th C}}$. t in hours.

Of the fraction $(1-a)$ Th A atoms reaching the electrode,[9] one-half disintegrate inwards and are lost as counts. Hence the total alpha-count from thoron and Th A is given by

$$\lambda_{\text{Tn}}N_{\text{Tn}}[1+a+(1-a)/2]=\lambda_{\text{Tn}}N_{\text{Tn}}(3+a)/2. \quad (11)$$

The fraction $(1-a)$ Th A atoms reaching the electrode disintegrate through the beta-rayer Th B[10] to $(1-a)$ $N'_{\text{Th C}}$ atoms. Of the fraction a all the resulting Th B atoms will be collected. Since half the alphas are again lost in the electrode, the contribution from Th C (or Th C') is given by

$$\lambda_{\text{Th C}}N_{\text{Th C}}\tfrac{1}{2}[a+(1-a)]=0.50\lambda_{\text{Th C}}N'_{\text{Th C}}. \quad (12)$$

The sum of (11) and (12) gives the total theoretical count Q_{Tn} alpha-particles per sec.

$$=1.62\lambda_{\text{Tn}}N_{\text{Tn}}+0.50\lambda_{\text{Th C}}N'_{\text{Th C}}. \quad (13)$$

In Fig. 4 the terms in (13) have been separately plotted for the case of starting streaming at $t=20$ hr. and a 10-hour period of streaming to $t=30$ hr. The alpha-particle emission from the Th C is at first barely sufficient to balance the decay of the supply of thoron and Th A, namely, the Th X, but after two hours the accumulation of the Th C and the consequent Th C alpha-emission is more than sufficient to balance the decay. The average value of Q_{Tn} for $t=20$–21st hr. is 0.9756 times the

[9] The calculation of the fraction reaching the electrode $(1-a)$ is given by Evans, Rev. Sci. Inst. **6**, 99 (1935), and has the value 0.76 for the particular chamber and conditions. Under the same conditions this fraction for Th B and Th C = 1 and recoils from the electrode will be recaptured. The mobility of these atoms is of the order of 1000 times the linear streaming velocity and hence there is no loss from the chamber.

[10] Recoils of Th B or Th C atoms into the electrode will lengthen the path within the electrode of the alpha-particle later ejected but insufficiently to prevent a count. This effect must be considered, however, in total ionization measurements.

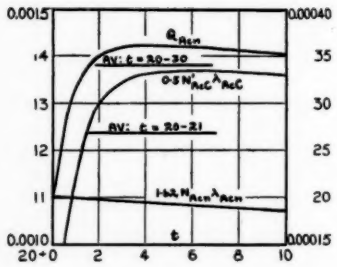

FIG. 5. Ordinate scale in alpha-particles per sec. per 1000 atoms of Ac X at $t=0$; left, Q_{Acn} and $1.62\ N_{Acn}\lambda_{Acn}$; right, $0.5\ N'_{Ac\ c}\lambda_{Ac\ c}$. t in hours.

average of the ten hourly recordings. This factor is independent of the time of commencing streaming and dependent only on the duration of the streaming. In practice the mean of the n hourly consecutive recordings is reduced to the mean for the first hour of streaming with the appropriate factor. The same functions for actinon and Ac C are given in Fig. 5. The mean of ten hourly consecutive runs is here 10.9 percent greater than for the first hour owing to the shorter half-life of Ac B (36 min.).

Thoron deposit

In measurements of the thoron deposit the procedure is to aspirate for about 20 hours, cut off the streaming, and measure the activity of the Th B and Th C or in the case of counting that of Th C. Curve III, Fig. 3, shows the number of Th C atoms $N''_{Th\ C}$ present at any time after streaming from $t=20$ to 40 hours and then cutting off the thoron supply to the chamber. It is the sum of the decay curve (a) for the Th C already present and the build-up curve (b) of the Th C from the Th B present at the moment of cutting off. The measured activity is decaying with the half-life of Th B (10.6 hr.) instead of Th X (3.64 days) and it is difficult to obtain a sufficient number of recordings to reduce the statistical error to a reasonable quantity. The relative efficiency of this method compared to the direct measurement of the thoron is quite low. For a comparison of collecting the deposit from $t=20$–40 hr. with a direct measurement on the thoron at $t=20$ hr., the relative efficiency is given by $(0.50\lambda_{Th\ C}N''_{Th\ C\ 40})/(1.62\lambda_{Tn}N_{Tn\ 20})$, equals 0.205 and requires twenty hours longer. If streaming is continued to $t=60$ hr. to reach peak Th C this rises only to 0.235, the maximum relative efficiency independent of the time of commencing streaming.

The presence of actinon

The solution contains in addition to Th X, the isotopes Ra and Ac X. It is required to determine the contribution of the resulting radon and actinon to the chamber count. $Z=f\cdot\alpha\cdot Q$ where Z is the count per sec. due to given emanation and the other symbols have the significance previously given. The fraction f can be taken the same for all three isotopes Acn, Tn and Rn (masses 219, 220 and 222). $\alpha_{Rn}=4.2\times10^{-4}$ and $\alpha_{Acn}=0.094$ from Eq. (4) for the same experimental conditions as in the routine thoron measurements where $\alpha_{Tn}=0.78$. If we take as an example a rock analysis: $Ra=2\times10^{-13}$ g per g ($U=5.88\times10^{-7}$ g per g.) $Th=1.5\times10^{-6}$ g per g and hence $Th/U=2.55$; assuming von Grosse's value for the half-life of protactinium and the isotope theory of the origin of the actinium series[11] the ratio of Pa to Ra should be the same in all rocks at the present geological time, namely, 0.8 g Pa to 1 g Ra, hence $Pa=1.6\times10^{-13}$ g per g. From these figures the number of Ra, Th X and Ac X atoms in the solution can be computed. With the small value of α_{Rn} and the long half-life of radon compared to thoron and actinon, the radon contribution is negligible for the Th/U ratio in rocks. Table I shows the method of determining the correction for actinon. From Eqs. (5), (6), (8a) and (13) and the analogous expressions for the actinium series (see Fig. 5) the theoretical counts Q_{Tn} and Q_{Acn} are calculated and an average for the period in question determined (column 3). For this particular example column 6 shows that at $t=20$–21st hour, 0.0219 of the total count is due to actinon and its products. In practice this correction factor must be computed after the Ra determination since the Pa is a function of the Ra. The half-lives of Th X (3.64 days) and Ac X (11.2 days) differ appreciably; the fraction due to actinon, etc., at time 240–241 hours is therefore considerably different (column 8), and the correction will depend upon the time of commencing streaming. This difference in ratio with time makes it possible, from two counts, one shortly after separation, the second ten to eleven days later,

[11] A. V. Grosse, Phys. Rev. **42**, 565 (1932).

TABLE I.

CONTENT PER g ROCK	ATOMS AT $t=0$	Q, α-PARTICLES PER SEC. FOR $t=20$–21ST HR.	α	COUNT Z PER SEC. $Z=f\cdot\alpha\cdot Q$	$\frac{Z_{Acn}}{Z_{Tn}}$	Z FOR $t=240$–241ST HR.	$\frac{Z_{Acn}}{Z_{Tn}}$
Th $1.5\times10^{-6}\cdot$g	Th X 2354	0.007144	0.78	0.00557f	0.0219	0.00097f	0.071
Pa $1.6\times10^{-13}\cdot$g	Ac X 1049	0.001299	0.094	0.00012f		0.00007f	
	Th X 2354	0.007144	0.90	0.00643f	0.1414	0.00113f	0.458
	Ac X 1049	0.001299	0.70	0.00091f		0.00052f	

to compute separate values of Q_{Tn} and Q_{Acn} and so find Pa and Th separately with no assumptions as to the Pa/Ra ratio. With the above values of α the apparatus is arranged to favor the thoron to cut down the correction which is one of the considerations in not making τ/T too small. By reducing the dead space volume so that τ/T is 1/100 and maintaining the same streaming velocity, values of α in the lower half of Table I are obtained and the ratio Z_{Acn}/Z_{Tn} rises as shown. It is important in verifying the isotope theory of the origin of the actinium series, based at present on a few Pa/Ra ratios in radioactive minerals, to determine the Pa/Ra ratio in rocks. The procedure is therefore outlined in the following equations. Let Z' be the average count (less the background) at time t' and Z'' at time t''. Then

$$Z'=\bar{Z}'_{Tn}+\bar{Z}'_{Acn} \tag{14}$$

and

$$Z''=\bar{Z}''_{Tn}+\bar{Z}''_{Acn}, \tag{15}$$

where $\bar{Z}'_{Tn}$ is the mean of the hourly readings for Tn and its products at time t' and $\bar{Z}''_{Tn}$ at time t''. $\bar{Z}'_{Acn}$ etc., the same for Acn and its products. In addition

$$\bar{Z}''_{Tn}=K_{Tn}\bar{Z}'_{Tn} \tag{16}$$

and

$$\bar{Z}''_{Acn}=K_{Acn}\bar{Z}'_{Acn}, \tag{17}$$

where

$$K_{Tn}=e^{\lambda_{ThX}(t'-t'')} \quad \text{and} \quad K_{Acn}=e^{\lambda_{AcX}(t'-t'')}.$$

The solution of Eqs. (14) to (17) is given by

$$\bar{Z}'_{Tn}=(K_{Acn}Z'-Z'')/(K_{Acn}-K_{Tn}) \tag{18}$$

and

$$\bar{Z}'_{Acn}=(Z''-K_{Tn}Z')/(K_{Acn}-K_{Tn}). \tag{19}$$

These means of n hourly recordings are now corrected to the mean at the first hour of streaming:

$$Z'_{Tn}=k_{Tn}\bar{Z}'_{Tn} \tag{20}$$

and

$$Z'_{Acn}=k_{Acn}\bar{Z}'_{Acn}, \tag{21}$$

where $k_{Tn}=0.9756$ and $k_{Acn}=0.891$ for $n=10$ (see Figs. 4 and 5). Then $Z'_{Tn}=\alpha_{Tn}\cdot f\cdot Q'_{Tn}$ and $Z'_{Acn}=\alpha_{Acn}\cdot f\cdot Q'_{Acn}$ and the amounts of Th X and Ac X at time $t=0$ or the corresponding equilibrium amounts of any other member of each series, e.g., Th and Pa, can be computed from Q'_{Tn} and Q'_{Acn} as shown below. The radium determination which always follows gives the Pa/Ra ratio.

STANDARDIZATION

From the relation $Z=f\cdot\alpha\cdot Q$, the factor $f\cdot\alpha$ for the apparatus described was determined with several solutions of Th X of known strengths, prepared in an analogous manner to the unknown solutions from a carefully analyzed 3.4 percent Th monazite and a 42.8 percent Th thorite, and ranging from thorium equivalents of 2 to 30×10^{-6} g. The calibrations from the two sources being in good agreement it is assumed that radioactive equilibrium has been established in these geological specimens. $f\cdot\alpha$ was found to be 0.42 independent of Th concentration. α having the value 0.78 from Eq. (4), by knowing the volumetric distribution of the apparatus and the streaming rate (maintained constant at the value giving the maximum of the function α), $f=0.54$ at the room temperature 20°C.

Computation of Th in unknown solutions

Z is the mean of n hourly recordings, corrected for background count, reduced to the mean for the first hour of streaming, corrected for the

presence of actinon, and expressed in alpha-particles per sec. The average value of Q_{Tn} for the first hour of streaming from $Z=f\cdot\alpha\cdot Q_{Tn}$ equals the true value at some given time after commencing streaming independent of when this began (1290 sec. for the present chamber and conditions). With the value of Q_{Tn} so obtained, Eqs. (5) and (6) where t=time elapsed since separation of the Th X from Ra Th, Eq. (8a) where $t=1290$ sec. and Eq. (13) are solved for X_0 which is converted by the radioactive equilibrium law into the number of atoms of thorium and hence the weight present in the original specimen. A graphical solution usually suffices. For two chosen values of the Th concentration, values of Z for $t=0$–1st hour after separation from the Ra Th are obtained by the converse of the above procedure and Z plotted against Th concentration. The relation is linear since $f\cdot\alpha$ is independent of the concentration. Z for the unknown solution is reduced to $t=0$–1st hour by the factor $N_{Th\ X_0}/N_{Th\ X_t}=e^{\lambda_{Th\ X}t}$ where t is the time elapsed since separation of the Th X to the commencement of streaming, and the concentration read off from the plot. A similar procedure is adopted for the determination of protactinium from Q_{Acn}.

Probable Error

The nature of statistical fluctuations in counting experiments has been dealt with in detail by Evans and Neher.[12] The probable error of a single observation is given by

$$r=\pm 0.67(2x+y)^{\frac{1}{2}} \qquad (22)$$

where x is the background count per hour and $y=3600Z$. When $x=18$ the observational limit given by Evans and Neher's Eq. (9) is found to be 2.9 alphas per hour. For the mean of ten hourly intervals the probable error varies from 49 percent for a count of 3 to 2 percent for a count of 160 per hour. The count due to Th A is directly controlled by the thoron and hence is not an independent random process. As a first approximation the value of y may be taken to be

$$\frac{3600Z(\lambda_{Tn}N_{Tn}+0.50\lambda_{Th\ C}N'_{Th\ C})}{(1.62\lambda_{Tn}N_{Tn}+0.50\lambda_{Th\ C}N'_{Th\ C})}. \qquad (23)$$

The bracketed portion of the numerator is the theoretical count were there no alphas from Th A. Since the mean background x remains reasonably constant, a family of curves is drawn plotting the probable error expressed as a percentage against y for values of n (number of observational intervals) from 3 to 12 hours. Having determined y from Eq. (23) the probable error is read off the appropriate curve.

The results of a long series of thorium measurements on rocks, with the helium and radium contents necessary to calculate ages are given in *Determination of the Radium Content of Rocks*.[2]

I wish to express my thanks to the American Philosophical Society for their generous support of this research.

[12] Evans and Neher, Phys. Rev. **45**, 144 (1934).

JANUARY, 1936 JOURNAL OF CHEMICAL PHYSICS VOLUME 4

Determination of the Radium Content of Rocks*

Wm. D. Urry,[1] *Massachusetts Institute of Technology*
(Received July 1, 1935)

The determination of the age of common rocks by the "helium method" necessitates accurate measurements of the radium content. The method of compensating the background by the use of two opposed ionization chambers is applied to radium determinations and the apparatus has an observational limit of $5.5\times10^{-14}\times n^{-\frac{1}{2}}$ g radium for n hourly readings. With the thorium content determined as in the preceding article a summary of results for a suite of rocks from a single horizon and the present status of a geological time scale is given.

* This research was supported by a grant from the Penrose Fund of the American Philosophical Society.

[1] Contribution No. 356 from the Research Laboratory of Physical Chemistry.

THE measurement of the radium content of certain naturally occurring material like the iron meteorites and even the accurate determination of this quantity in some basic rocks falls beyond the scope of the ordinary single ionization chamber system. The difficulty lies in the fact that the very small ionization due to the radon is superimposed on a much larger background. The work of G. Halledauer[2] constitutes a step forward in these measurements in that variations in the background with time were canceled out with a second ionization chamber. After a certain charging interval the charge from each chamber, one containing the radon, the other only the background gas, was shared in turn with an electrometer the difference being the charge due to the ionization by the radon. Paneth and Koeck[3] have considerably improved the technique of this method but the practical difficulties of maintaining constant capacity in a charge sharing system are well known. In cosmic-ray work the subtracting of the background from the background plus the effect to be measured has for some time been conducted automatically by connecting the electrodes of two identical equal and oppositely charged chambers permanently to an electrometer. Such a system has been described by Steinke[4] and Schindler,[5] was personally suggested by Steinke to Paneth for radon measurements and is now in operation in Königsberg, Germany[6] and at this Institute. At the same time the adoption of this differential system to the measurement of radon has been developed independently at the California Institute of Technology by Evans.[7] The advantages of the system are in the elimination of errors due to variations in the background exterior to the chambers, battery variations and contact potentials and particularly in the added accuracy of the differential reading insofar as this can now be spread over a larger scale. The one disadvantage is that the statistical variation is $\sqrt{2}$ times that for the single chamber as Schindler[5] and Evans[8] have noted. However, the same statistical error is obtained by increasing the number of observations to $2n-1$, where n is the number of observations on a single chamber and with automatic registration this is easily accomplished.

The Apparatus

The apparatus is shown schematically in Fig. 1. The two chambers A and B are constructed identically, having a volume of 2500 cc. The chambers are grounded and the collecting voltage applied to a net placed at a distance of 0.6 cm from the walls and made of 40-mesh copper gauze. One end of each of the copper chambers is sealed with a steel block and lead washer in such a way that no lead is exposed to the chamber. The $\frac{1}{8}$-inch brass electrode leads are coned into amber plugs in turn coned into brass guard rings (made of the same brass stock as the electrodes) which are packed into the steel heads. Similar leads without guard rings are provided for the collecting voltage to the nets. Two packed leads to each chamber provide pumping and filling facilities. The chamber nets are charged to + and −200 volts with regard to the center ground tap on a potentiometer across a center 6-volt storage battery. This variable center tap is adjusted as described by Schindler[5] until $E_A C_A = -E_B C_B$ whereupon battery fluctuations should show no effect on the electrometer. In the head of the 2-inch diameter lead casing is arranged a small ring condenser C. A remote control switch allows a platinum to platinum contact directly with the electrometer lead whereby charges of either sign can be applied to the electrodes and electrometer, or the same grounded. Two potentiometers supply voltages to the remote control switch and the ring condenser C. These voltages can be accurately read by throw-over switches to a Leeds and Northrup potentiometer. The electrode lead casing and shielding to the electrometer is hermetically sealed and any water vapor removed with a P_2O_5 drying tube. The Compton electrometer E (sputtered quartz fiber suspension) is operated for

[2] G. Halledauer, Ber. Wien Akad. **134**, 39 (1925).
[3] F. Paneth and W. Koeck, Zeits. f. physik. Chemie, Bodenstein-Festband, 145 (1931).
[4] E. Steinke, Physik. Zeits. **31**, 1019 (1930).
[5] H. Schindler, Zeits. f. Physik **72**, 625 (1931).
[6] Publication deferred. I am indebted to Professor F. Paneth for his kind assent to the portion of this article relating to the electrical apparatus.
[7] R. D. Evans, Phys. Rev. **39**, 1014 (1932), Rev. Sci. Inst. **6**, 99 (1935).
[8] R. D. Evans, Phys. Rev. **45**, 144 (1934).

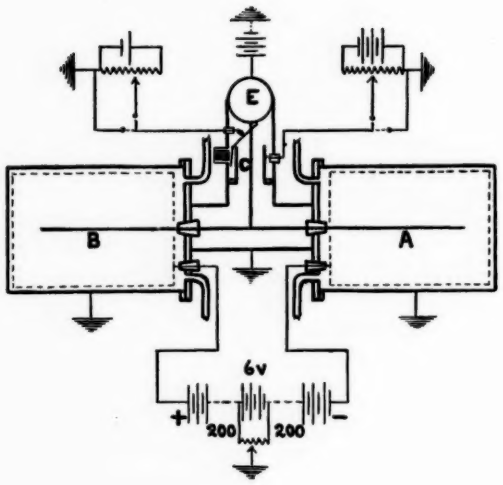

FIG. 1.

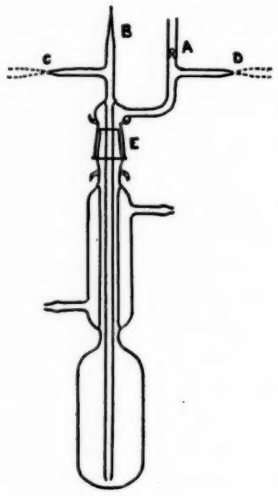

FIG. 2.

visual observations at a sensitivity of about 2500 mm per volt at 1 meter distance.

Fig. 2 shows the flask used for storing the solution[9] containing the radium. The flask is of 150 cc capacity fitted with a condenser for use when boiling and passing air through the solution to remove the emanation. With the magnetic break seal *A* and the tip *B* sealed the solution is deemanated through *C* and *D* which are then sealed off. The ground glass joint *E* is lubricated over the upper quarter with P_2O_5. This design of storage flask avoids any possible adsorption of radon by grease. The period of storing from the time of sealing off *C* and *D* to the time of introduction into the chamber gives the fraction of the equilibrium amount of radon generated, accurately known from the tables of Meyer and Schweidler.[10] In most cases sufficient radon has accumulated in fifteen to twenty days (0.934–0.973).

Likewise the introduction train shown in Fig. 3 is designed to avoid all contact with possible adsorbers of emanation. The spiral and charcoal *A* immersed in liquid air removes the emanation from the background gas—air—drawn through a drying train from outside the laboratory. The air passes through a sulphuric acid trap *B* as a flow indicator. Connection to the vacuum pump or air supply is made through stopcock *C*. This vacuum connection serves to pump out the connecting lines only. Stopcock *D* splits the air line to the solution flask and the line *E*. Stopcock *F* further splits the line *E* to the compensating chamber and the flush lead through the stopcock *G*. The two manometer columns *H* and *K* indicate the pressure in the chambers and are used to balance this pressure at a few mm below atmospheric pressure. The storage flask *L* when ready for measurement is connected at *M* with rubber pressure tubing and sealed to the line at *N* with the magnetic break system installed. The only stopcock *O* (necessary to control the streaming rate) in the emanation train is lubricated with P_2O_5. To *O* is sealed a soda-lime tube *P*, to absorb most of the HCl gas, which is then connected to the first mercury valve 1. To this is sealed the saturated NaOH bubbler *Q*, completing the HCl absorption. To *Q* is connected the mercury valves 2 and 3 with a common lead to the $CaCl_2-P_2O_5$ drying tube *R*. The leads to the emanation and compensating chamber pass through the mercury backstops *S* and *T*. The portion of the train through which the emanation passes is thus seen to be free from any organic adsorbing matter. The adsorption of emanation in the various chemicals used has been shown to be negligible. After considerable use the NaOH solution showed only a very slight trace of chloride and has been left out in the

[9] See Urry, "Determination of the Thorium Content of Rocks," preceding article, for the preparation of the solution.

[10] St. Meyer and E. v. Schweidler, *Radioactivität*, second edition (Teubner, Leipzig, 1927).

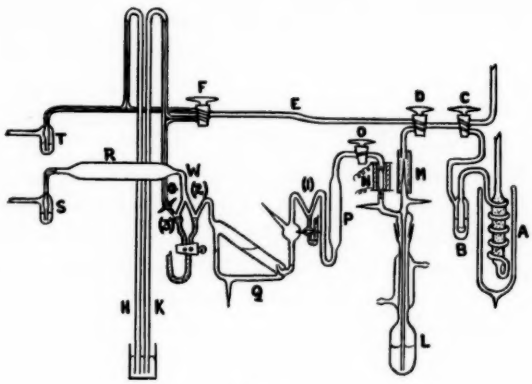

FIG. 3.

later work. It is significant that the standardization remained the same.

OPERATION

A is immersed in liquid air for one hour. The air lines as far as *F* and *M* are evacuated through *C* and filled with emanation-free air. With 0, 1, 2, 3 and *G* open the chamber and line as far as the magnetic break bulb is evacuated through the emanation-chamber pump lead. *G* is then closed and 3 run up to prevent contact of the emanation with the greased stopcock *G*. The pump lead to the chamber and *O* are closed. The magnetic break-off is brought into action, *O* carefully opened to start the air out of *L* into the train and the tip *B* (Fig. 2) broken off inside *M*. *C* is opened to *D* in turn opened to *M*, and the solution brought to a temperature slightly below boiling and maintained there. The introduction time of the radon into the chamber is taken as fifteen minutes after starting streaming. When the pressure in the chamber reaches about 73 cm *D* and *O* are closed and 2 run up. 3 is lowered and the train from *W* on flushed through line *E* and stopcocks *F* and *G* until the manometer *K* is nearly level with the mercury in the reservoir. The valve 1 serves to prevent back diffusion of water vapor from *Q* to *P* while not in use. The compensating chamber is then filled through the line *E* and the stopcock *F*, until the same pressure in the two chambers is indicated by *H* and *K*. Electrometer readings are commenced immediately after the filling process in order to follow the build-up curve of the decay products in the chamber. This affords a check on the presence of spurious ionization by a comparison of the build-up curve with the theoretical.

ELECTRICAL MEASUREMENTS

With the circuit given in Fig. 1 three methods of measurement, all of which have here been employed, are possible.

(1) Measurement of the rate of charge starting from the electrical null point.

(2) Measurement of the rate of charge starting from a predetermined charge on the electrometer system imparted through the remote control switch such that the time of drift in a given observation interval is approximately equal on either side of the null point. Leakage errors if constant with regard to corresponding points on either side of the null point should then cancel out.

(3) Compensation of the charge on the electrometer system by application of a potential to the ring condenser *C* with the electrometer as a null instrument. The electrical symmetry of the system permits this method of operation whereas in the single chamber induced effects will make the standardization doubtful. By this method the apparatus is calibrated in terms of volts applied to *C* per unit of radon or radium. Since the capacity of the system remains constant and the electrometer calibration does not enter, this method is the most direct, but does not lend itself readily to automatic control.

The correspondence of all three methods (observations by each method over many intervals) within 2 percent and random with respect to sign is indicative of the very low losses and absence of spurious effects with this type of electrometer when guard rings of exactly the same material or plating are used at all insulated leads and a thoroughly dry system is maintained. Consequently methods 1 and 2 have been mostly employed in the routine work, 2 more particularly when the observational interval is long.

Electrical capacity of the system

The apparatus has been calibrated with standard solutions of radium but a rough check is afforded by the Duane and Laborde[11] equation. This requires a knowledge of the electrometer system capacity to convert e.s. units of current into electrometer volts per hour. The capacity of the ring condenser *C* was determined by Steinke's[12] method to be 0.61 cm. On setting up

[11] Reference 10, p. 305.
[12] E. Steinke, Zeits. f. Physik **48**, 650 (1928).

the capacity relations for the circuit given in Fig. 1 it is found that, by maintaining all other values constant

$$dV_e/dV_r = -c_r/C_e, \qquad (1)$$

where the subscripts e and r refer respectively to the electrometer system and the ring condenser and C_e is the total capacity of the electrometer, leads and electrodes. The capacity of the electrometer system at zero deflection was determined from Eq. (1). With a series of voltages applied to the electrometer system, the voltage that must be applied to the ring condenser to return the electrometer to zero in each case was determined. The average value of C_{e0} (zero deflection) was found to be 34.8 ± 0.3 cm. The change of capacity with deflection was determined by finding the value of dV_e for a given deflection and of dV_r for the same deflection. The capacity varied from $C_{e0} = 34.8$ cm to 32.5 cm for a deflection of 150 mm nearly linearly. In practice the electrometer is calibrated after each observational interval over the same deflection as was obtained in that interval. The length of the observational interval varies from 15 minutes to two hours according to the amount of radon present and the required accuracy of the determination. Observations last over at least nine intervals.

Standardization

From the equation of Duane and Laborde, the saturation current per 10^{-13} curie of radon in equilibrium with its decay products to Ra C′ is found to be 4.72×10^{-7} e.s.u. From the average volumetric field intensity (16.3 volts/cm for a collecting voltage of 200 v in the chambers used) the ionization saturation parallel to the field is given by Moulin[13] as 76 percent and perpendicular to the field as 88 percent, averaging 82 percent. Assuming a uniform volumetric distribution of the ions, 16 percent are captured between the net and the wall leaving 84 percent collected within the net (total volume of the chamber 2494 cc, volume inside the net 2113 cc). The saturation current is therefore $0.82 \times 0.84 \times 4.72 \times 10^{-7} = 3.23 \times 10^{-7}$ e.s.u per 10^{-13} gram radium. With the value of the capacity C_{e0} previously given this corresponds to 0.010 v per hour per 10^{-13} gram $\mathrm{Ra} = K$. Values of K from standard radium solutions[14] varying in strength from 2 to 62.6×10^{-13} gram radium were found as follows: 0.009506, 0.009441, 0.009447, 0.009406 mean 0.00945 v per hour. A comparison of the calibrations with standards and the Duane and Laborde formula agrees with the work of other authors on similar chambers in the direction and approximate difference found. The value of K as found from the standard solutions has been taken as the calibration. The radium content of an unknown solution is found as follows: Let m be the deflection (mm), less the net background difference in the two chambers if any, in a given observational interval reduced to an hour unit of time and s the sensitivity of the electrometer in volts per mm. If

$$U = \frac{\text{radon generated in the storing period}}{\text{equilibrium radon}}$$

(from the duration of the storing period and the aforementioned tables), and

$$u = \frac{\text{radon in the chamber during the observational interval}}{\text{radon at the time of introduction into the chamber}}$$

(from the same tables) then the charge rate reduced to equilibrium amount of radon and zero time of the radon in the chamber is given by ms/Uu. The readings used are those for $t > 3$ hours to allow the establishment of equilibrium with the decay products. The n observations reduced in like manner to this standard state can now be averaged. If W is the weight of the original rock sample and R the radium per gram in units of 10^{-13} gram

$$R = \left[\frac{ms}{Uu}\right]_{\text{Av.}} \times \frac{1}{WK}. \qquad (2)$$

Any difference in the background ionization between the two chambers is determined by averaging a like number of observational intervals after removing the radon and refilling with emanation free air, allowing sufficient time for

[13] Moulin, Ann. chim. phys. **21**, 550 (1910); **22**, 26 (1911).

[14] The standard stock radium solution was kindly supplied by S. C. Lind and was diluted from the main stock used for a radium-uranium ratio determination. See Lind and Roberts, J. Am. Chem. Soc. **42**, 1170 (1920). A correction for the decay of radium since the date of standardization following the preparation (1919) has been applied.

the radon decay products to disintegrate. The average background difference is nearly always negligible corresponding to <0.003 v per hour and may be of either sign showing that it is due to the statistical fluctuation residual since $n \neq \infty$. The individual background observations, however, are quite readable and enable an analysis of the background ionization to be made. The computation in the case of the null method is similar, substituting in Eq. (2) V_r, the voltage applied to the ring condenser to maintain zero charge on the electrometer system less any background difference, in place of ms, and K_r the calibration in ring condenser volts for K. The ionization in the 2-cc quadrant box of the electrometer even assuming as high a value as 12 ions per cc per sec. contributes a negligible charge to the quadrants connected to the electrodes.

The Probable Error

Let x_1 be the number of contamination alpha-particles per hour in the one chamber of specific effect, a electrometer volts per particle and y_1 the number of betas, gammas and cosmics per hour of specific effect b in the same units. (The last three sources of ionization are grouped together since the contribution to the fluctuations is found to be negligible compared with that due to the alpha-particles and the specific effect of each source is not greatly different.) Let the subscript $_2$ refer to the second chamber and $_3$ to the radon measurement. If E is the electrometer reading in v per hour,

$$E_1 = ax_1 + by_1 \tag{3}$$

and

$$E_2 = ax_2 + by_2 \tag{4}$$

and

$$E_1 - E_2 = (ax_1 + by_1) - (ax_2 + by_2). \tag{5}$$

From measurements on each chamber in turn it is found that $E_1 = E_2$ and on the reasonable assumption that $y_1 = y_2$ we have

$$E = E_1 = E_2 = ax_1 + by_1 \tag{6}$$

and hence

$$E_1 - E_2 = (ax_1 + by_1) - (ax_1 + by_1). \tag{7}$$

The nature of statistical fluctuations has been treated in full by Evans.[15] From Evans' Eq. (4) the Gaussian mean deviation D_B for the background $E_1 - E_2$ in Eq. (7) is given by

$$D_B^2 = 2a^2x_1 + 2b^2y_1. \tag{8}$$

Now the actual quantity measured is given by

$$E_3 + (E_1 - E_2) = ax_3 + by_3 + (ax_1 + by_1) - (ax_1 + by_1) \tag{9}$$

and the mean Gaussian deviation of this sum of effects D_S is given by

$$D_S^2 = 2a^2x_1 + a^2x_3 + 2b^2y_1 + b^2y_3. \tag{10}$$

To derive E_3 Eq. (7) is subtracted from Eq. (9) and by neglecting b^2 terms compared with a^2, since the specific effect of the alpha-particle greatly exceeds that of the other sources of ionization, by the principle of propagation of errors the mean deviation of E_3 is given by the sum of (8) and (10):

$$D^2_{S-B} = 4a^2x_1 + a^2x_3. \tag{11}$$

Now $4a^2x_1 = 2D_B^2$ from Eq. (8) by neglecting b^2 terms and since $r = 0.6745D$ (Evans' Eq. (7) where r is the probable error of a single observation)

$$r_{S-B} = 0.6745[(2D_B^2 + a^2x_3)/n - 1]^{\frac{1}{2}} \tag{12}$$

for n observations. D_B has the value 8.08×10^{-3} v per hour (1-hour intervals) from the residuals of over 300 observations on the background difference from the relation

$$0.6745D_B = r_B = 0.6745[\Sigma v_B^2/(n-1)]^{\frac{1}{2}} \tag{13}$$

where v is the observed variation from the arithmetic average. a having the value 5.25×10^{-4} volt per alpha-particle with due regard to the ionization saturation, Eq. (12) reduces to

$$r_{S-B} = 0.6745\left[\frac{1.306 \times 10^{-4} + 5.25 \times 10^{-4} ax_3}{n-1}\right]^{\frac{1}{2}} \tag{14}$$

for 1-hour intervals and the probable error is calculated by substituting the average value of ms/Uu from n observations for ax_3. The value of D_B appropriate to the observational interval in use must be substituted for intervals other than one hour. One point of practical importance

[15] R. D. Evans, Phys. Rev. **45**, 144 (1934).

TABLE I. *Ages of the Keweenawan trap rocks.*

Sp. No.	Location	He $\times 10^5$ (cc/g)	Ra $\times 10^{13}$ (g/g)	U $\times 10^7$ (g/g)	Th $\times 10^6$ (g/g)	Th/U	Age (10^6 years)
3		3.27 ± 0.06	0.90 ± 0.08	2.65	0.98 ± 0.12	3.70	520 ± 25
5		8.09 .16	2.62 .09	7.70	1.30 .12	1.69	600 15
6L		5.55 .28	1.79 .08	5.26	1.24 .19	2.36	540 30
8		7.80 .31	3.23 .07	9.50	1.01 .15	1.06	535 20
12	Normal lower mine levels	9.28 .19	4.16 .06	12.23	2.00 .24	1.64	450 15
14		11.23 .34	3.21 .06	9.44	2.40 .22	2.54	585 20
18		2.42 .10	0.57 .07	1.66	0.81 .12	4.88	530 35
19		1.94 .04	0.57 .06	1.68	0.65 .08	3.87	480 25
20		2.47 .05	0.74 .06	2.18	0.68 .12	3.12	520 30
							530
17	Conglomerate felsite pebble	23.54 .70	7.23 .07	21.26	6.75 .40	3.17	500 15
23		20.00 .40	0.79 .05	2.32	3.68 .22	15.86	1290 45
24	Abnormal lower mine levels	20.20 .70	1.29 .08	3.79	3.63 .23	9.58	1190 45
25		1.69 .03	4.71 .05	13.85	11.0 .4	7.94	32 1
1		1.36 .03	0.33 .06	0.97	0.70 .20	7.22	405 50
16	Surface and upper levels with	2.99 .15	1.10 .08	3.23	1.14 .17	3.53	405 20
28	exposure to waters	3.40 .07	1.54 .07	4.53	1.79 .45	3.95	310 25
7		5.45 .22	3.73 .07	10.97	1.00 .15	0.91	340 20
9		1.50 .02	0.71 .02	2.09	<0.40	<1.91	>400 <630
11	Surface and upper levels, no	6.82 .27	2.44 .09	7.17	1.67 ± .21	2.33	490 ± 20
22	apparent exposure to cir-	3.16 .16	0.97 .06	2.85	1.10 .15	3.86	460 30
29	culating waters	1.87 .04	1.22 .10	3.59	— —	—	440 —
31		1.45 .10	0.87 .03	2.56	0.10 .04	0.39	435 60
26	Freshly dumped rock	5.36 .22	1.15 .06	3.38	1.73 .15	5.12	555 25
27Ph		2.30 .16	0.58 .09	1.71	0.63 .16	3.68	565 60

arising out of the foregoing analysis is that the b^2y term is negligible compared with the a^2x term unless there is a very large extraneous source of radiation in the neighborhood of the apparatus. In order to reduce the probable error and the observational limit the alpha-particle contamination must be reduced and shielding precautions will have little effect, an important observation first pointed out by Evans.[15] The specific effect of these wall particles can be reduced by the introduction of the net but adjustment must be made between the reduction of probable error on decreasing the residual ionization of such contamination particles and the loss of ionization between the net and the wall. The net was finally placed at a distance of 0.6 cm from the wall. For alpha-particles of 4-cm range in air the fractional absorption is therefore 0.15 and from Evans[16] the fractional ionization appearing inside the net is about 0.62. The mean deviation D_B from Eq. (8) is therefore 0.62 of the mean deviation with no net. From Eq. (12) we obtain the following expression for the ratio of the percentage probable error with and without the net (0.84 of the total ionization available when the net is present).

$$\frac{r \text{ with net}}{r \text{ without net}} = \frac{[2D_B^2 + a(ax_3)]^{\frac{1}{2}}/ax_3}{(2[D_B/0.62]^2 + a[ax_3/0.84]^2)^{\frac{1}{2}}/ax_3/0.84}. \quad (15)$$

For small values of ax_3 (0.01 v per hour) this ratio is about 0.7 whereas for large values (1.00 v per hour) the ratio is sensibly 1. The probable error is therefore more likely to be diminished by the further removal of contamination sources than by the use of nets. For this reason the following analysis of the background ionization has been made. Solving Eqs. (6) and (8) for x_1 we have

$$x_1 = (D_B^2 - 2bE)/2a(a-b), \quad \text{but since } a \gg b,$$
$$x_1 = (D_B^2 - 2bE)/2a^2, \quad (16)$$

where a is here the specific effect of the fractional

[16] R. D. Evans, Phys. Rev. **45**, 29 (1934).

TABLE II. *Geological time scale by the helium method.*

HORIZON	ROCK AND SOURCE		He×10⁶ (cc/g)		Ra×10¹³ (g/g)		U×10⁷ (g/g)	Th×10⁶ (g/g)		Th/U	AGE (10⁶ YEARS)	
Miocene	Basalt, Douglas Creek	(1)	0.23	±0.03	2.17	±0.06	6.40	2.02	±0.20	3.17	17	± 1.3
	Washington.	(2)	0.21	.02	2.16	.04	6.38	2.10	.23	3.30	15.5	1.0
	Columbia River, Ore.		0.27	.03	2.20	.07	6.45	2.52	.23	3.88	18	1.4
Early Eocene?	Tinguaite, Montreal		6.44	.26	20.40	.17	59.98	14.5	.29	2.42	57	1.5
Early Cretaceous	Porphyrite Dike, Cal.		1.17	.09	1.68	.08	4.93	1.58	.16	3.2	110	7
Jurassic	Diabase, N. Star Mine, Cal.		1.76	.11	1.65	.08	4.82	1.98	.16	4.1	150	8
Triassic	West Rock Sill, Conn.	(1)	1.82	.13	1.96	.15	5.76	1.30	.38	2.26	170	12
		(2)	1.88	.13	2.13	.16	6.26	1.21	.35	1.93	170	12
	Buttress Dike, Conn.		1.52	.09	1.55	.07	4.56	1.06	.11	2.28	175	9
	Palisade Intrusive, King's	(1)	1.60	.10	1.44	.08	4.23	1.79	.12	4.24	155	8
	Bluff, Weehawken, N. J.	(2)	1.66	.10	1.30	.07	3.81	1.77	.14	4.64	165	9
		(3)	1.68	.10	1.38	.07	4.05	1.80	.12	4.45	165	8
	Basalt Watchung, Mt. Clifton, N. Y.		1.13	.08	1.00	.06	2.94	0.90	.10	3.06	180	11
	Cape Spencer Flow, N. S., Can.		1.33	.08	1.05	.07	3.08	1.53	.11	5.00	160	8
Ordovician	Stark's Knob, Adirondack Mts.		0.485	.04	0.34	.06	1.00	<.08		<0.80	<340>410	
	Basalt flow,* Martinsburg	(1)	1.90	.11	2.25	.09	6.6	1.98	± .18	3.0	140	± 7
	shale, Penn.	(2)	1.15	.08	1.16	.06	3.41	1.27	.11	3.71	145	8
	Diabase in above shale	(1)	3.88	.17	1.30	.06	3.81	1.83	.12	4.80	375	15
		(2)	2.61	.13	1.29	.07	3.78	0.91	.10	2.40	355	15
Cambrian	Basalt, Unicoi formation,	(1)	1.62	.11	0.87	.08	2.56	0.15	—	0.59	465	30
	Tenn.	(2)	1.51	.10	0.85	.08	2.50	0.15	—	0.60	440	30
Pre-cambrian												
Keweenawan	Mean from Table I										530	
	Diabase Dike, Noranda	(1)	6.00	.24	1.26	.08	3.70	2.50	.20	6.76	485	20
	Horne Mine, Quebec	(2)	6.40	.25	1.13	.07	3.32	2.57	.20	7.74	525	25
		(3)	6.34	.25	1.13	.07	3.32	2.57	.20	7.74	520	25
Latest Huronian?	Diabase Dike, Gogebic	(1)	6.50	.26	2.17	.08	6.38	1.30	.19	2.04	550	25
	Iron Range, Wis.	(2)	21.14	.64	2.02	.08	5.94	9.56	.33	16.09	560	15
		(3)	21.20	.64	2.44	.09	7.18	8.60	.30	12.0	580	25
		(4)	14.81	.44	3.50	.09	10.29	4.28	.25	4.16	570	15
?	Woollen Mill gabbro, N. Y.		2.09	.13	0.19	.09	0.86	0.75	.15	8.75	670	85
Algoman?	Diabase Dike, Great Bear Lake, Can.		11.01	.34	1.71	.07	5.05	1.80	.18	3.55	900	35

* Metamorphosed.

ionization appearing inside the net. $2bE$ is a second-order term and b need not be accurately known. It was computed from the average path of a beta, etc., through the chamber at 100 ion pairs per cm. E was found to be 0.2002 v per hour. From (16) $x_1 = 116$ alpha-particles per hour $= 11.1$ alpha-particles per 100 cm² per hour and $ax_1 = 0.0609$ v per hour or 1.88 ions/cc/sec. From Eq. (6) the background from the beta, gamma and cosmic-radiation $= by_1 = 0.1393$ v per hour or 4.29 ions/cc/sec. Not until the alpha-particle background is reduced by special cleaning precautions to 1.6 alphas per hour per 100 cm² does the b^2y_1 term come within 10 percent of the term a^2x_1 although by_1 is now contributing 94 percent of the total background ionization. If the alpha-background can be so far suppressed, shielding must be used for a further diminution of D_B. The observational limit is also dependent upon the value of x_1 being given by $0.36\times10^{-14}[2x_1/n]^{\frac{1}{2}}$ gram radium for one-hour intervals and n readings with the differential apparatus.

RESULTS

The "helium method" for the determination of the geological age of rocks has been dealt with elsewhere.[17] A full discussion of the results given in Table I for the Keweenaw Point, Upper

[17] Wm. D. Urry, Chem. Rev. **13**, 2 (1933).

Michigan, basaltic flows is in course of publication by the Geological Society of America. The undue variations of certain results are owing to the inclusion of obviously unsuited material, to determine the influence of geological and physical factors on the result. Table II shows the progress in the present project of building a geological time scale by the examination of authenticated basic rocks from all geological horizons. The advantage of the helium method when once substantiated lies in the wealth of suitable material available. The results recorded here, interdigitate well with lead ratios in radioactive minerals. The helium determination has been described previously.[18] The thorium measurements are described in the immediately preceding article.[9] The age result probable error is calculated from the usual differentiation of Eq. (1) for t in the same article.[9] The uranium content is calculated from the equilibrium factor, uranium $= 2.94\times10^{6}$ Ra. The average radium content of all the basic rocks in the two tables is 1.65×10^{-13} g per g. This value may be somewhat low for a general basic rock average since the Keweenawan basalts are low compared to material from other sources. Thus the average Keweenaw content (27 specimens) is 1.60×10^{-13} g per g, somewhat higher than was given in the preliminary Keweenawan report—15 specimens averaging 1.3×10^{-13} g per g[19]—but lower than an average of 1.9×10^{-13} g per g for 20 non-Keweenawan basic rocks. The average thorium content of all the basic rocks is 2.0×10^{-6} g per g and the mean Th/U ratio 4.1. The individual ratios are often higher than has previously been supposed, a finding in agreement with the results of R. D. Evans (private communication). As a comparison, the radium contents of various suites of granites as given in the literature vary from 9 to 17×10^{-13} g per g.[20] Individual measurements with the present apparatus give results from 5 to 20×10^{-13} g per g for granites.

This research was made possible by the support of the American Philosophical Society. The Geological Society of America has generously contributed to the support of the routine analyses.

[18] Paneth and Urry, Zeits. f. physik. Chemie **A152**, 110 (1931).

[19] Urry, "Radioactivity Measurements. I," Proc. Am. Acad. **68**, 125 (1933).

[20] Urry, "Radioactivity Measurements. II," Proc. Am. Acad. **68**, 137 (1933). See also Evans and Williams, Am. J. Sci. **22**, 441 (1935).

JANUARY, 1936 JOURNAL OF CHEMICAL PHYSICS VOLUME 4

Rotatory Dispersion of Aliphatic Aldehydes

P. A. LEVENE AND ALEXANDRE ROTHEN, *Rockefeller Institute for Medical Research, New York*

(Received October 11, 1935)

Rotatory dispersion curves of configurationally related aldehydes of the type

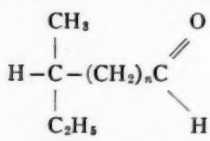

(n being equal to 0, 1, 2, or 3) have been determined in the visible and the ultraviolet regions of the spectrum. Their analysis has shown first, that the band of the aldehydic group at λ2950 is rotatory active and that the sign of its contribution in the first member ($n=0$) is opposite to that of the higher members and second, that the magnitude of that contribution varies periodically with the number of carbon atoms located between the aldehydic group and the asymmetric carbon atom.

PREVIOUS observations in this laboratory[1] have established the fact that in substances of the general type

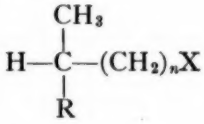

(R = an alkyl or aryl group, $n = 0$ or an integer, X = a chromophoric group with an absorption region situated in the near ultraviolet region of the spectrum) the change of the value of n from 0 to 1 brings about a change in the direction of rotation, this direction remaining constant for the substances with higher values of n. In the few cases[2] where no change of sign was observed, the analysis of the dispersion curve showed that the dispersion was anomalous, i.e., the sign of the rotation was opposed to that of the first contribution. These facts led to the belief that in all other cases, the observed changes of rotation were due to changes in the first contribution. Further, there was observed a periodicity in the values of the rotations of the individual members with the progressive increase in the value of n.

The group of substances thus far analyzed, however, was of a nature which did not permit direct measurement of the course of rotation within the region of the nearest absorption band. Hence the direction and value of its partial rotation were obtained by the analysis of the rotatory dispersion curve outside the band.

It was therefore desirable to analyze a group of substances of the same general type but with a chromophoric group which permitted the measurement of its rotation within the region of the absorption band. The group 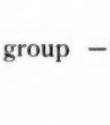 held out the promise of presenting these advantages. The first absorption band of this group at 2950A is weak ($E \leq 20$) well isolated without any overlapping, thus permitting calculation of its partial rotation from the experimental dispersion curve within the region of the absorption band.

Hence, the following series of configurationally related aldehydes of the above general type were prepared:

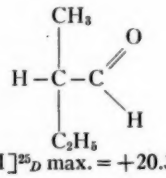

$[M]^{25}_D$ max. = +20.3°

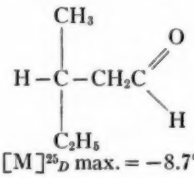

$[M]^{25}_D$ max. = −8.7°

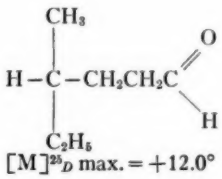

$[M]^{25}_D$ max. = +12.0°

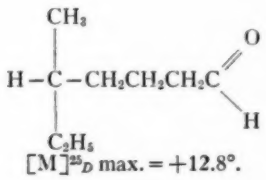

$[M]^{25}_D$ max. = +12.8°.

The mode of preparation of these substances has been described elsewhere.[3] The present communication deals with the analysis of the rotatory dispersion curves of the above four aldehydes. The results of the observations are summarized in Fig. 3. The ordinate represents the absolute magnitude of the partial rotation (which is proportional to the circular dichroism) of the band λ2950, the abscissa the number of carbon atoms between the asymmetric center and the aldehydic group (the numerical value of n).

It is evident that there is a periodicity in the value of the rotatory component of the band λ2950. This partial rotation is comparatively small in the third and fourth members ($n = 2$ and 3). However, its magnitude in the fourth member is twice that of the third. Thus it is clear that the periodic variations of rotation with the increase of the numerical value of n, observed in the visible part of the spectrum are due to periodic variations in the partial contribution of the band λ2950. These observations are significant for they add weight to the conclusions reached earlier regarding substances whose nearest absorption bands were not accessible to direct analyses.[4]

[1] P. A. Levene and R. E. Marker, J. Biol. Chem. **103**, 299 (1933).

[2] P. A. Levene, A. Rothen and R. E. Marker, J. Chem. Phys. **1**, 662 (1933).

[3] P. A. Levene and A. Rothen, J. Biol. Chem., **111**, 739 (1935).

[4] In an interesting and recent article, H. Hudson, M. L. Wolfrom and T. M. Lowry, J. Chem. Soc. 1179 (1933),

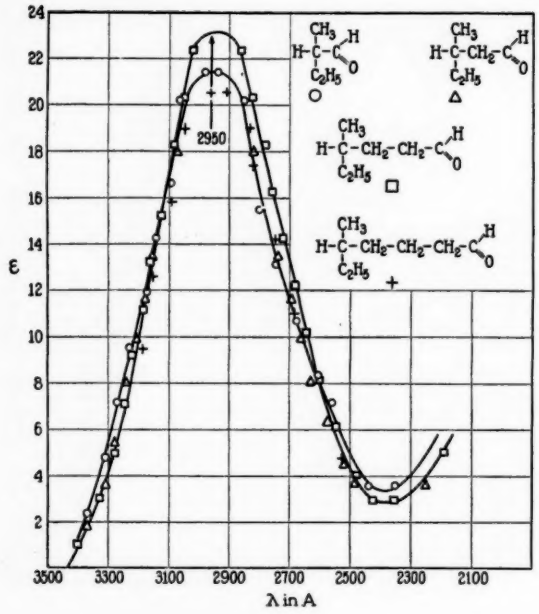

FIG. 1.

The physical basis of the observed changes in rotation still remains a matter of speculation. Among all the theories concerning optical activity, none is able to predict, first, that a change of sign occurs in the function $(\varphi)_\lambda{}^* = f(n)$ when n is changed from 0 to 1; second, that for $n > 1$ this function keeps the same sign but varies periodically with the successive values of n in magnitude only. It is possible to deduce from the mechanical model used by W. Kuhn[5] that a change of sign should occur when the distance between the two coupled oscillators increases, but the wave-length should be of the order of magnitude of interatomic distances, which is, of course, excluded in the case here considered. The more recent theory of Born[6] shows that one could expect a short periodicity in the function $(\varphi)_\lambda = f(n)$ but no change of sign can be predicted.

In the absence of any other explanation for the observed facts, we venture to suggest one which is in harmony with the deduction from Kuhn's mechanical model and with the theoretical consideration of Born[6] and others. The facts to be remembered are: First, that the configuration remaining constant, it is only the change of n from 0 to 1 which brings about inversion of sign of a given $(\varphi)_\lambda$, the sign remaining the same in all the other members of a homologous series. Second, there is no change in direction of rotation and no periodicity if $X = CH_3$ so long as the length of the chain $(CH_2)_nCH_3$ does not exceed that of R. Thus it is evident that the polar nature of X is a requisite for the phenomenon. On the other hand, it is known that the polar groups induce alternating polarities in the consecutive carbon atoms of the chain, which naturally is extended to the asymmetric carbon atom. Hence it is reasonable to assume that the dissymmetry of the asymmetric carbon atom will alter with the change of the electric charge of the neighboring carbon atom.

studied the rotatory dispersion of aldehydic sugars. They report a strong partial rotation of the band λ2900 which, in one case, is practically the only rotatory component of the rotation observed. But the presence, in those compounds, of three or four asymmetric carbon atoms renders interpretation more difficult.

* The symbol $(\varphi)_\lambda$ will be used to denote the partial rotatory contribution of the band λ due to the group X.

[5] W. Kuhn and K. Freudenberg, "Drehung der Polarisationsebene des Lichtes," *Hand- und Jahrbuch der chemischen Physik* (Leipzig, 1932), p. 47.

[6] M. Born, Proc. Roy. Soc. **A869**, 84 (1935).

ANALYSIS OF THE ABSORPTION BAND

The absorption curves of the aldehydes may be seen in Fig. 1. It is apparent that the position of the band is identical in all four compounds, the intensity being of the same order of magnitude. The absorption curves can be expressed by an exponential equation based on a Maxwellian distribution.

TABLE I. *Rotatory dispersion of dextro-2-methylbutanal-1 in heptane.*

Concentration: 1.337M. Visible region: $l = 40$ cm. U.V.: $l = 5$ cm from 3640 to 3460A, 1 cm for 3420A, 0.1 cm for $\lambda < 3420$.

λ(A)	α^{25}	$[M]^{25}_{max.}$	$[M]^{25}_{max.} = \frac{5.104}{\lambda^2 - 0.0932}$
5875.6	+5.140	+20.28	+20.25
5780.1	+5.369	+21.19	+21.19
5460.7	+6.315	+24.92	+24.92
4358.3	+13.37	+52.76	+52.76
4046.6	+18.30	+72.21	+72.36
3640	+3.98	+125	+130
3588	+4.48	+141	+144
3540	+4.99	+157	+159
3500	+5.49	+173	+174
3460	+6.00	+189	+188
3420	+1.35	+215	+215
3320–3070	+0.20	+325	—
2980	0.00	0	—
2930	−0.10	−160	—
2770	−0.35	−450	—
≂2350	−0.15	−240	—

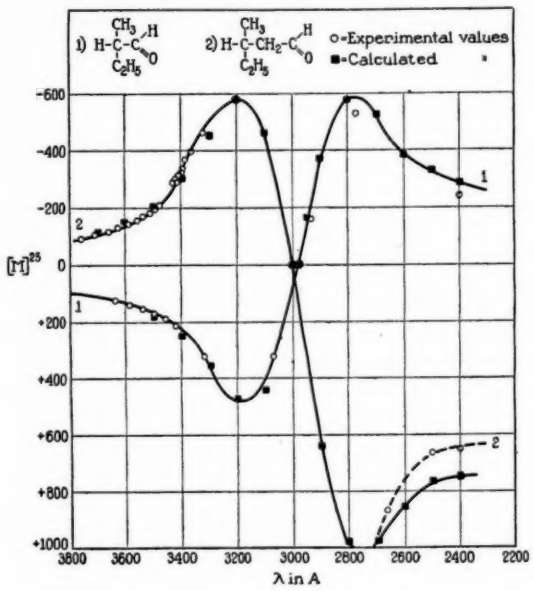

FIG. 2.

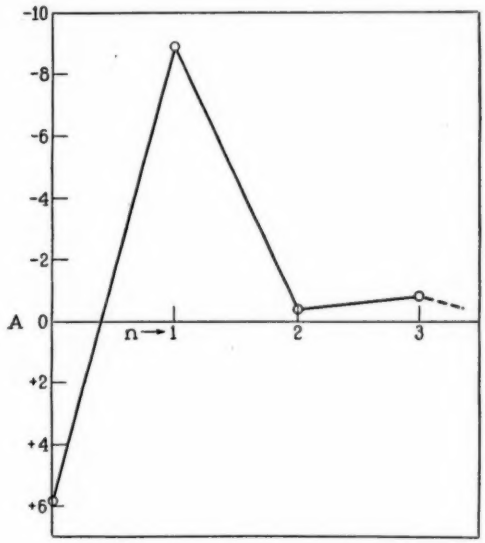

FIG. 3.

TABLE II. *Rotatory dispersion of levo-3-methylpentanal-1 in heptane.*

Constants of sample: δ_4^{25} 0.8010, $n^{25}D$ 1.3989. Concentration 1.338M. Visible region: l = 40 cm. U.V.: l = 10 cm from 3970 to 3475A 1 cm for *a*, 0.5 cm for *b*, 0.1 cm for *c*.

λ(A)	α^{25}	$[M]^{25}_{max.}$	$[M]^{25}_{max.} = -\frac{7.569}{\lambda^2-0.093} + \frac{6.693}{\lambda^2-0.032}$
5875.6	−1.320	-8.67_9	−8.64
5780.1	−1.409	-9.26_4	−9.24
5460.7	-1.786_5	-11.74_6	−11.75
4358.3	−5.43	−35.7	−35.7
4046.6	−8.54	-56.1_5	−56.1
3885	−2.75	−72.3	−74.3
3850	−3.00	−78.9	−79.5
3710	−4.00	−105	−106
3660	−4.50	−118	−119
3630	−5.00	−131	−128
3590	−5.50	$-144._5$	−142
3555	−6.00	−158	−156
3535	−6.50	−171	−165
3510	−7.00	−184	−177
3492	−7.50	−197	−188
3475	−8.00	−210	−198
3430	−1.11 (a)	−292	
3420	−1.17 (a)	−323	
3395	−1.25 (a)	−329	
3360	−0.76 (b)	−400	
3320	−0.70 (b)	−460	
3200	−0.22 (c)	−580	
3000	−0.00 (c)	0.0	
2730	+0.43 (c)	+1100	
2660	+0.33 (c)	+870	
2500	+1.26 (b)	+670	
2400	+2.46 (a)	+650	

ANALYSIS OF ROTATORY DISPERSION CURVE

The measurements of the rotatory dispersions may be found in Tables I, II, III, IV and on Fig. 2. The values found in the fourth column of the tables have been calculated, using in one case a one-Drude term, and in the others a two-Drude term formula. The constants of the formulas have been so chosen as to reproduce as well as possible the experimental data in the visible and very near ultraviolet regions. The agreement between experimental and calculated values is quite satisfactory especially if one considers that in the case of 3-methylpentanal-1 the two terms of opposite sign are of the same order of magnitude. The dispersion constants of the first terms come very close to the position of the absorption

TABLE III. *Rotatory dispersion of dextro-4-methylhexanal-1 in heptane.*

Constants of sample: δ_4^{25} 0.8132, $n^{25}D$ 1.4081. Concentration 1.016M. Visible region: l = 40 cm. U.V.: l = 10 cm for 3490A and 0.5 cm for 2350A.

λ(A)	α^{25}	$[M]^{25}_{max.}$	$[M]^{25}_{max.} = -\frac{0.371}{\lambda^2-0.087} + \frac{4.114}{\lambda^2-0.036}$
5875.6	+0.800	+12.01	+11.87
5780.1	+0.819	+12.30	+12.30
5460.7	+0.930	+13.96	+13.93
4358.3	$+1.54_0$	$+23.1_2$	+23.12
4046.6	+1.82	+27.3	+27.37
3490	+0.60	+36	+37
2350	+0.20	+240	+228

TABLE IV. *Rotatory dispersion of dextro-5-methylheptanal-1 in heptane.*

Constants of sample: δ^{25}_4 0.8164, n^{25}_4 1.4144. Concentration 0.616M. Visible region: $l=100$ cm. U.V.: $l=20$ for 3770 and 3580A, 5 cm for 3450A, 1 cm for 2460A.

λ(A)	α^{25}	$[M]^{25}_{max.}$	$[M]^{25}_{max.}=-\frac{0.8158}{\lambda^2-0.087}+\frac{4.9102}{\lambda^2-0.036}$
5875.6	+1.596	+12.79	+12.72
5780.1	+1.643	+13.17	+13.17
5460.7	+1.856	+14.88	+14.86
4358.3	+2.99	$+23.9_7$	+23.97
4046.6	+3.47	$+27.8_2$	+27.81
3770	+0.80	+32	+31.5
3580	+0.90	+36	+33.5
3450	+0.20	+32	+33.6
2460	+0.30	+240	+230

band, with a slight displacement towards the red. The dispersion curves of the first two compounds ($n=0$ and 1) are reproduced in Fig. 2. It was impossible to obtain a two-term formula representing accurately the experimental data over the whole wave-length range covered. The smallness of the angles observed as well as a gradual decrease in the rotations due to decomposition prevented any accurate determinations in the immediate neighborhood of the band. The calculated values have been obtained from a two-term formula, the first term being a Kuhn-Braun[7]-Lowry-Hudson[8] term. The general formula used was

$$[M]^{25}_{max.}=\frac{\phi\lambda_\phi}{m\lambda}\left[e^{-[(\lambda-\lambda_0)/\theta]^2}\int_0^{(\lambda-\lambda_0)/\theta}e^{x^2}dx+\frac{\theta}{2(\lambda+\lambda_0)}\right]+\frac{B}{\lambda^2-\lambda_1^2},$$

where: $\phi=+500°$, $m=0.560$, $\lambda_\phi=0.3166$, $\lambda_0=0.2980$, $\theta=0.0207$, $B=-0.798$, $\lambda_1^2=0.036$ for levo 2-methylbutanal-1 and $\phi=-700°$, $m=0.560$, $\lambda_\phi=0.3180$, $\lambda_0=0.2980$, $\theta=0.0223$, $B=+8.07$, $\lambda_1^2=0.036$ for dextro-3-methylpentanal-1. (To comply with the usual convention adopted in polarimetry, wave-lengths are expressed in microns.) As known,[7] the first term of this formula reduces to a simple Drude term $A/(\lambda^2-\lambda_0^2)$ for values of $\lambda>4\theta+\lambda_0$ where $A=\phi\lambda_\phi\theta/m$.

The following facts should be brought out: First, the center of the active part of the band is slightly displaced towards the red as compared to the absorption band; second, the active band does not spread over the entire width of the absorption band: The constants θ determined from absorption measurements are very much larger than θ determined to fit the dispersion formulas; third, the high value of the dispersion constants of the second terms for all compounds indicate that the second contribution is also located for the most part in the aldehydic group.

Experiments were attempted to determine directly the dichroism in the band λ2950. As expected, it could be detected only in the first two compounds. The measurements remained of a qualitative nature because of the small angles, but were, however, of the right order of magnitude.

EXPERIMENTAL

The instruments used have been previously described[9] and the same precision is claimed. The method followed to determine the circular dichroism was that described by W. Kuhn.[10]

The compounds used were not resolved to the maximum. All observed α values as given in the tables were multiplied by an appropriate coefficient to bring them to the maximum. The decrease of rotation due to decomposition was taken into account when the series of measurements extended over a long period of time.

[7] W. Kuhn and E. Braun, Zeits. f. physik. Chemie **B8**, 281 (1930).

[8] T. M. Lowry and H. Hudson, Phil. Trans. Roy. Soc. London **A232**, 117 (1933).

[9] P. A. Levene and A. Rothen, J. Chem. Phys. **2**, 681 (1934).

[10] W. Kuhn and E. Braun, Zeits. f. physik. Chemie **B8**, 445 (1930).

On the Zero-Point Energy of an Activated Complex and the Reaction $2NO+O_2 \rightarrow 2NO_2$

O. K. RICE, *Department of Chemistry, University of California, Berkeley*

(Received October 14, 1935)

Considerations, based on the uncertainty principle, have been brought forward which indicate that a reaction, whose rate is determined solely by a transitory activated complex in the formation of which classical degrees of freedom must be frozen out into vibrations, must have a positive activation energy at all temperatures, which increases with the temperature. A negative activation energy must mean the formation of a more or less stable intermediate compound, or "molecular complex." The theory has been applied to the reaction $2NO+O_2 \rightarrow 2NO_2$.

§1

RECENTLY Gershinowitz and Eyring[1] have considered the reaction $2NO+O_2 \rightarrow 2NO_2$ from a theoretical point of view. In so doing they set up an expression for the rate constant, K, of the reaction in the form

$$K = A_0 e^{-\epsilon_{a,0}/kT}, \tag{1}$$

where $\epsilon_{a,0}$ is the activation energy at absolute zero[2] and consequently independent of temperature, while A_0 is a quantity which may depend on temperature. A_0 was determined on the assumption that the rate-determining step is the passage of the system over a potential energy saddle, the rate then being proportional to the number of activated complexes (an activated complex being simply the system of three molecules in the act of passing over the barrier) and to the rate at which they get over the barrier. It was assumed that in forming the activated complex from the two NO molecules and the O_2 molecule seven rotational and translational degrees of freedom were frozen out into vibrations. Then by making estimates of the vibrational frequencies and the various moments of inertia involved it was possible to get an estimate of A_0. They concluded that $\epsilon_{a,0}$ should be zero (this roughly corresponds to making the height of the potential energy barrier zero), so the whole burden of the explanation of the negative temperature coefficient was placed on A_0.

In order to get a clear idea of the significance of the negative temperature coefficient there is a certain advantage in writing the equation for the rate constant in the more usual form

$$K = A e^{-\epsilon_a/kT} \tag{2}$$

where ϵ_a is the average energy of reacting triplets minus the average energy of all triplets, and the quantity A differs from A_0 just enough to counteract the difference between ϵ_a and $\epsilon_{a,0}$. If we use the activated complex picture, ϵ_a is the average energy of all activated complexes minus the average energy of all triplets, and it is directly related to the temperature coefficient by the relation[3]

$$d \ln K/d(1/T) = -\epsilon_a/k. \tag{3}$$

Eq. (3) tells us at once that a negative temperature coefficient means that the average energy of all activated complexes or reacting triplets is less than the average energy of all the molecules; though the use of Eq. (1) is perfectly justified it tends to make one forget this fact, which should be borne constantly in mind.

In order to get a better idea of the various factors involved in such a reaction let us consider a simple two-dimensional case, in which we may suppose that the reaction occurs on the passage of one of the degrees of freedom over a potential energy saddle of height zero. The representative point of the system in coordinate space will be supposed, nevertheless, to go through a pass, the other degree of freedom

[1] Gershinowitz and Eyring, J. Am. Chem. Soc. **57**, 985 (1935).

[2] This is the same as the E_0 of Gershinowitz and Eyring.

[3] Tolman, *Statistical Mechanics* (Chemical Catalog Co., 1927), Chapter 21. This equation holds quite universally for all orders of reaction if ϵ_a is defined in such a way as to include all the energy. See the discussion of Gershinowitz and Rice (J. Chem. Phys. **2**, 273 (1934), footnote 11) on bimolecular reactions.

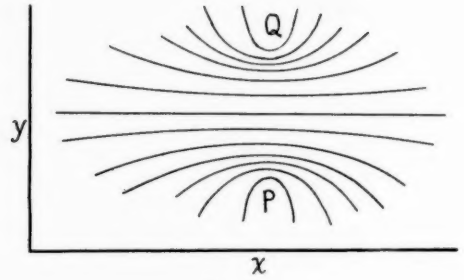

FIG. 1.

being hemmed in by potential energy hills. A schematic contour diagram of the potential energy surface is shown in Fig. 1. As the representative point moves in the x direction it is necessary for it to pass between the highlands at P and Q. However, even though the lowest contour line goes straight through the middle of the valley the system will need a finite energy in order for it to have any reasonable probability of getting through the pass. For in the pass oscillations in the y direction are possible and these oscillations will have a zero-point energy.[4] The energy levels corresponding to these oscillations cannot be sharp, as Kassel[5] has noted, but their diffuseness cannot be sufficient to erase effectively the zero-point energy. A system with less than this amount of energy in the y direction has a small probability of getting through the pass on the fringes of the diffuse state, but it will not have a probability approaching the classical value until its energy approaches the zero-point energy. This is connected with the fact that, by the uncertainty principle, it is not possible by any conceivable experiment to locate definitely a system in the pass until the product of the probable ranges of the y coordinate and the corresponding momentum is sufficiently great, and this first occurs at the energy of the lowest vibrational state. The effective zero-point energy could, indeed, be lowered if it were possible for the system to tunnel into the negative kinetic energy regions under the highlands Q and P, for this would effectively widen the pass. But this latter phenomenon would necessarily lower the vibration frequency to an amount corresponding, roughly at least, to the lowered zero-point

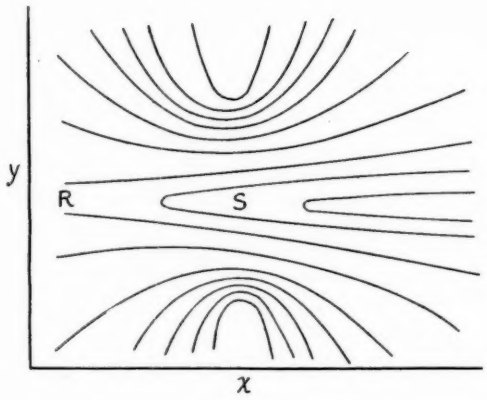

FIG. 2.

energy. Thus the actual effective frequency of the oscillator must, at least approximately, determine the zero-point energy.

So, in assigning certain frequencies to the activated complex, Gershinowitz and Eyring also unavoidably assign certain zero-point energies, and it is clear that if their potential energy barrier were of zero height the value of ϵ_a could not possibly be less than zero. It might, perhaps, be supposed that this difficulty could be overcome if, instead of the contour diagram in the analogous two-dimensional case being like Fig. 1, it were like Fig. 2, sloping off to the right (for reaction to take place the representative point is supposed to move from left to right). According to this picture the original idea of an activated complex as being determined by the state of a system as it goes over a potential energy barrier has pretty well disappeared, but one might still expect, even if the valley in the neighborhood of S is deep, that the degree of freedom represented by y would have to be effectively frozen out to a vibrational state such as would occur at S where the valley is narrow.[6] For we should

[4] Compare, e.g., Wigner, Zeits. f. physik. Chemie **B19**, 203 (1932), especially p. 213.

[5] Kassel, J. Chem. Phys. **3**, 399 (1935).

[6] If there were other degrees of freedom of the system than x and y, and these had a high probability of exchanging energy with x and y while the representative point for x and y was in the region between R and S, then of course this representative point would not be able to get to the left again, and y would have to be frozen out to an extent corresponding to its frequency at the point between R and S where exchange of energy with the other degrees of freedom became important. The thing to note here is that there would be a corresponding zero-point energy.

Very similar considerations have been brought forward by Rice and Gershinowitz (J. Chem. Phys. **3**, 479 (1935), especially p. 482) in their treatment of unimolecular reactions. In this paper these authors discuss the relation between Eyring's special type of activated complex (J. Chem.

anticipate that in order to pass through the valley the representative point of the system would have to be pretty well aimed, otherwise it would most probably be eventually forced back toward the left because of the general slope of the potential energy diagram in that direction. To the vibration at S there would correspond a zero-point energy, but now one might suppose that, with a potential energy surface such as shown in Fig. 2, it could be balanced by the difference in potential energy at the points R and S. This assumes, of course, that it is possible for enough transfer of energy to take place between the x and y motions to supply the zero-point energy. Since the broadening of the energy levels for the y motion is connected with the coupling between the x and y motions, and since it is clear that the energy levels must be broad, unless a very great obstacle to the passage of the system through the valley is to be encountered, considerable transfer of energy between the x and y degrees of freedom is to be anticipated. Thus it looks at first sight as though the necessary condition for the neutralization of the zero-point energy is fulfilled.

However, closer scrutiny of the situation seems to indicate that this is not actually the case. For the passage of the representative point down the valley still represents a restriction on the coordinate y. If this restriction is to be effective in determining the number of systems which can get through the valley, it must be possible to refer it back to the motion of the representative phase points which are still far to the left of R. We have, effectively, a certain target area, or better a target length, in the y direction at which any representative point must be aimed if it is to go through the pass. The same argument used above, based on the uncertainty principle, will indicate that systems which are thus restricted must exhibit a zero-point energy for their motion in the y direction, and since the energy in the x direction cannot be less than zero, there will be a positive activation energy even in this case.[7] This of course does not imply that a system whose energy in the y direction is less than the zero-point energy has no chance of going through the pass; just as in the case where the potential energy surface was like Fig. 1, the zero-point energy is a sort of average affair, and there is a finite probability of the representative point going through because of the broadening of the energy levels, but the probability of its getting through must continually increase as the energy increases. When the temperature is so low that the change with the energy of the intensity of the broadened vibrational state is small (at the average energy corresponding to the temperature) compared to the change of probability with energy given by the distribution law, the average energy in the y direction of systems going through the pass will be nearly equal to the average energy of all systems and so the activation energy will be nearly zero; but the number of systems getting through under these circumstances will be small and as it approaches a more normal value the activation energy will become positive, approaching $kT/2$ for every classical degree of freedom frozen out into a vibration, the average energy of the weakly quantized oscillator varying from $kT/2$ at low temperatures to its normal high temperature value of kT. On account of the broadening of the energy levels this limiting high temperature value will be reached at a lower temperature than is the case for a strongly quantized oscillator of the same frequency.[8]

Phys. **3**, 107 (1935)) and their idea of freezing out of degrees of freedom (ibid. **2**, 853 (1934)). In the present paper we speak both of an activated complex and of the freezing out of degrees of freedom.

[7] If we demand that the energy in the y direction be less than the zero-point energy, the target length will necessarily be increased. Thus the aim of such low energy systems will be poor, and the probability of going through must be lowered in at least the ratio in which the target length is increased over that necessary to insure passage through the valley.

[8] It may be possible some time in the future to treat the questions considered here in a more quantitative fashion by an extension of the methods of Wigner, reference 4.

Added in proof: Some correspondence with Dr. Gershinowitz prompts me to add the following two remarks (which are not necessarily to be considered as expressing his views). (1) The method of estimating the energy of activation implies a close relation between the motion in the y direction at S and the motion in the y direction to the left of R. Though in general the variables will not be strictly separable, some such condition is to be inferred from the arguments of the first part of the paragraph. (2) The arguments in the text are based on the assumption that the effective target length does not decrease (due perhaps to some peculiarity of the potential energy surface) with the energy of the approaching system; in fact, it increases because of the increase with energy of the distance across the valley, this being automatically taken care of by assuming the oscillator at S to be harmonic. A decrease in target length could indeed be imagined to give a negative temperature coefficient (above a certain temperature

It may appear rather strange that we thus have an oscillator, even a weakly quantized one, whose specific heat retains a finite value at absolute zero (or, rather, down to such a temperature that the specific heat of the connected "classical" degree of freedom begins to fall off), for this indicates that at low temperatures the entropy of the oscillator must become negative. However, this is really just what is to be expected, for at these temperatures the oscillator occupies a state at the lower fringe of a broadened discrete state, and the statistical weight of the *whole* broadened discrete state is just that of a *single* sharp state. At high temperatures the entropy of the oscillator must approach that of an oscillator with discrete levels, and at ordinary temperatures it will be a sufficiently good approximation to take the entropy of a sharply quantized oscillator of the same frequency if, for example, one desires to use it in calculating the order of magnitude of an absolute reaction rate; such an approximation, however, will not always suffice to give the change of entropy with temperature in the lower temperature ranges. The use of this approximation will in general give too low an estimate of the rate of reaction, because it does not take into account the chance of a system getting through on the fringe of a broadened discrete state, but at the same time it will give too high an energy of activation. If now the energy of activation is arbitrarily altered (by adjusting $\epsilon_{a,0}$) so as to give the observed value, this will more than compensate for the deficiency in the estimate of the rate of reaction; since this is what is ordinarily done in practice the resulting theoretical estimate of the rate of reaction will be too high and a correction to lower it somewhat will be needed. The size of this correction is difficult to estimate, but, as stated, at reasonable temperatures it may surely be assumed to be small.

§2

We may now consider the application of the principles discussed in §1 to the trimolecular reaction $2NO+O_2 \rightarrow 2NO_2$. In Fig. 3 we have

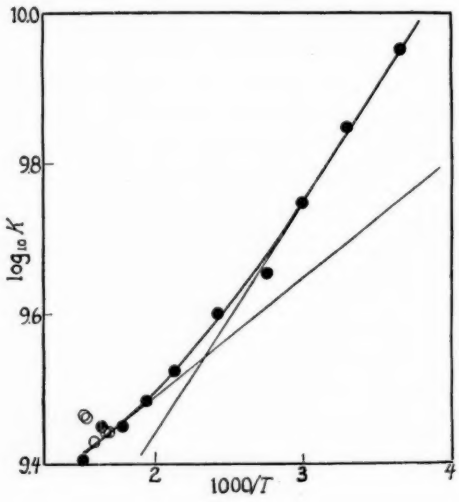

FIG. 3.

plotted the experimental values of $\log K$ against $1/T$. The black circles give the values obtained by Bodenstein and co-workers;[9] the open circles give the values calculated by Bodenstein and Ramstetter[10] from the equilibrium and the rate of the reverse reaction. Though these latter were believed to be more accurate than the values obtained by the study of the direct reaction, it is seen that two of them fall rather badly out of line. On the basis of these two points the rate constant would attain a minimum value around 630°K; it is seen, however, that this would necessitate a rather sudden change in activation energy around this temperature, and I think that one is justified in supposing that the slopes of the straight lines shown in Fig. 3 may be used to give the activation energies at 310°K and 570°K, which are found to be −1410 and −720 calories per mole, respectively.

This brief presentation of some of the aspects of the experimental results brings out two points which need consideration. In the first place, we have to explain the negative activation energy, and, in the second place, we must try to understand its variation with temperature.

The activation energy, ϵ_a, for this reaction may be written in the form

$$\epsilon_a = \epsilon_{a,0} + \sum_{i=1}^{i=n} E_i - nkT/2 + kT/2. \qquad (4)$$

depending on the target length at absolute zero), but this would be a purely *ad hoc* assumption which seems to me to be extremely unlikely and to involve a radical departure from the idea of an activated complex with simple freezing out of degrees of freedom, as equilibrium considerations would not then suffice to treat the problem.

[9] Bodenstein, Zeits. f. Elektrochemie **24**, 183 (1918); Zeits. f. physik. Chemie **100**, 87 (1922).

[10] Bodenstein, Zeits. f. physik. Chemie **100**, 106 (1922).

In this equation n is the number of classical degrees of freedom which must be frozen out into vibrations in order for reaction to occur, E_i is the average energy of these vibrations and may range from $kT/2$ to kT as explained in §1, and the extra $kT/2$ term takes care of the fact that the average energy of systems going over a potential barrier (even if its height is zero) is kT greater in that degree of freedom than the energy of the top of the barrier, while the average energy of that degree of freedom in the dissociated state of the system is $kT/2$. For the reaction under consideration Gershinowitz and Eyring take $n=7$, but it may be 6 or 8.

Now the difference between the activation energies at 310° and 570°K is quite small compared to $nkT/2$. This suggests that the E_i do not exceed $kT/2$ very greatly nor change very much in the temperature range under consideration. It may seem that the temperatures considered are a little high for this to be the case, but in view of the complications which may arise in a process of the kind we are dealing with, it is rather difficult to see whether the assumption is reasonable or not. Under these circumstances it may not be without interest to see what would happen if we should use the usual expression for the energy of a harmonic oscillator, $h\nu_i(e^{h\nu_i/kT}-1)^{-1}+h\nu_i/2$ for E_i. It is then found that the experimental trend of ϵ_a with the temperature can only be explained by taking the average value of ν_i to be about 700 cm^{-1}, which is rather high—higher, for example, than would be expected from the frequencies of N_2O_4 which were used by Gershinowitz and Eyring to estimate the frequencies of their activated complex.[11] Gershinowitz and Eyring did not try to fit the activation energies at different temperatures, but in estimating rate constants at different temperatures they met with a somewhat similar difficulty, as may be seen from an examination of their Table I, in which it is to be observed that there is a considerable difference in the trends of calculated and experimental values. This difference could only be overcome by using higher frequencies than they did, by assuming $\epsilon_{a,\,0}$ to be less than zero (which I believe may fairly be said to be contrary to their theory), or by taking n greater than 7; but setting $n=8$, without making other changes, would not help much.

Returning now to the matter of the negative temperature coefficient, we note that if the considerations of §1 are correct, it is not possible to account for such a phenomenon by the use of an activated complex, even when modified in the way suggested in §1. The indications are that we must go back to the old idea[12] of a more or less stable intermediate molecule, or "molecular complex," with a negative energy of formation.[13] Then its energy of formation at absolute zero will contribute effectively to $\epsilon_{a,\,0}$ and can make this quantity sufficiently negative to counteract the net positiveness of the rest of the terms on the right-hand side of Eq. (4). If the E_i are not much greater than $kT/2$, as postulated above, then the energy of formation of the molecular complex need not be very greatly negative. Now it is known that nitric oxide is associated in the liquid phase,[14] and it seems probable that the associated molecule has an energy of dissociation of[15] 2–3000 calories per mole of $(NO)_2$, which is quite adequate for the present purposes. It is thus very likely that the molecular complex is a double nitric oxide molecule, and that the final step of the reaction is the reaction of this double molecule with an oxygen molecule, this latter step involving a true *activated* complex in the modified sense of §1. Most of the vibrations of the $(NO)_2$ molecule may be expected to be pretty loose; reaction with the O_2 molecule may be expected to require further freezing out of these vibrations, and in any event it will require some mutual orientation of the $(NO)_2$ and O_2 molecules; besides this there will be a certain activation energy, due to the zero-point energy of the new vibrations formed, to the increase of the zero-point energy of other vibrations, and possibly to other causes. This activation energy will be less than the energy required to dissociate the double molecule by the amount of the negative

[11] This assumes $n=6$. If n were greater than 6 the average value of ν_i would have to be higher.

[12] For an account of the older theories see Kassel, *Kinetics of Homogeneous Gas Reactions* (Chemical Catalog Co., 1932), Chapters IV and IX.

[13] As we shall see, this does not mean that the reaction does not go through an activated complex (in the modified sense of §1), but simply that prior formation of a molecular complex is necessary.

[14] The entropy of vaporization is abnormally high. See Johnston and Giauque, J. Am. Chem. Soc. **51**, 3208 (1929); also p. 3213.

[15] Rough estimate from the heat of vaporization.

activation energy of the trimolecular reaction, and if this factor were the only one involved one would expect the reaction with oxygen to proceed faster than the dissociation of the $(NO)_2$ through energy received by collision with other molecules. However, except at very low temperatures, it seems probable that this effect of the activation energy will be more than counterbalanced by the necessity of orientation for the trimolecular reaction with oxygen. The latter reaction will therefore be much slower than the breaking up of the $(NO)_2$ molecules. We may therefore expect that there will always be present an equilibrium concentration of the molecular complex. The concentration of *activated* complexes may then be calculated in the usual way, just as though the intermediate steps were not necessary, except that the negative energy of formation of the molecular complex is added to the activation energy; in other words, the intermediate formation of a molecular complex, by allowing a lower starting point for the activated complex, makes it possible for $\epsilon_{a,0}$ to be negative. The important difference between an activated complex and a molecular complex is that the latter is in what may be called "back-and-forth equilibrium" with the molecules from which it is formed. The flux type of equilibrium which we get, or at least conceivably may get, with an activated complex, in which there is no return of the systems from the activated state to the initial state, is not capable, in my belief, of yielding a negative activation energy.

It is, of course, not impossible that the actual details of the mechanism are different than those suggested above. The intermediate may be $NO \cdot O_2$ or the trimolecular complex $(NO)_2 \cdot O_2$. This, however, is not of importance as regards the point which we wish chiefly to bring out.

There is one matter, however, which requires some further attention. In §1 we discussed the average energy of a vibrational degree of freedom which had been frozen out from a classical degree of freedom and which was still broadened by the contact with the classical degree of freedom. In the present situation we have in the activated complex some vibrations which were not directly frozen out from classical degrees of freedom, but are the result of a further freezing out of the vibrations of the molecular complex, which are strongly quantized. The situation is not changed on this account, however, provided the latter frequencies are low enough. This can be seen by a consideration of the two-dimensional analogy. The analogy to the present case would be obtained if, in Fig. 2, we had a valley with sides of gentle slope instead of a plain to the left of R. If the slopes of this valley were gentle enough, only its central portion, where the potential energy is practically constant in the y direction, would be of importance; the average kinetic energy in the y direction of the particles in the central part of the valley would be $kT/2$, just as before, and the broadening of the levels at S would occur as before, though the probability of a given energy would not be as smooth a function of the energy, but would have a banded structure. The effect of this rather uneven or banded broadening of the levels at S would nevertheless be expected to have very nearly the same effect as the smooth broadening considered in §1, provided the bands were not too far apart, compared to the spacing of the levels of S. Inasmuch as the spacing of the bands of high probability in the broadened level would be determined by the spacing of the levels in the original vibrator to the left of R, the requirement is that the latter should have a low frequency compared to that at S; that is to say the frequencies of the molecular complex must be low compared to those of the activated complex, the former being represented by the point to the left of R, the latter by the point at S. If, on the other hand, some of the frequencies of the activated complex were no greater than those of the molecular complex, then some vibrations of the activated complex would have sharp energy levels, and we should have to use the usual formula for the energy of a harmonic oscillator to calculate the average energies of these vibrations. If, however, this were true of any considerable number of the vibrations of the activated complex we would find it difficult to explain the slow change of the activation energy with the temperature, as the calculations made earlier in this section of the paper will indicate. We are thus led to suppose that the frequencies of the molecular complex are actually considerably lower than those of the activated complex, though it must be granted that this is not a

completely satisfactory resolution of the point at issue, and the matter cannot be considered closed.

We turn now to a consideration of the results at very low temperatures obtained by Briner, Pfeiffer and Malet.[16] Their results indicate that the rate at 80°K is not as great as one would expect by extrapolation from higher temperatures. This is well brought out by the calculations of Gershinowitz and Eyring, which, while they give too small an increase in the rate constant on going from 600°K to 300°K, increase far more than the experimental values at low temperatures. At very low temperatures the experimental value of the rate constant appears to be approaching a maximum. A possible explanation was suggested by Kassel,[17] who assumed that the reaction goes through an intermediate, $NO \cdot O_2$. His explanation is that this complex becomes so stable at low temperatures that with excess of O_2 (such as was present in the experiments of Briner, Pfeiffer, and Malet) most of the NO is removed. If $(NO)_2$ is the intermediate molecule no similar explanation can hold, however, for the association in the gas phase is known to be extremely small at the boiling point of nitric oxide, and at lower temperatures the vapor pressure goes down so rapidly that this will continue to be true at all attainable pressures. However, another possibility has been brought to my attention by Professor W. F. Giauque. The NO molecule has two low electronic states, a $^2\Pi_{1/2}$ and a $^2\Pi_{3/2}$. The latter has the higher energy, and there is only about one-fourth as much of it at 80°K as around room temperature.[18] If, now, the $(NO)_2$ molecule is formed from NO's in the $^2\Pi_{3/2}$ state, then the number of NO's which can react with O_2 will be only 1/16 as great as would be expected from the situation at room temperature if the difference in the electronic states were neglected, and this factor appears to be of the correct order of magnitude to account for the small rate at 80°K. Another possible explanation might be found in the supposition that at very low temperatures the rate of dissociation of the molecular complex $(NO)_2$, requiring as it does a higher activation energy than the reaction with oxygen, becomes less than the rate of reaction with oxygen. This would mean that the complex would no longer be present in equilibrium numbers, and so the rate would fall off, the rate of formation of the molecular complex ultimately becoming the rate determining step. Further data at low temperatures might enable one to distinguish between these three possible explanations. Kassel's hypothesis would make the reaction rate proportional to the first power of the NO concentration, instead of the second, and proportional to the O_2 concentration; the explanation based on the suggestion of Giauque would leave the order of the reaction unchanged; the last explanation would make the rate independent of the oxygen concentration at low enough temperatures and high enough oxygen pressures.

In closing we should make a statement about the absolute rate of the reaction. Not much need be said, for the discussion in the last paragraph of §1 makes it appear obvious that the calculation of Gershinowitz and Eyring should be reasonably adequate in that respect above room temperatures. Even if their value of n is not quite correct, the difference caused by changing it by 1 should be within the unavoidable uncertainty of the reaction.

We thus see that it is possible to construct a theory for the reaction $2NO+O_2 \rightarrow 2NO_2$ consistent with the principles laid down in §1, which is reasonably satisfactory in most respects. As pointed out already, however, it is not possible to make any dogmatic statement that any particular mechanism is necessarily the correct and final one, but it is believed that the points brought out in this paper will have to be taken into account in any theory of the reaction which may be brought forward.

[16] Briner, Pfeiffer and Malet, J. chim. Phys. **21**, 25 (1924). Recent work by Temkin and Puizhov, Acta Physicochim. U. R. S. S. **2**, 473 (1935), abstracted in C. A. **29**, 6522 (1935), indicates that complications may arise at low temperatures on account of a heterogeneous reaction; however, it appears probable that the conditions under which the reaction was studied by the latter investigators were such as to favor the heterogeneous reaction.

[17] Kassel, reference 12, p. 166.

[18] Johnston and Chapman, J. Am. Chem. Soc. **55**, 164 (1933), especially Table V (in the heading of which one should apparently read $^2\Pi_{3/2}$ for $^2\Pi_{1/2}$).

The Structure of Ice II

RONALD L. MCFARLAN, *Research Laboratory of Physics, Harvard University*

(Received October 31, 1935)

The stability of the high pressure ice forms discovered by Tammann and Bridgman at very low temperatures and atmospheric pressure has made it possible to obtain x-ray powder diffraction photographs of these forms. The experimental procedure is very briefly discussed. An analysis of the ice II diffraction patterns leads to a side-centered orthorhombic cell with $a=7.80$A, $b=4.50$A, and $c=5.56$A. This cell contains eight molecules, has the symmetry of space group V^5-C222_1, and gives a value for the density of 1.21. The proposed arrangement of the hydrogen atoms indicates that the transition from ice I to ice II breaks up the water molecule, and that ice II is an ionic crystal. According to the model described the effect of a pressure of 2100 atmospheres in forming ice II is: (1) To decrease the packing volume of the oxygen ion approximately three percent; (2) To break down the open ice I structure by a slipping of the oxygen ion layers relative to each other; (3) To give a four-coordinated structure where each oxygen is surrounded by a badly distorted tetrahedron of oxygen ions.

INTRODUCTION

THE existence of polymorphous ice forms at high pressures was first discovered by Tammann,[1] and was later thoroughly investigated by Bridgman[2] who discovered several additional forms. As these ice forms are not stable at ordinary pressures and temperatures their structure has not as yet been determined by x-ray methods. A knowledge of the crystal structure of the various high pressure ice forms would provide valuable information regarding the following points:

1. The effect of pressure on the coordination of the water molecule.
2. The effect of pressure on the angle between the OH directions of the water molecule.
3. The mechanism of the solid-solid reaction that takes place when a phase line separating two ice forms is crossed.

The present investigation was undertaken to determine the crystal structure of the different ice forms by x-ray diffraction methods.

EXPERIMENTAL WORK

The pressure-temperature range over which each ice form is stable is shown in Fig. 1 taken from Bridgman's paper. A detailed description of the technical difficulties involved, and the methods devised to overcome them will be made in a separate paper which will appear in the *Review of Scientific Instruments*. A brief account will be given here.

If the temperature of any high pressure ice form is maintained sufficiently low it will remain stable at ordinary pressures indefinitely, and consequently can be irradiated with x-rays outside the press. The problem of extracting the high pressure ice crystal from the press was solved by Professor Bridgman, at whose suggestion this work was undertaken. The crystal was frozen under pressure, and before releasing the pressure the lower part of the press was immersed in liquid air. The crystal could then be removed without reverting to ice I.

The x-ray diffraction camera was of the standard powder design modified:

1. To maintain the crystal temperature near that of liquid air during exposure.

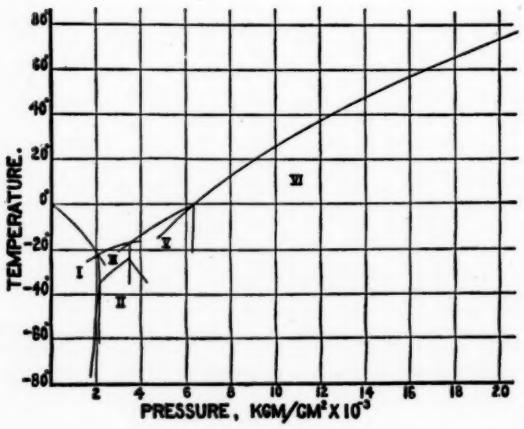

FIG. 1.

[1] Tammann, *Kristallisieren und schmelzen* (Barth, Leipzig, 1903), pp. 315–344.
[2] P. W. Bridgman, Proc. Am. Acad. **47** (1912).

2. To permit rapid insertion and centering of the crystal.

The actual crystal temperature during exposure —as measured by a thermocouple—was −155°C, and after some practice it was found possible to center and insert the crystal in the camera in from ten to fifteen seconds. The time of stability before a crystal would revert to ice I upon removal from liquid air was about twelve seconds.

With the exception of ice II it was found necessary to grind each crystal under liquid air in order to obtain good powder patterns. Attempts to form small crystal fragments by crossing the solid-solid phase lines several times were not very satisfactory.

The camera was calibrated in two different ways:

1. With an ice I diffraction pattern using Barnes'[3] data as a standard.
2. With a NaCl-gum tragacanth diffraction pattern.

Both calibration patterns were obtained in exactly the same way as the high pressure crystal patterns. These two methods gave identical calibration curves within the ordinary limits of experimental error. Cu $K\alpha$ radiation filtered through nickel was used to irradiate the crystal.

The possibility of frost forming on the outside of the high pressure crystal made it necessary to test for the presence or absence of ice I lines on the high pressure ice films. The complete absence of ice I lines on the patterns of the other ice forms was inferred from the following observations:

1. The NaCl-gum tragacanth pattern showed no ice I lines.
2. An empty cellophane cylinder exposed under the usual conditions showed no powder lines.
3. A single crystal rotation photograph of ice VI showed no trace of any powder lines.

It is also possible that the diffraction patterns might be produced by a mixture of two kinds of crystals as a result of the solid-solid reaction not going to completion after crossing a phase line. To eliminate this possibility patterns were obtained from several crystals of each ice form, each crystal being formed by crossing a different phase line into the desired region. In this way it was easy to identify the lines that were characteristic of a particular ice form.

[3] W. H. Barnes, Proc. Roy. Soc. **A125**, 670 (1929).

The Crystal Structure of Ice II

Two methods of computing the density from the Bridgman[2] data were used. In the first of these it was assumed that ice II would show the same relative change of volume over the pressure range 2100–1 atmospheres as does ice I. Temperature-volume relations were neglected. In the second method the ice II compressibility-pressure curve was extrapolated to one atmosphere, whence the density could be computed from the average compressibility. Both of these methods gave values of approximately 1.15 for the density, which value is probably accurate to within ten percent.

An excellent match between the observed and calculated interplanar spacings can be obtained on a hexagonal lattice with an axial ratio of 1.24. This leads to a unit cell 4.50 by 5.56 Angstroms, containing four molecules and giving a density of 1.21, a value which differs by approximately five percent from the extrapolated Bridgman value. However, no space group of the hexagonal system permits a distribution of oxygen atoms which predicts intensities in agreement with those observed. But it is possible to arrange the four atoms on a hexagonal lattice in such a way as to obtain a good fit between the observed and calculated intensities. This arrangement—which does not have the trigonal symmetry required of all hexagonal space groups—is shown projected on the xy plane in Fig. 2. As appears in the diagram the oxygen atom distribution may also be represented by an orthorhombic lattice whose axial ratios are 1.73 : 1 : 1.24. The symmetry is that of space group V^5-C222_1, and there are eight molecules in a unit cell of dimensions $a=7.80$A, $b=4.50$A, and $c=5.56$A. The oxygen atoms appear in the following positions:

xyz;	$x\bar{y}\bar{z}$;
$x+\frac{1}{2}, y+\frac{1}{2}, z$;	$x+\frac{1}{2}, \frac{1}{2}-y, \bar{z}$;
$\bar{x}, y, \frac{1}{2}-z$;	$\bar{x}, \bar{y}, z+\frac{1}{2}$;
$\frac{1}{2}-x, y+\frac{1}{2}, \frac{1}{2}-z$;	$\frac{1}{2}-x, \frac{1}{2}-y, z+\frac{1}{2}$;

where the best agreement with observed intensities is obtained for $x=0.167$, $y=0.205$, and $z=0.178$. The calculated and observed interplanar spacings and intensities are shown in Table I. Each oxygen atom is surrounded by a badly distorted tetrahedron of oxygen atoms,

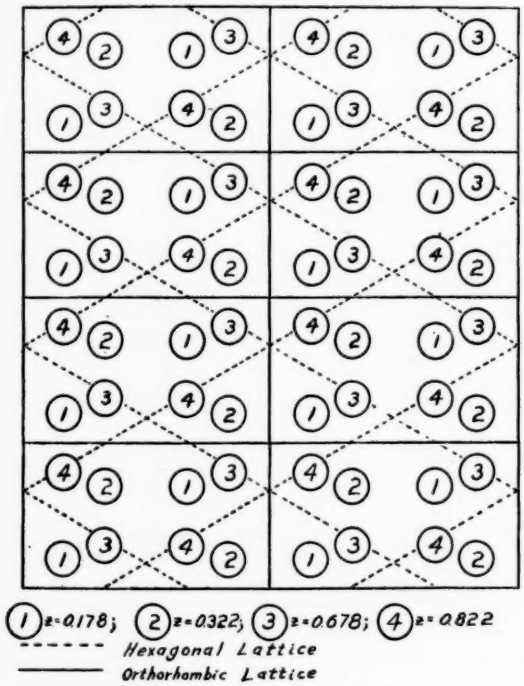

FIG. 2. Oxygen atoms—ice II.

giving a coordination of four as in ice I. The number and distance of various oxygen neighbors is shown below.

No. neighbors	4	2	1	2	6	2
Distance (A)	2.71	3.09	3.31	4.23	4.50	4.65

This compares with four neighbors at 2.74A and thirteen at 4.47A for ice I. This shows the increased density of ice II to be the result of a relatively small change in nearest neighbor distances of ice I, i.e., actual ionic compression, and a considerable decrease in the ice I next nearest neighbor distances, i.e., geometrical compression.

The assignment of the hydrogen atom positions is necessarily arbitrary, since no x-ray evidence is available regarding this point. It is not possible to follow the procedure of Bernal and Fowler[4] with ice I in assigning positions to the hydrogen atoms in the ice II structure. The distribution of oxygen atoms is such that the angle between the OH directions cannot be made the same for all the oxygen atoms, and at the same time a reasonable structure obtained. Consequently, it

TABLE I.

hkl	d(calc) (A)	d(obs) (A)	I(calc)	I(obs)	hkl	d(calc) (A)	d(obs) (A)	I(calc)	I(obs)
110	3.90	3.8	33.7	v.s.	131	1.43			
200	3.90				511	1.43			
111	3.20	3.0	81.4	v.v.s.	313	1.43	1.43	4.6	m.
201	3.20				023	1.43			
002	2.78	2.7	17.0	s.	421	1.43			
020	2.26				223	1.34			
202	2.26	2.19	52.1	v.s.	403	1.34	1.34	3.4	m.
112	2.26				114	1.31			
310	2.26				204	1.31			
311	2.09	2.10	43.5	v.s.	600	1.30			
021	2.09				330	1.30	1.29	9.2	s.
400	1.95	1.94	5.9	m.	422	1.30			
220	1.95				512	1.30			
221	1.84	1.85	7.2	m.	132	1.30			
401	1.84				331	1.27	1.26	1.3	m.
022	1.75	1.74	3.7	m.	332	1.18			
312	1.75				314	1.18	1.18	0.5	w.
113	1.68	1.70	6.7	m.	024	1.18			
203	1.68				133	1.15			
222	1.60	1.59	4.4	m.	513	1.15	1.14	2.1	m.
402	1.60				423	1.15			
510	1.48								
420	1.48	1.46	1.6	m.					
130	1.48								

is necessary to assume that the ice I–ice II transition breaks up the water molecule, and that the ice II crystal is made up of oxygen and hydrogen ions which do not form molecules. The simplest way to build up such a structure is to assume that each hydrogen ion lies on a line joining the center of an oxygen ion to the center of one of its nearest neighbors, and further that each hydrogen ion lies midway between the neighboring oxygen centers. This arrangement gives the necessary 16 ions of hydrogen per unit cell, is consistent with the accepted value for the O−H−O packing distance, and satisfies all the symmetry requirements of space group V^5-C222_1. The coordinates obtained in this way for the hydrogen ions are as follows:

$u00$; $\bar{u}0\frac{1}{2}$; $u+\frac{1}{2}, \frac{1}{2}, 0$; $\frac{1}{2}-u, \frac{1}{2}, \frac{1}{2}$, where $u=0.167$; $0u\frac{1}{4}$; $0\bar{u}\frac{3}{4}$; $\frac{1}{2}, u+\frac{1}{2}, \frac{1}{4}$; $\frac{1}{2}, \frac{1}{2}-u, \frac{3}{4}$, where $u=0.250$; xyz; $x\bar{y}\bar{z}$; $\bar{x}, y, \frac{1}{2}-z$; $\bar{x}, \bar{y}, z+\frac{1}{2}$; $x+\frac{1}{2}, y+\frac{1}{2}, z$; $x+\frac{1}{2}, \frac{1}{2}-y, \bar{z}$; $\frac{1}{2}-x, y+\frac{1}{2}, \frac{1}{2}-z$; $\frac{1}{2}-x, \frac{1}{2}-y, z+\frac{1}{2}$,

where $x=0.250$, $y=0.455$, $z=0.250$.
A projection on the xy plane of this arrangement is shown in Fig. 3.

The angle between the OH directions of the water molecule, which Mecke's[5] measurements on steam and Barnes[3] ice I data give as 103°–107°, loses its significance in this structure. For four of the oxygen atoms of the ice II structure the H−O−H angle is 103°, but the departure from this value for the other four atoms is large.

[4] Bernal and Fowler, J. Chem. Phys. **1**, 515 (1933).

[5] Mecke and Baumann, Physik. Zeits. **33**, 833 (1932).

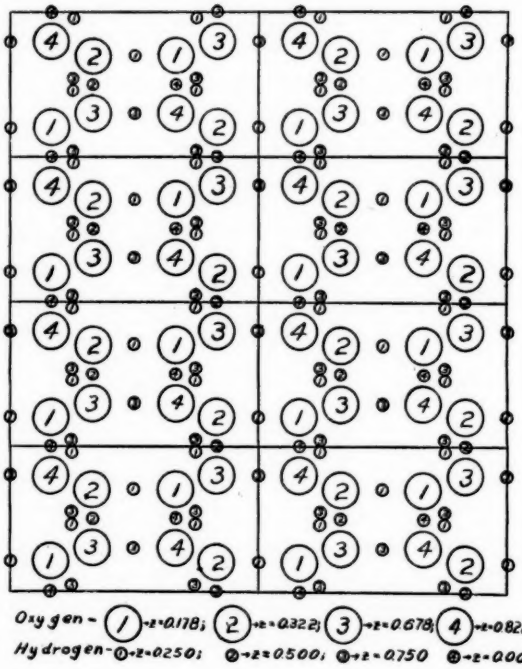

FIG. 3. Atomic distribution—ice II.

The change from ice I to ice II is, according to the model proposed, a slipping of adjacent oxygen ion layers, as shown in Fig. 4. If, in Fig. 2 the layers marked 3 and 4 were moved so as to make the *xy* coordinates of 3 and 2, and 4 and 1 coincide the resulting structure would be that of ice I. The mechanism of the ice I–ice II reaction can thus be pictured as a slipping of oxygen ion layers accompanied by a hydrogen displacement, as a result of the electrostatic attraction between the hydrogen and oxygen ions. The extent to which this slipping takes place is determined by the repulsive forces between the oxygen ions which are next nearest neighbors. In Fig. 3 this would mean the repulsive forces between the oxygen ions marked 1 and 3, and those marked 2 and 4. The proposed model places no hydrogen atoms between these next nearest neighbors, and consequently the effective distance of closest approach will be much larger than for the 2.71A nearest neighbor distance.

Additional evidence as to the reasonableness of the assumption that the water molecule is broken up in the course of the ice I–ice II transition is furnished by some recent, and as yet unpublished

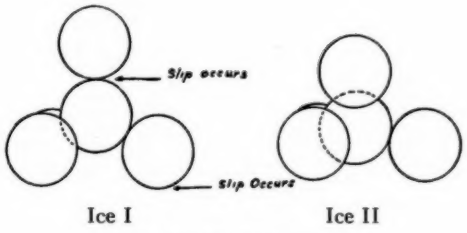

FIG. 4. Ice I–ice II reaction.

work of Professor Bridgman. He found that a high pressure plus a shear stress applied to lead oxide reduced it to pure lead. The reduction was purely a mechanical disruption of the PbO_2 molecule, no thermal effect being possible.

The only other analysis of a high pressure crystal that has appeared so far is the black phosphorus analysis of Hultgren, Gingrich, and Warren.[6] In their solution the bond angles of phosphorus were found to fit the expected near tetrahedral values for bond angles of the lighter elements. However, black phosphorus contains but a single kind of atom, and further is stable under ordinary conditions whereas ice II satisfies neither of these conditions.

It is of interest to calculate what portion of the volume decrease in the ice I–ice II change is due to a difference in packing, and what portion is due to a redistribution of ions. The x-ray measurements give the O−H−O packing diameter as 2.71A, a decrease of 0.03A from the 2.74A value of ice I. This represents a decrease in molecular volume—assumed to be spherical—of 3.4 percent. Some estimate as to the reasonableness of this result can be obtained by assuming—as suggested by Bernal and Fowler[4]—that the volume change of any one ice over its range of pressure stability represents molecular compression. Then according to Bridgman's[2] data for ice I there would be a three-percent decrease in packing volume upon increasing the pressure 2000 atmospheres. The volume change on going from ice I to ice II is 22.3 percent at atmospheric pressure according to the x-ray measurements, and is 20 percent at 2000 atmospheres according to the Bridgman data. The difference between these volume changes, 2.3

[6] Hultgren, Gingrich and Warren, J. Chem. Phys. 3, 351 (1935).

percent, corresponds roughly to the three-percent change in packing volume over 2000 atmospheres. The stability of ice II at very low temperatures would thus seem to be due to a thermal contraction of the oxygen ion of the same order of magnitude as the volume change under 2000 atmospheres pressure. Accordingly, the density obtained from the x-ray measurements is not necessarily the same as that under pressure in the press. As both the phase diagram of Bridgman[2] and the low temperature ice I measurements of Barnes[3] show, the thermal contraction is not in itself sufficient to cause the formation of ice II. The expenditure of external work is necessary to change the OH bond angles of ice I. This is in agreement with the giving off of latent heat during the course of the ice I–ice II reaction.

Further information regarding the effect of pressure on the water molecule can be obtained from the crystal structure of ice III. The results of the analysis of the ice III photographs already obtained will appear in the near future.

JANUARY, 1936 JOURNAL OF CHEMICAL PHYSICS VOLUME 4

Studies on Glass

XII. Some New Heat Capacity Data for Organic Glasses. The Entropy and Free Energy of *dl*-Lactic Acid

GEORGE S. PARKS, S. BENSON THOMAS* AND DONALD W. LIGHT, *Department of Chemistry, Stanford University*

(Received October 14, 1935)

Heat capacity measurements by the Nernst method have been made upon samples of secondary butyl alcohol and 3-methylhexane in the glassy and liquid condition and upon a sample of *dl*-lactic acid (1) in an incompletely crystallized state, (2) in the form of an *acid* glass and liquid, and (3) in the form of a *mixed* glass and liquid. From these results the specific heats and heat of fusion of pure crystalline *dl*-lactic acid also have been derived. The data for the several glasses and undercooled liquids show a rapid rise from the heat capacity characteristic of a crystalline solid to that for the liquid state within a transition region of about 10° and the nature of this transition region has been discussed. A calculation of the molal entropy and free energy of formation of liquid *dl*-lactic acid at 298.1°K yields 45.9 (±1.0) e.u. and −124,300±(2300) cal., respectively.

IN previous studies[1] dealing with organic glasses heat capacity data have been presented for ethyl alcohol, *n*-propyl alcohol, propylene glycol, and glucose, and for two mixed glasses or solutions containing glycerol and glucose and propylene glycol, glycerol and glucose, respectively. The data showed in every case a marked increase in heat capacity within a comparatively small temperature interval or *transition region*, the rate of increase being somewhat less rapid in the mixed glasses than with the pure substances. The materials represented in these earlier studies, however, were all primary alcohols or polyhydroxy compounds; and accordingly it seemed desirable to extend the measurements to other types of substances. In the present study specific heat determinations have been made upon secondary butyl alcohol, *dl*-lactic acid, and 3-methylhexane—i.e., upon a typical secondary alcohol, a hydroxy acid, and a paraffin hydrocarbon. These substances all form stable glasses on cooling from the liquid state, although the lactic acid may also be obtained in the crystalline condition. It is interesting to note that in each case the molecule contains an asymmetric carbon atom and that the materials involved in the present study were in reality mixtures of equal amounts of the dextro and laevo forms.

MATERIALS

A very pure sample of secondary butyl alcohol was kindly prepared for us by H. E. Buc of the Standard Oil Development Company. Its boiling range was 99.52–99.55°C.

* Shell Research Fellow at Stanford University for the academic year 1930–31.

[1] (a) Parks and Huffman, J. Phys. Chem. **31**, 1842 (1927); (b) Parks, Huffman and Cattoir, J. Phys. Chem. **32**, 1366 (1928); (c) Parks, Thomas and Gilkey, J. Phys. Chem. **34**, 2028 (1930).

To obtain the *dl*-lactic acid for this investigation a C. P. commercial syrup was subjected to two successive vacuum distillations at 115° and 2 to 3 mm pressure. The middle fraction of the final distillate was kept frozen in an ice bath until used in the calorimeter. As shown by Thurmond and Edgar[2] and by others, lactic acid samples ordinarily contain some lactide ($C_6H_8O_4$), lactic anhydride ($C_6H_{10}O_5$) and water, formed from the acid. These are inevitable concomitants of the distillation process; although in an investigation, carried out subsequently to this one, Borsook, Huffman and Liu[3] have discovered that such anhydro compounds can be practically eliminated by fractional crystallization of the lactic acid from a mixture of ethyl and isopropyl ethers. In the present case the free acid was determined by titration with standard sodium hydroxide solution, with phenolphthalein as an indicator. Excess sodium hydroxide was next added; the solution was boiled to complete the hydrolysis of the anhydro forms; and then a back titration with standard hydrochloric acid sufficed to give the percentage of these anhydro forms, calculated as lactide, in the original sample of acid. The amount of water was determined by difference. Our final product, freshly prepared, gave in duplicate analyses (by weight): 98.4 percent lactic acid; 1.4 percent lactide; and 0.2 percent water. A portion of this product, subsequently kept for thirty days around −5°C, changed to 97.2 percent lactic acid and 2.2 percent lactide. At higher temperatures alterations were much more rapid. Thus a portion kept for ten days at 22°C analyzed 94.7 percent lactic acid and 4.4 percent lactide, and a sample heated at 82°C for forty-six hours changed to 68.3 percent lactic acid and 26.4 percent lactide.

The 3-methylhexane was prepared in very pure form by Edgar, Calingaert and Marker[4] and has been fully described by them in other places. A sample of this material was loaned to us for the present investigation by the Ethyl Gasoline Corporation.

These three substances showed practically no optical rotation when tested with a polariscope.

[2] Thurmond and Edgar, Ind. Eng. Chem. **16**, 823 (1924).
[3] Borsook, Huffman and Liu, J. Biol. Chem. **102**, 449 (1933).
[4] Edgar, Calingaert and Marker, J. Am. Chem. Soc. **51**, 1483, 1540 (1929).

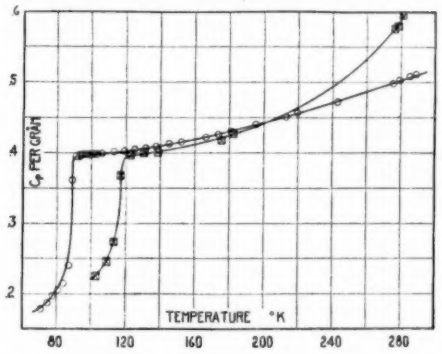

FIG. 1. The specific heats in cal. per degree of glassy and liquid secondary butyl alcohol (squares) and 3-methylhexane (circles) plotted against the absolute temperature.

METHOD AND EXPERIMENTAL RESULTS

In principle, the method of Nernst was employed with an aneroid calorimeter in determining the "true" specific heats. The apparatus and details of experimental procedure have been fully described in other places.[5] In view of the accuracy of the various measurements involved, the absolute error in the experimental values thereby obtained is probably less than 1 percent; the fortuitous errors, which are naturally of greater importance in a comparative study of heat capacities over a range of temperatures, were usually under 0.3 percent. The results have been expressed in terms of the 15° calorie (=4.185 joules) per gram, with all weights reduced to a vacuum basis.

The specific heat data for secondary butyl alcohol and 3-methylhexane are given in Tables I and III. They are also represented graphically in Fig. 1. Neither of these substances showed any tendency to crystallize; with progressive cooling they simply became more viscous and finally hardened to glasses at the lower temperatures. The individual heat capacity determinations

TABLE I. *Specific heats in cal. per degree for sec.-butyl alcohol, glass and liquid.*

T(°K)	C_p	T(°K)	C_p	T(°K)	C_p
102.8	0.225	123.0	0.397	182.3	0.427
109.3	.246	130.2	.399	276.5	.576
113.5	.274	138.5	.401	278.3	.580
116.7	.368	175.5	.418	281.7	.596

[5] Parks, J. Am. Chem. Soc. **47**, 338 (1925); also Parks and Kelley, J. Phys. Chem. **30**, 47 (1926).

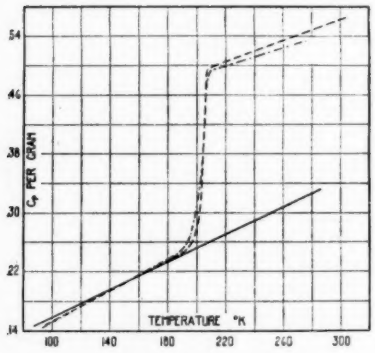

FIG. 2. The specific heat curves for lactic acid in the pure crystalline form (solid line), in the form of the acid glass and liquid (broken line), and in the form of the mixed glass and liquid (dot-and-dash line). Specific heats are in cal. per degree.

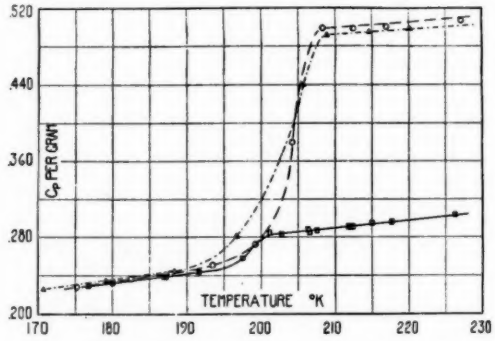

FIG. 3. The specific heat curves for lactic acid in the immediate neighborhood of the transition region. The squares refer to the 87.8 percent crystallized system; the circles to the acid glass and liquid; and the triangles to the mixed glass and liquid. Specific heats are in cal. per degree.

were made consecutively, with intervals of at least one hour, proceeding up the temperature scale.

The *dl*-lactic acid sample was transferred to the calorimeter as a liquid, promptly frozen therein by maintenance around 0°C, and then the calorimeter was installed in the specific heat apparatus. During this installation, which took about a day, the sample undoubtedly melted and underwent some alteration. To determine the approximate extent of this alteration, a portion of our purified lactic acid was given similar treatment; subsequent analysis yielded 97.0 percent lactic acid, 2.4 percent lactide and 0.6 percent water. The lactic acid sample in the calorimeter was first carefully crystallized again and a series of heat capacity measurements and a heat of fusion determination were made. Some of the specific heat values thus obtained are represented by the squares and solid line in Fig. 3. They disclose an appreciable sudden rise around 200°K, indicative of the presence of considerable amorphous or glassy material. Subsequent quantitative comparison of this curve with the two curves representing lactic acid in a completely uncrystallized state showed that this amorphous phase in contact with the crystals represented about 12.2 percent of the material.

TABLE II. *Specific heats in cal. per degree for dl-lactic acid.*

Acid Glass and Liquid		Mixed Glass and Liquid		Pure Crystals and Liquid	
T(°K)	C_p	T(°K)	C_p	T(°K)	C_p
103.5	0.1572	95.8	0.1471	90	0.148
110.3	.1612	101.3	.1533	100	.158
122.6	.1753	108.1	.1611	120	.177
135.4	.1876	156.1	.2109	140	.196
141.0	.1940	170.7	.2263	160	.214
154.8	.2075	179.1	.2357	180	.233
169.4	.2207	188.3	.2444	200	.252
175.2	.2283	196.7	.2809	210	.261
182.5	.2364	205.7	.4409	230	.280
187.9	.2421	208.8	.4921	250	.298
193.5	.2512	214.6	.4946	280	.326
199.2	.2729	220.2	.4986	289.9	Fusion
204.2	.3700	262.7	.5254	290	.554
208.3	.4988	267.4	.5282	300	.563
212.5	.4982				
217.0	.5003				
227.2	.5070				
293.5	.5562				
297.5	.5585				
303.0	.5655				

The lactic acid sample, now a liquid, was next cooled very quickly in liquid air to produce what we have designated as the *acid glass*, and a series of heat capacity measurements was made on this material in the glassy and liquid condition. The specific heat values thereby obtained are given columns 1 and 2 of Table II and are represented graphically by broken lines in Figs. 2 and 3.

Following the completion of these measurements the calorimeter and contents were heated to a temperature of 70°C for forty-eight hours to promote the partial conversion of the acid to water and anhydro forms. The calorimeter was next cooled to liquid-air temperatures, whereupon the material formed a noncrystallizing glass which will be subsequently designated as the *mixed glass*, in view of the fact that it contained such appreciable quantities of the anhydro

TABLE III. *Specific heats in cal. per degree for 3-methylhexane, glass and liquid.*

T(°K)	C_p	T(°K)	C_p	T(°K)	C_p
71.1	0.178	96.7	0.398	151.8	0.415
74.7	.187	99.1	.398	166.2	.422
78.0	.197	101.1	.399	173.8	.426
81.1	.205	103.1	.399	181.0	.430
84.0	.215	106.3	.400	195.7	.440
86.9	.240	112.7	.402	212.9	.451
89.2	.362	118.9	.403	219.8	.457
91.0	.395	125.1	.405	243.1	.473
92.8	.397	131.4	.407	275.8	.502
93.0	.395	137.6	.409	285.4	.514
95.1	.397	144.8	.413	289.2	.517

forms. The series of specific heat values represented in the third and fourth columns of Table II and by the dot-and-dash lines in Figs. 2 and 3 was then obtained. The material taken out of the calorimeter immediately after these measurements analyzed: 69.6 percent lactic acid, 24.2 percent lactide and 6.2 percent water.

From the relations of the three curves in an enlargement of Fig. 3 it was possible to deduce easily, in two successive approximations, the percentage of the amorphous material in the first series of measurements on the two-phase, crystalline-amorphous system, the heat capacity of this amorphous fraction at various temperatures, and finally the specific heats of the pure crystalline and liquid lactic acid. These last are given for various even temperatures in Table II and the crystal values also are represented by the practically straight, solid line in Fig. 2. It is interesting that at the lowest temperatures these specific heats for the crystals are slightly higher than those for the glasses. This is a rather unusual situation, although White[6] has observed it previously in the case of certain silicates. The heat of fusion of the crystals, with allowance for 12.2 percent amorphous phase, was calculated as 30.1 cal./gram at 289.9°K.

DISCUSSION

The glasses

In general characteristics the heat capacity curves for these three substances in the glassy and liquid condition are strikingly similar to those found previously for various glass-forming organic materials of a predominantly alcoholic character. Of course, such behavior might be expected for the secondary butyl alcohol and probably for the lactic acid, but the 3-methylhexane is a distinctly novel case.[7] Here we encounter a nonpolar hydrocarbon, while the other organic glasses have been formed from oxygen-containing compounds that yield highly associated liquids.

Three rather distinct regions appear in all these heat capacity curves. At the lower temperatures, where the material forms a hard glass, the specific heats are of the order of magnitude of those found for the same substances, or for closely related ones, in the crystalline state. At the higher temperatures the material is a more or less viscous liquid and the specific heats even below the melting point of the crystals, as in the case of lactic acid, lie on a portion of the curve which is clearly characteristic of the ordinary liquid state and considerably above that of the corresponding crystalline state. Intermediate between these two portions of the curve appears a *transition region*, 8° to 20° in magnitude depending on the nature of the glass-forming material and its thermal history, within which the specific heats increase very rapidly. Its suddenness is reminiscent of a change of state, although there is nothing comparable to a heat of fusion and two phases are never present. The middle point of this transition region has been found to be associated with a viscosity of the order of 10^{13} or 10^{14} poises in a number of cases.[8]

For secondary butyl alcohol this transition centers around 115°K. The corresponding temperatures in the cases of other simple glass-forming compounds have been found as follows: 3-methylhexane 88°; ethyl alcohol 94°; *n*-propyl alcohol 98°; propylene glycol 159°; glycerol 185°; lactic acid 204°; glucose 282°; boron trioxide 510°. Among the organic compounds the mean temperature of the transition evidently rises with increasing polarity and increasing molecular weight, the former factor being the more important. However, at present there seems to be no way of quantitatively determining this temperature in advance of experiment.

[6] White, Am. J. Sci. **47**, 1 (1919).

[7] Some preliminary heat capacity values for this heptane were published in a general study of the nine isomeric heptanes by Huffman, Parks and Thomas, J. Am. Chem. Soc. **52**, 3241 (1930).

[8] Parks and Spaght, Physics **6**, 69 (1935).

TABLE IV. *C_v values in cal. per degree for 3-methylhexane.*

T(°K)	C_p per mole	C_p-C_v per mole	C_v per mole	T(°K)	C_p per mole	C_p-C_v per mole	C_v per mole
82	20.9	0.6	20.3	200	44.3	6.6	37.7
92	39.7	2.7	37.0	250	47.9	8.7	39.2
100	39.9	2.9	37.0	290	51.9	10.6	41.3

In the case of the lactic acid the *mixed glass*, which presumably represents a greater variety of molecular composition, exhibits a distinctly more gradual transition than the *acid glass*, as may be seen in Fig. 3. This result is in agreement with the previous studies on mixed alcohol glasses.[1]

Some interesting points come out in the case of the nonpolar 3-methylhexane if we deal with C_v instead of the experimentally measured C_p values. The molecular volume (V) and the coefficients of isothermal expansion (α) and compressibility (β) have been reported for this compound at 20°C by Edgar and Calingaert.[9] By use of the thermodynamic relationship

$$C_p-C_v=\alpha^2VT/\beta$$

we then find $C_v=41.3$ cal. per mole at 290°K. Taking the quantity α^2/β above the transition region as constant with temperature, we have then derived the additional values given in columns 3 and 4 of Table IV. The lone value for C_p-C_v below the transition region constitutes a somewhat cruder guess, based on fragmentary data concerning the change of α and β for the analogous case of glucose.[1b]

The tabulated data show that C_v changes relatively little for the liquid heptane above 92°K, and its order of magnitude can be readily accounted for. If we neglect the vibrations of the hydrogen atoms attached to carbon, which are generally regarded as negligible below 250°K, there are left twenty-one degrees of freedom for the heptane molecule. Postulating only harmonic vibrational motion within the liquid, we thus obtain for the upper limit of C_v $21R$ or 41.7 cal./deg., which is merely 4.7 to 0.4 calories higher than the actual values above 92°K. The much lower C_v value of 20.3 cal./deg. at 82° may be interpreted either on the basis of a very rapid decline of the heat capacity associated with these vibrational degrees of freedom consequent to a rapid increase in their characteristic frequencies within the temperature interval 92°–82°, or perhaps to the actual loss of some of these degrees of freedom with lowering temperature. Of course this glass at 82°K, which is the apparent lower edge of the transition region, must be regarded as a comparatively inert material. Thus on the assumption of a characteristic frequency of the order of 10^{13} per second (which seems plausible in view of Andrews' studies on several organic crystals[10]) we have estimated that the average heptane molecule acquires between the absolute zero and 82°K only about one quantum of energy, distributed between these twenty-one degrees of freedom.

Throughout this discussion the interval of 10° or so, in which the specific heats rise suddenly, almost discontinuously, has been termed the *transition region*. Previous studies in this series[1, 11] have shown that the character of the curve here depends upon the way in which the heating is carried out and to some extent upon the thermal history of the glass. With the Nernst method the transition in organic materials becomes somewhat more abrupt with increased annealing during the initial formation of the glass and also with enlargement of the time intervals between successive heat capacity determinations. Such considerations make very plausible the earlier suggestion of Gibson and Giauque[12] that "if it were possible to obtain a glass free from strain at all temperatures, the liquefaction would occur at a definite temperature"; and recently several students of the glass problem, including Berger[13] and Tammann,[14] have adopted this notion of a *transformation point* (analogous to the melting point of a crystal) separating the glassy and viscous liquid conditions. This idealization of the transition region into a transformation point certainly fits in with the conception of a glass as

[9] Edgar and Calingaert, J. Am. Chem. Soc. **51**, 1540 (1929).

[10] Andrews, Chem. Rev. **5**, 533 (1928); *Colloid Symposium Annual*, Vol. 7 (John Wiley and Sons, New York, 1930), pp. 119–128.

[11] Thomas and Parks, J. Phys. Chem. **35**, 2091 (1931).

[12] Gibson and Giauque, J. Am. Chem. Soc. **45**, 95 (1923).

[13] Berger, J. Am. Ceram. Soc. **15**, 647 (1932).

[14] Tammann, Zeits. f. anorg. allgem. Chemie **190**, 48 (1930).

an amorphous solid,[15] or a fourth state of matter[16] —a conception that has much to be said for it from the purely practical standpoint of classifying our knowledge of the properties of glasses. Other investigators, however, consider that a glass is simply an undercooled liquid of great viscosity; and some adherents of this theory, notably Littleton[17] and Morey[18] in recent years, maintain that with *true* internal equilibrium within the glass at all temperatures the transition in a property, such as specific heat, must become more gradual and apparent discontinuities will disappear. The attainment of such complete internal equilibrium in glasses at the lower temperatures would presumably require long periods of time—months or even years. Accordingly, a thorough test of these opposing views of the transition region, which are both plausible in their way, is probably impossible in the case of heat capacity data because calorimetric procedures, at least at the present day, do not permit accurate measurements over such periods of time.

The present study also throws some light upon the nature of organic glass-forming materials. All three of the substances here investigated contained dextro and laevo molecules in equal numbers. The secondary butyl alcohol and 3-methylhexane could not be crystallized; the lactic acid, which probably forms a racemic compound, exhibited only a moderate tendency to crystallize. Apparently in many types of compounds, and notably in the hydrocarbons, the presence of the two varieties of molecules with equal intermolecular forces and energy contents strongly militates against any crystallization process. In the case of some very polar organic liquids, ethyl alcohol for example, a somewhat comparable variety of molecular species may undoubtedly be attained through a variable association of the ultimate molecular units; but this association, being rather temporary in character, produces a glass which more readily crystallizes.

The entropy and free energy of *dl*-lactic acid

The heat capacity data for the lactic acid provide a basis for a calculation of its molal entropy and free energy at 298.1°K by means of the third law of thermodynamics.

By application of the extrapolation method of Kelley, Parks and Huffman[19] to the data for the crystals in Table II, the entropy increase between the absolute zero and 90° was estimated as 11.51 e.u. (cal. per degree) per mole. According to Borsook, Huffman and Liu[3] the melting point of pure *dl*-lactic acid is 289.9°K, i.e., about 0.8° higher than that found by us with acid of somewhat lower purity. The entropy increase for the crystals between 90° and 289.9°K, calculated from the data in Table II, is 23.62 e.u. The molal entropy of fusion is $(30.1)\times(90.05)/289.9$ or 9.36 e.u. From the heat capacity values in Table II the entropy increase of the liquid between 289.9° and 298.1° is found to be 1.44 e.u. Addition of these various increments then yields $S_{298}^\circ = 45.9(\pm 1.0)$ e.u. for the molal entropy of *dl*-lactic acid in the liquid state.

By using 326,000 cal., a revision by Kharasch[20] of the value of Emery and Benedict for the heat of combustion of lactic acid at constant pressure, in conjunction with the values 68,310 cal. and 94,240 cal.[21] for the heats of combustion of hydrogen and graphitic carbon, respectively, we find for the process

$$3C(\text{graph.}) + 3H_2 + 1\tfrac{1}{2}O_2 = dlCH_3-CH(OH)-CO_2H(1)$$

$$\Delta H_{298} = -161{,}700(\pm 2000)\ \text{cal.}$$

Taking for the atomic entropies[21] 1.36 e.u. for carbon, 15.615 e.u. for hydrogen and 24.52 e.u. for oxygen, we next find $\Delta S_{298}^\circ = -125.4$ e.u. (cal. per degree) for this process. By the fundamental thermodynamic relation, $\Delta F = \Delta H - T\Delta S$, we then obtain $\Delta F_{298}^\circ = -124{,}300(\pm 2300)$ cal. for the free energy of formation of a mole of liquid *dl*-lactic acid from its elements. The uncertainty in this last value can be greatly reduced when a more reliable combustion value for lactic acid becomes available.

[15] Warren, Rev. Sci. Inst. **4**, 520 (1933).
[16] Parks and Huffman, Science **64**, 363 (1926).
[17] Littleton, Ind. Eng. Chem. **25**, 748 (1933).
[18] Morey, J. Am. Ceram. Soc. **17**, 315 (1934).
[19] Kelley, Parks and Huffman, J. Phys. Chem. **33**, 1802 (1929).
[20] Kharasch, Bur. Standards J. Research **2**, 390 (1929).
[21] Parks and Light, J. Am. Chem. Soc. **56**, 1512 (1934).

Studies on Glass

XIII. Glass Formation by a Hydrocarbon Polymer

JOHN D. FERRY* AND GEORGE S. PARKS, *Department of Chemistry, Stanford University*

(Received October 14, 1935)

Polyisobutylene, with an average molecular weight of about 4900, is at room temperature a highly viscous liquid. When cooled, it has been found to form a glass, with the same transitions in thermal properties characteristic in the vitrification of substances of low molecular weight. The heat capacity of polyisobutylene has been measured from 118°K to 295°K. It increases by 32 percent between 192°K and 202°K. The thermal expansion coefficient of polyisobutylene has been measured from 160°K to 300°K. It increases by 200 percent between 185°K and 205°K. The mean temperature of transition corresponds to a viscosity of about 10^{13} poises, in agreement with a rule observed generally for glass-forming materials. The factors on which the transition temperature depends are discussed.

INTRODUCTION

GLASSES have been described as amorphous solids, characterized by optical isotropy and by lack of symmetry or periodicity in the microscopic arrangement of structural elements. On the other hand, a very clear characterization of the vitreous state of matter from a macroscopic standpoint is given by thermal properties. When a glass is heated through the temperature range in which it softens to a viscous liquid, there is in nearly every case a rapid—almost discontinuous—increase in the heat capacity and thermal expansion coefficient, taking place in a small temperature interval. In contrast to the fusion of a crystalline solid there is no latent heat effect or sudden increase in volume. This type of phenomenon is termed by Ehrenfest[1] a "transition of the second order," since discontinuities appear, not in the heat content and volume of the substance, but in the temperature derivatives of these quantities.

Transitions of this sort have been observed not only for silicate glasses[2] and various amorphous materials,[3] but also for many simple organic compounds and for boron trioxide[4] and elementary sulphur[5] and selenium.[5] In several cases (silicate glasses, boron trioxide, glucose,[6] and glycerol[7]), the viscosity of the viscous liquid above the transition range of temperature has been studied. Extrapolation or continuation of measurements into the transition range indicates that, at the midpoint of the latter, the viscosity of the material is between 10^{13} and 10^{14} poises. This rule appears to hold irrespective of the nature of the material or of the mean temperature at which the transition takes place (510°K for boron trioxide; 185°K for glycerol).

All of the organic compounds previously studied are simple substances of low molecular weight, which can be undercooled without crystallization. As examples may be cited 3-methylhexane,[8] ethyl alcohol,[9] propylene glycol,[9] lactic acid,[8] and glucose.[10, 11] The present study deals with a polymeric substance whose molecular size is of an entirely different order of magnitude. This substance, polyisobutylene, is an example of the linear or "chain-molecular" polymers which have been the subject of much investigation by Staudinger[12] and others.

Many organic polymers of very high molecular weight have been briefly described as "glassy" solids because of transparency and brittleness. It was anticipated that a lower polymer, being a viscous liquid at room temperature, would vitrify upon cooling and undergo the characteristic transition observed for simple organic compounds.

* Shell Research Fellow at Stanford University for the academic year 1934–35.

[1] Konink. Akad. Wetensch. Amsterdam **36**, 153 (1933).
[2] Jenckel, Zeits. f. anorg. allgem. Chemie **216**, 367 (1934).
[3] Samsoen, Comptes rendus **181**, 354 (1925); **182**, 517 (1926).
[4] Spaght and Parks, J. Phys. Chem. **38**, 103 (1934).
[5] Mondain-Monval, Ann. chim. **3**, 5 (1935).
[6] Parks, Barton, Spaght and Richardson, Physics **5**, 193 (1934).
[7] Parks and Gilkey, J. Phys. Chem. **33**, 1428 (1929).
[8] Parks, Thomas and Light, preceding article.
[9] Parks and Huffman, J. Phys. Chem. **31**, 1842 (1927).
[10] Parks and Thomas, J. Am. Chem. Soc. **56**, 1423 (1934).
[11] Parks, Huffman and Cattoir, J. Phys. Chem. **32**, 1366 (1928).
[12] Staudinger, *Die Hochpolymeren Organischen Verbindungen* (Julius Springer, Berlin, 1932).

This was amply confirmed in the present study on polyisobutylene, which is found to have a transition at a mean temperature of about 197°K. Data for the heat capacity and thermal expansion are here presented; the viscous properties of the material are described elsewhere.[13]

Material

The sample of polyisobutylene employed in this work was a mixture of polymers with a wide range of molecular weights. The average molecular weight, as determined by cryoscopic measurements in benzene solution, was about 4900.

The molecules of polyisobutylene, like those of other "linear" polymers, are generally supposed to be unbranched chains of great length. This hypothesis, while not at present susceptible to proof, is supported by the viscosity studies of Staudinger,[12] and (in the case of polystyrene and other polymers) by various physical measurements in dilute solution, such as diffusion[14] and streaming double refraction.[15] The most probable arrangement for the isobutylene units in polyisobutylene is:

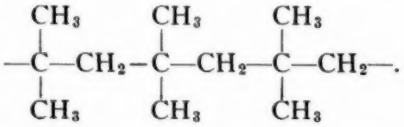

If bond lengths and angles are the same as in normal paraffins, a molecular weight of 4900 corresponds to a length of about 220A. Actually, more complicated arrangements may be involved, with side chains longer than the methyl groups.

The density of our sample, determined at three temperatures, is given in Table I. The refractive index at 27.1°C was $n_D = 1.50451$.

TABLE I. *Density of polyisobutylene.*

Temperature (°C)	23.4	100.2	178.2
Density (g/cc)	0.9074	0.873	0.835

Heat Capacity Measurements

Method

Heat capacity measurements were carried out by a modification of the Nernst method of aneroid calorimetry. The apparatus and procedure have been fully described elsewhere.[16, 17] The absolute errors in the values reported are probably within less than 1 percent, except in the temperature interval of transition, where the thermal conductivity of the material is lower, and uncertainty in attainment of complete thermal equilibrium arises.

Results

In the first series of determinations, low temperatures were reached always by very slow cooling, to insure a well-annealed sample. The measurements involved occasional alternate heating and cooling, and overlapping series of values showed the results to be quite reproducible and unaffected by this thermal treatment, so long as the cooling was slow (crossing the transition region in about 24 hours). The results, expressed in terms of the 15° calorie per gram, and with all weights reduced to a vacuum basis, are given in Table II. These values are plotted against the absolute temperature in Fig. 1 as curve I. The heat capacity of the sample thus "annealed" by slow cooling increases by 32 percent within the temperature interval 192°K to 202°K (the "transition interval"). The rise in the curve is quite sharp, in spite of the wide range of molecular weights in the material.

A second series of determinations was made to show the effect of absence of annealing. The same sample was cooled rapidly, the transition interval being crossed in less than an hour. The heat capacity values for this unannealed sample are given in Table III, and are plotted as curve II in Fig. 1.

TABLE II. *Specific heats in cal. per degree for polyisobutylene (annealed sample).*

T(°K)	C_p	T(°K)	C_p	T(°K)	C_p
121.0	0.167	193.4	0.283	242.6	0.410
127.2	0.176	197.5	0.325	247.9	0.415
133.4	0.185	200.2	0.363	253.3	0.421
139.7	0.194	201.4	0.371	258.5	0.426
145.4	0.202	201.5	0.367	263.5	0.431
150.9	0.210	205.2	0.376	268.6	0.436
156.9	0.218	208.9	0.379	275.1	0.445
162.4	0.227	212.5	0.384	278.7	0.448
167.9	0.235	216.7	0.387	282.0	0.451
174.1	0.243	221.1	0.390	286.5	0.456
179.3	0.252	225.7	0.394	291.2	0.462
184.3	0.260	231.5	0.399	294.9	0.466
189.1	0.269	237.0	0.404		

[13] Ferry and Parks, Physics **6**, 356 (1935).
[14] Herzog and Kudar, Zeits. f. physik. Chemie **A167**, 343 (1934).
[15] Signer and Gross, Zeits. f. physik. Chemie **A165**, 181 (1933).
[16] Parks, J. Am. Chem. Soc. **47**, 338 (1925).
[17] Parks and Kelley, J. Phys. Chem. **30**, 47 (1926).

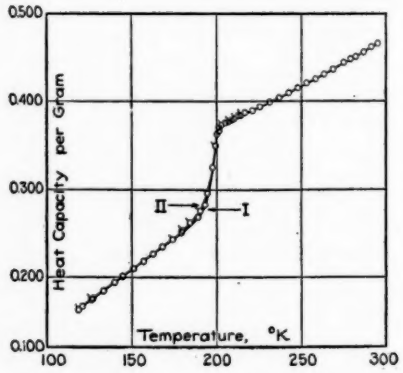

FIG. 1. The specific heat of polyisobutylene in calories per degree plotted against the absolute temperature. The plain circles (curve I) denote determinations made following slow cooling; the tailed circles (curve II), determinations made following rapid cooling.

TABLE III. *Specific heats in cal. per degree for polyisobutylene (unannealed sample).*

T(°K)	C_p	T(°K)	C_p	T(°K)	C_p
118.5	0.163	184.6	0.262	202.7	0.374
126.2	0.174	189.8	0.276	206.6	0.378
—		194.4	0.296	210.3	0.381
174.0	0.244	199.0	0.350	214.1	0.384
179.5	0.254				

The heat capacity rise is evidently slightly less sharp than in the case of the annealed sample. However, the values above and below the transition interval agree very closely in the two cases. Differences in thermal history apparently do not affect the heat capacity except at temperatures in and immediately below the transition region. This was also found to be true for propylene glycol,[9] boron trioxide,[18] and glucose[10] glasses.

THERMAL EXPANSION MEASUREMENTS

Method and apparatus

Thermal expansion measurements were carried out in two types of dilatometers, constructed of Pyrex glass and of brass, respectively, with an aqueous solution of ethyl alcohol as a dilatometric fluid.

The Pyrex dilatometer design was essentially a large model of a liquid-in-glass thermometer. A cylindrical bulb 1.9 cm in diameter and 10.8 cm long was provided with a thermocouple well sealed in from the bottom, and an 80-cm capillary tube of suitable bore (2.4 mm or 1.7 mm) sealed on the top. Introduction of the polyisobutylene was accomplished by cutting off the capillary to leave an aperture about 0.8 cm in diameter, filling with the polymer up to a point 3 cm below the break, and sealing the capillary back on.

The glass dilatometers were employed for measurements from room temperature down to 230°K. Below this point, the expansion coefficient of the polyisobutylene appeared to fall off steadily with decreasing temperature. This drop was attributed not to a real transition (which by analogy with the heat capacity results should appear only below 205°K), but to lack of internal mechanical equilibrium. The polyisobutylene, introduced at a temperature where it was moderately fluid (viscosity 10^5 poises), wetted the walls of the dilatometer and adhered firmly to them. When the temperature was lowered, the adherence to the walls prevented immediate contraction and uniform recession of the upper surface. Stresses were introduced, and these were relieved by viscous flow. Rough calculations based on a model of Poiseuille flow through a cylindrical tube[19] indicated that, below 220°K, the time required for relief of these stresses would become longer than the times ordinarily taken for measurements. Thus the Pyrex dilatometers were inapplicable below 220°K.

The metal dilatometer obviated adherence of the polyisobutylene to the walls. It consisted of a cylinder and cap which, when assembled with a solder gasket, had the same external dimensions as the Pyrex bulb. It was provided also with a thermocouple well, and with a strong iron capillary tube which was continued by a calibrated Pyrex capillary attached at a joint sealed by litharge and glycerine cement. In the cylinder was placed a cylindrical basket of fine brass gauze, with a hole in the bottom to accommodate the thermocouple well. The basket was lined with filter paper to confine the polyisobutylene. This arrangement kept the material from contact with the rigid walls of the dilatometer, and the mechanical flexibility of the container permitted free contraction at low temperatures.

The dilatometric fluid was introduced into either type of dilatometer by evacuating the system and then, by means of a three-way

[18] Thomas and Parks, J. Phys. Chem. 35, 2091 (1931).

[19] We are indebted to Professor F. Bloch for suggesting this model.

stopcock, allowing the freshly boiled-out liquid to flow over into it. Persistent bubbles were removed by introducing into the calibrated capillary a tube drawn out to a diameter of 0.8 mm and a length of a meter. This device also served in removing the dilatometric liquid, which was expelled by inverting the dilatometer and blowing air through the inner tube.

For temperature control, the dilatometer was surrounded by a cylindrical copper jacket, provided with a heating coil and copper-constantan thermocouple. A similar thermocouple measured the temperature in the well of the dilatometer; while a differential thermocouple, with one junction in the well and the other on the outside of the dilatometer, provided a control on radial temperature gradients. The thermoelectric forces of these thermocouples were measured with a White double potentiometer. The jacket was separated by an air gap from a brass can which was immersed in a cooling bath to attain and maintain low temperatures. Baths of ice, ice and alcohol, and alcohol and solid carbon dioxide were employed. For temperatures below the sublimation point of carbon dioxide, the outer can was provided with a coil of 3-mm copper tubing, through which liquid air was pumped, the whole system being immersed in a bath of precooled alcohol. The apparatus is illustrated in Fig. 2.

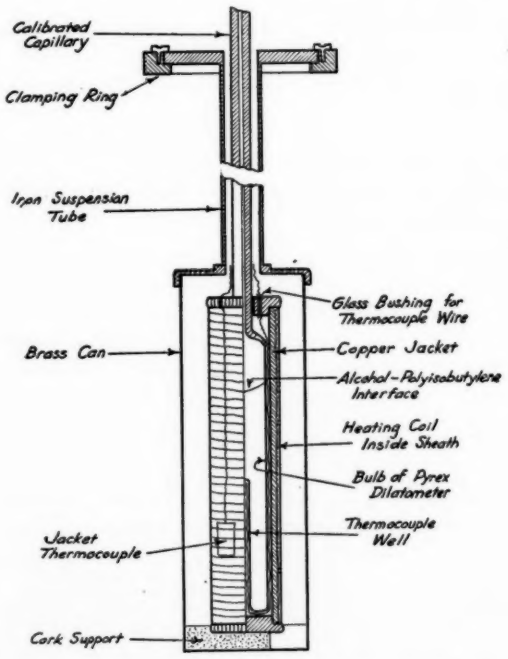

FIG. 2 Apparatus for measurement of thermal expansion.

Each series of expansion measurements was commenced at the bottom of the temperature range to be covered. Thermal equilibrium at any desired temperature was maintained by electrically heating the jacket sufficiently to compensate for the loss of heat from it to the outer can. Criteria for equilibrium were constancy of dilatometer temperature and absence of radial thermal gradients. The height of the liquid column in the capillary was read by a cathetometer. Determinations of corresponding temperatures and column heights were made at intervals of about 6°. The thermal expansion coefficient of volume was calculated over each such interval, and was assumed to represent the instantaneous value at the midpoint of the interval ($\alpha=(1/V)(dV/dT)$).

Thermal expansion of 92.5 percent aqueous ethyl alcohol

Ethyl alcohol fulfilled all the requirements for a dilatometric fluid over the appropriate temperature range. A sample from the ordinary laboratory supply was employed; the presence of water was an advantage, since it assured undercooling of the liquid below its melting-point (159°K). The density of the solution at 22.0°C was 0.8089 g/ml in vacuum, corresponding to a weight-concentration of 92.5 percent ethanol, according to the data of the *International Critical Tables*.

Since no expansion data for such a solution were available, measurements were first made for this alcohol with Pyrex dilatometers. The thermal expansion coefficients were calculated by the equation

$$\alpha_1=\alpha_0+(v_T/v_R)(A/V)(\Delta h/\Delta T), \qquad (1)$$

where α_1 and α_0 are the expansion coefficients of the alcohol and Pyrex, respectively, v_T and v_R the specific volumes of the alcohol at the mean temperature of the dilatometer and at that of the capillary column, respectively, A the cross section area of the capillary, V the volume of that part of the dilatometer system whose temperature is controlled by the jacket, and Δh and ΔT the observed changes in height and temperature. The values for α_0 were calculated

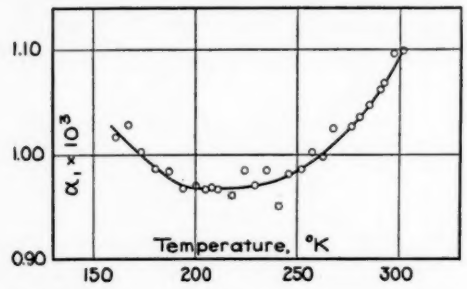

FIG. 3. The thermal expansion coefficient of 92.5 percent aqueous ethyl alcohol plotted against the absolute temperature.

from the data of Buffington and Latimer.[20] The values for v_T were calculated by rough numerical integration of α_1, proceeding by successive approximations. The results for α_1 are plotted against the absolute temperature in Fig. 3. Above 0°C, these results are in very satisfactory agreement with values obtained by differencing density data from the *International Critical Tables*.

The expansion of the metal dilatometer was determined by calibration measurements with the same stock alcohol.

Thermal expansion of polyisobutylene

The expansion coefficients of polyisobutylene were calculated by the equation

$$\alpha_2 = 1/V_p\{dV/dT - (V - V_p)\alpha_1 + (v_T/v_R)A(\Delta h/\Delta T)\}, \quad (2)$$

where V_p is the volume of the polyisobutylene at the mean temperature of the measurement. This was obtained by numerical integration of α_2 from room temperature (where the density of the polymer was known accurately) down, proceeding by successive approximations. The term dV/dT was given by the calibration for the metal dilatometer, or by $V\alpha_0$ for the Pyrex apparatus.

The results of six series of determinations are plotted in Fig. 4. The results from the metal dilatometer are more subject to fortuitous error, because the basket arrangement contained a much smaller sample of polymer than did the Pyrex bulb, and the contribution of the alcohol to the observed expansion was much greater. The absolute errors in the values above 230°K are believed to be within 4 percent.

[20] Buffington and Latimer, J. Am. Chem. Soc. **48**, 2305 1926).

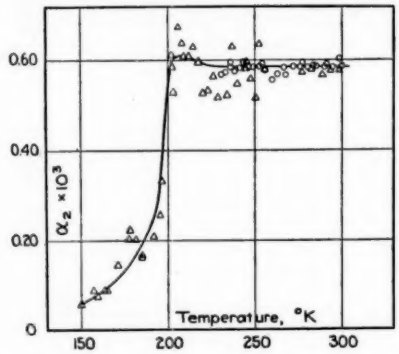

FIG. 4. The thermal expansion coefficient of polyisobutylene plotted against the absolute temperature. The triangles denote measurements with the metal dilatometer; the circles, measurements with Pyrex dilatometers.

The thermal expansion coefficient of polyisobutylene evidently increases by 200 percent within the temperature interval 185°K to 205°K.

It is of interest to note the complete similarity between these results and the expansion measurements of Bekkedahl[21] on rubber hydrocarbon, a natural product obtained from latex.

DISCUSSION

The transitions in heat capacity and thermal expansion for polyisobutylene are entirely similar to those observed for simple organic glass-forming liquids and for boron trioxide, except that the magnitude of the increase in heat capacity is considerably less in the present case. Further, the viscosity-temperature curve of polyisobutylene,[13] when extrapolated to 197°K (the midpoint of the transition interval), shows a viscosity of about 10^{13} poises, in agreement with the rule found generally for glass-forming systems.

The tendency toward vitrification as an alternative to crystallization has been discussed by Randall and others.[22] If a liquid can be supercooled through its melting-point without crystallization starting, and the cooling is continued to a sufficiently low temperature, the material becomes so viscous that orientation of molecules into a crystal lattice is henceforth virtually impossible. Ease of supercooling is the deciding

[21] Bekkedahl, Bur. Standards J. Research **13**, 411 (1934).

[22] Randall, *The Diffraction of X-Rays and Electrons by Amorphous Solids, Liquids, and Gases* (Wiley and Sons, New York, 1934), pp. 182–184. See also Cline and Andrews, J. Am. Chem. Soc. **53**, 3671 (1931); and Zachariasen, J. Am. Chem. Soc. **54**, 3841 (1932).

factor; this probably arises from optical isomerism in many cases and from a variable association in the case of simple alcohols.[8] In polyisobutylene, the steric hindrance of the long, clumsy chain molecules, and the variety of molecular species present, undoubtedly account for the failure to crystallize under any circumstances.

The temperature at which the transitions in heat capacity and thermal expansion occur seems in general to be connected with a viscosity of 10^{13} poises, and hence with a certain definite degree of intermolecular interaction. When glass-forming substances are arranged in the order of the mean temperatures of their transition regions, the series progresses regularly from nonpolar compounds through compounds of increasing dipole moment to a substance like boron trioxide, whose structure involves a network of valence bonds throughout. For equal dipole moments, the compounds fall in the order of increasing molecular weights. Polyisobutylene, although virtually nonpolar, has a mean temperature of transition corresponding to rather polar compounds, falling between glycerol and lactic acid. This may be qualitatively explained on the basis of its huge molecular weight, which may be considered to overbalance the effect of the nature of the intermolecular forces. More specifically, we may consider the binding among the isobutylene units in the material. Binding between units in different macromolecules is of a purely van der Waals character, similar to the intermolecular interaction in nonpolar compounds. Units in the same macromolecule, however, are connected by chemical bonds—a type of binding more analogous to that in boron trioxide than to that in any other organic glass-forming material. The resultant of these two types of binding places the transition temperature of polyisobutylene somewhere between those of nonpolar heptanes (about 88°K) and boron trioxide (about 510°K).

JANUARY, 1936 JOURNAL OF CHEMICAL PHYSICS VOLUME 4

The Kinetics of the Oxidation of Gaseous Hydrocarbons

III. The Oxidation of Acetylene

E. W. R. STEACIE AND R. D. MCDONALD, *Physical Chemistry Laboratory, McGill University, Montreal*

(Received October 7, 1935)

An investigation of the kinetics of the oxidation of gaseous acetylene has been made by the static method. The results show marked irregularities due to variations in the surface. The rate of the reaction is given by

$$-(d/dt)(C_2H_2) = K(C_2H_2)^{2\cdot7}/(O_2)^{0\cdot1}$$

when oxygen is in excess. In a packed bulb the order is diminished to about 1.4. Packing decreases the rate at high pressures and has little effect at low pressures. In an empty vessel the CO/CO_2 ratio of the products is independent of the pressure. Packing decreases this ratio, and it further decreases rapidly with diminishing pressure. The apparent heat of activation of the reaction is about 35,000 calories. The addition of glyoxal to the reaction mixture causes no change in the rate of the reaction, while formaldehyde causes a marked retardation. The products of the reaction are discussed in the light of recent work on the oxidation and decomposition of glyoxal.

INTRODUCTION

THERE have been a number of previous investigations of the oxidation of acetylene. Bone and Andrew[1] interpreted their work by postulating the formation of the unstable dihydroxy compound $C_2(OH)_2$, which was assumed to decompose directly into CO and HCHO. In a more recent investigation, Kistiakowsky and Lenher[2] found that the reaction was a chain process with the rate proportional to the square of the acetylene concentration, and a slight retardation by oxygen. The condensable products

[1] Bone and Andrew, J. Chem. Soc. **87**, 1232 (1905).

[2] Kistiakowsky and Lenher, J. Am. Chem. Soc. **52**, 3785 (1930).

were mainly glyoxal, formaldehyde, and formic acid. They suggested that the primary step in the reaction was the formation of glyoxal, which subsequently was oxidized or decomposed. They did not attempt to arrive at the chain process. The investigation was further extended by Spence and Kistiakowsky.[3] After a further investigation, Spence[4] proposed a mechanism for the reaction based in principle on the Bodenstein scheme, activated glyoxal being assumed to carry the chains.

The present paper deals with an investigation of the acetylene oxidation by the static method, with special emphasis on high oxygen concentrations and on the effect of surface. Experiments have also been made on the oxidation of mixtures of acetylene and glyoxal, and of acetylene and formaldehyde to determine the possibility of these substances acting as carriers of the reaction chains.

Experimental

The change in pressure accompanying the oxidation of acetylene is too small to permit its use as a method of following the reaction, and it was therefore decided to investigate the reaction by withdrawing samples of gas for analysis from time to time. The apparatus was similar to that employed in previous investigations.[5] Mixtures of oxygen and acetylene were made up and introduced into silica or Pyrex reaction vessels of about 200 cc capacity at the desired temperature. After a definite time the gaseous mixture was withdrawn and analyzed in a Burrell gas analysis apparatus.

The oxygen used was taken directly from cylinders of the commercial gas and dried over phosphorus pentoxide. Analysis showed it to contain from 1.0 to 1.4 percent nitrogen. Acetylene was generated from calcium carbide, and was washed with solutions of potassium hydroxide, chromic acid, mercuric chloride in hydrochloric acid, and alkaline hydrosulphite. It was then dried and condensed with liquid air and fractionated. From 98.7 to 99.4 percent was absorbed in fuming sulphuric acid.

In theory the use of the analytical method is extremely simple. A number of experiments are performed under identical conditions, and are interrupted and a sample taken at various times. We may then construct a rate curve and from it determine either the velocity constant or the time to half-value. The great disadvantage of the method is that each experiment gives only a single point on the amount reacted-time curve, and the investigation is thus exceedingly laborious.

The method used here to avoid this is as follows. The value of, say, T_{50} is obtained under one set of conditions from a series of experiments as described above. Then to determine the order another experiment is performed at a higher pressure and the sample is withdrawn at a time which would correspond to 50 percent reaction if the reaction had some plausible assumed order, say 2. Since the order is not exactly 2, the amount reacted as determined by analysis is not 50 percent, but say 55 percent. The order is thus more than 2, and since the percent reacted is not very different from 50, the time for 50 percent reaction can be calculated to a fair approximation still assuming an order of 2. An approximate graph of T_{50} against pressure is obtained in this way, and hence the approximate order. The calculations are then repeated with this more accurate value of the order, and the real order is thus found by successive approximations from only one experiment at each pressure.

The amount of reaction has in every case been inferred from the percentage of unchanged acetylene in the gaseous reaction products. The calculation can only be made, however, provided that no condensable products are present, or that the amount and composition of such products is known. As will be shown later, on the average about 5 percent of the total carbon goes to form such condensable products, and all calculations of the amount of reaction have been made on this assumption.

Experimental Results

The pressure change accompanying the reaction

As mentioned at the outset, the pressure change accompanying the reaction is comparatively small. The actual pressure increase found

[3] Spence and Kistiakowsky, J. Am. Chem. Soc. **52**, 4837 (1930).
[4] Spence, J. Chem. Soc. **1932**, 686.
[5] Steacie and McDonald, J. Phys. Chem. **38**, 1031 (1934).

varied widely with the experimental conditions. The pressure-time curves, however, always had roughly the same form, the pressure decreasing very slightly at the start and then rising. Almost without exception, it was found that, for corresponding stages of the reaction, the relative pressure changes were greater the lower the initial pressure. Depending upon the conditions, the pressure increase corresponding to 50 percent reaction varied from 3 to 11 percent. With a packed reaction vessel the form of the pressure time curves was completely altered, and the pressure decreased steadily but very slightly.

The order and the rate of the reaction

The rate of the reaction was found to be very variable, and to be strongly dependent upon the condition of the surface of the reaction vessel. On this account a number of different vessels were used which had been subjected to various surface treatments. The different series of experiments are described below.

Series I. A mixture consisting of $2O_2+1C_2H_2$ was used at 320°C. The reaction vessel was a spherical Pyrex bulb. It was washed and given a prolonged evacuation at 550°C. The rate was found to increase steadily for some 40 runs. Heating to 550°C with and without air between runs had no effect on the results. Little information could be obtained from this series, except that the over-all order of the reaction was between 2 and 3.

Series II. The reaction vessel was a Pyrex bulb as before. It was rinsed with a normal solution of NaCl, and then once with distilled water, a treatment which Lenher and Kistiakowsky found to speed up the reaction and to make the results more reproducible. In the present work the rate was increased, but the drift was very pronounced and after a few runs the bulb was discarded.

Series III. A spherical Pyrex vessel of 200 cc capacity was used. It was rinsed with a saturated solution of potassium chloride and evacuated. The aging in this case was much less pronounced, but was still somewhat troublesome. The results will therefore not be given in detail. Runs were made with 2:1, 3:1, and 5:1 mixtures. These indicated an order between 2.4 and 2.6, and that oxygen had a very slight retarding effect on the reaction.

Series IV. The same vessel as in III was used after a further treatment with saturated potassium chloride solution. The reproducibility in this case was excellent and about 25 runs were made. The gas analyses are given in detail in Table I. It will be seen from the constancy of the $(CO+CO_2)/C_2H_2$ ratio, which is obviously a measure of the amount of reaction, that the times chosen for sampling correspond almost exactly to equal amounts of reaction. The corrections which must be made, as described above, are very little greater than the experimental error. These corrections have been made, and the results are given in Fig. 1 in the form of a $\log T_{45}-\log P_{C_2H_2}$ graph.

As shown by Table I, the CO/CO_2 ratio of the products remains constant for any O_2/C_2H_2 ratio. It also varies very little with the different mixtures. Thus on going from a 1:1 to a 5:1 O_2/C_2H_2 mixture the CO/CO_2 ratio falls only about 10 percent.

From the slopes of the lines in Fig. 1, the over-

TABLE I. *Gas analyses from series IV.*

No.	$P_{C_2H_2}$, Initial. (cm)	t (min.)	Composition of sample—% CO_2	C_2H_2	O_2	CO	H_2	N_2	A	B
TEMPERATURE = 320°C A = CO/CO_2 B = $(CO+CO_2)/C_2H_2$										
ORIGINAL MIXTURE—O_2/C_2H_2 = 1										
18	21.5	9.8	8.8	31.6	20.2	37.4		2.0	4.25	1.46
20	19.6	11.6	8.3	32.1	20.0	37.4		2.2	4.50	1.42
21	15.7	17.8	8.2	31.4	21.3	37.2		1.9	4.54	1.44
22	12.5	27.6	8.0	31.5	21.6	37.0		1.9	4.63	1.43
19	10.8	36.4	8.1	31.6	20.6	37.5		2.2	4.63	1.44
ORIGINAL MIXTURE—O_2/C_2H_2 = 2										
1	20.5	10.6	6.1	20.3	48.0	23.9		1.7	3.92	1.48
2	16.5	16.0	6.0	20.2	47.6	24.2		2.0	4.03	1.49
13	14.6	19.6	5.6	20.1	48.0	24.3		2.0	4.34	1.49
3	13.2	23.6	5.8	20.3	47.8	24.3		1.8	4.20	1.48
4	10.5	34.6	5.6	20.5	48.4	23.7		1.8	4.24	1.43
5	8.4	51.8	5.4	20.5	48.2	24.1		1.8	4.27	1.44
ORIGINAL MIXTUEE—$O_2/C_2H_2/N_2$ = 2/1/1										
6	15.2	18.2	4.1	14.6	34.6	17.5	0.7	28.5	4.26	1.48
7	12.2	26.6	4.0	14.7	34.3	17.6	0.6	28.8	4.40	1.47
ORIGINAL MIXTURE—O_2/C_2H_2 = 3										
16	15.8	17.5	4.3	14.5	62.0	17.4		1.8	4.05	1.50
17	12.7	25.6	4.1	14.8	62.6	16.8		1.7	4.10	1.41
14	10.0	38.8	4.2	14.8	61.5	17.7		1.8	4.22	1.48
15	7.9	57.2	4.2	14.6	62.0	17.4		1.8	4.14	1.48
ORIGINAL MIXTURE—O_2/C_2H_2 = 5										
8	10.3	38.0	3.1	9.6	74.0	11.6		1.7	3.74	1.53
9	8.2	56.5	2.9	9.7	74.0	11.7		1.7	4.03	1.51
10	6.5	83.0	2.9	9.5	74.4	11.4		1.8	3.93	1.51
ORIGINAL MIXTURE—$O_2/C_2H_2/N_2$ = 5/1/1										
11	9.0	48.0	2.4	8.1	63.4	9.6	0.0	16.5	4.00	1.48
12	7.1	71.5	2.5	8.1	63.2	9.4	0.0	16.8	3.76	1.48

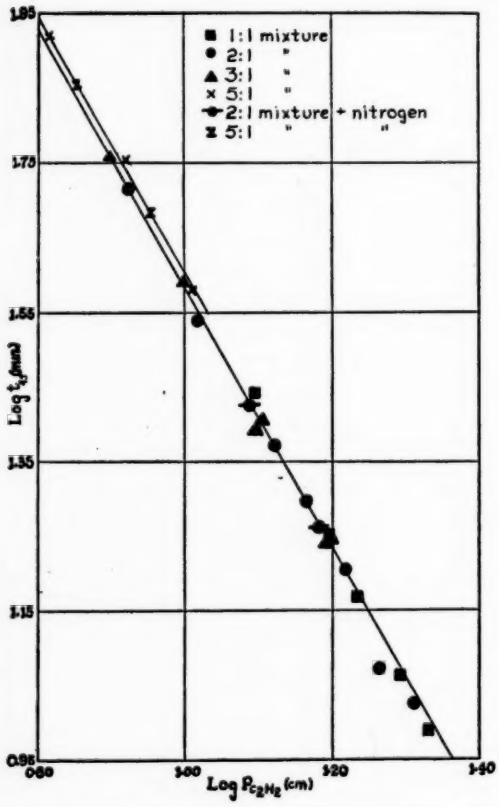

FIG. 1. The effect of pressure on the rate of reaction.

all order is calculated to be 2.7. The 5:1 mixture indicates a slight retardation by oxygen. In the other cases any effect of the oxygen concentration is smaller than the experimental error.

In the runs in which nitrogen was added it is possible to set up material balances and to calculate the amount of condensable products formed. A few typical results of this kind are given in Table II. It will be noted that approximately 5 percent of the total carbon present appears as condensable material. The amount of condensable products present is too small to permit of an accurate calculation of its composition.

Series V. After the completion of the above experiments in Series IV, aging effects again became apparent. A spherical 200-cc silica bulb was therefore tried. After a few experiments in which the rate increased progressively from run to run, conditions became steady and some 50 runs showed excellent reproducibility. These confirmed almost exactly the conclusions reached with the Pyrex bulb, showing an over-all order of about 2.6 and again a slight retardation due to oxygen. The absolute rates in the silica bulb were, however, about 30 percent higher than those in the Pyrex bulb. Material balances and the analyses of the products were also in excellent agreement with Series IV. The material balances, however, showed much better agreement among themselves and thus permitted a rough estimate of the composition of the condensable material. Some typical results are summarized in Table III.

TABLE II. *Material balances—series IV.*

RUN NO.	7			11			12		
	C	H	O	C	H	O	C	H	O
Calculated	53.6	53.6	107.0	29.1	29.1	143.0	29.6	29.6	145.4
Found	51.0	30.6	94.2	28.2	16.2	141.2	28.1	16.2	140.8
Difference	2.6	23.0	12.8	0.9	12.9	1.8	1.5	13.4	4.6

In view of the difference between the value of the order of the reaction found here and that found by Spence and Kistiakowsky, it was of importance to determine whether the order varied with the stage of the reaction as has often been reported for hydrocarbon oxidations. A number of experiments were therefore made at different pressures with a $3O_2 : 2C_2H_2$ mixture. Samples were withdrawn and analyzed at times corresponding approximately to T_{25} and T_{70} instead of to T_{45} as before. These indicated an order identical with the previously found value. The ratios $T_{25} : T_{45} : T_{70}$ were also in agreement with the calculated ratios for an order of 2.6. Hence it may be concluded that the over-all order of the reaction is 2.6 over at least 75 percent of its course.

The temperature coefficient

A separate series of experiments was made in a silica vessel to determine the temperature coeffi-

TABLE III. *Composition of condensable products in typical experiments.*

% COMPOSITION OF CONDENSABLE MATERIAL			% OF TOTAL CARBON IN THE CONDENSABLE PRODUCTS
C	H	O	
10.0	61.1	28.9	7.6
9.0	63.0	28.0	6.7
9.4	61.8	28.8	7.2
9.2	57.0	33.8	7.5
8.8	59.2	32.0	7.0
7.8	59.2	33.0	6.5
8.3	65.5	26.2	5.8
9.9	63.8	26.3	5.5

TABLE IV. *The temperature coefficient of the reaction.*

PRESSURE—13.0 CM $2O_2 : 1C_2H_2$ MIXTURE									
TIME (min.)	TEMP. (°C)	COMPOSITION OF SAMPLE—% CO_2	C_2H_2	O_2	CO	Res.	$\frac{CO}{CO_2}$	$\frac{CO+CO_2}{C_2H_2}$	T_{45} (calc.)
140	280	6.5	18.8	47.3	24.6	2.8	3.79	1.65	118
46.3	300	6.8	17.9	44.5	28.1	2.7	4.13	1.95	32.0
16.5	320	6.3	17.9	45.7	27.5	2.3	4.36	1.89	11.7
6.6	340	5.7	18.9	46.8	26.0	2.6	4.55	1.68	5.4

cient of the reaction. The results are given in Table IV. From the values of T_{45} the activation energy is calculated to be 33,500 calories, in good agreement with the value of 34,700 calories found by Spence and Kistiakowsky. The values of T_{45} in Table IV have been calculated on the assumption that the order does not change with changing temperature. While this may not be strictly true, the correction involved is comparatively small and the value of E would not be very much affected by a small change in order. In any case, in the absence of any very definite significance for the temperature coefficient, it was not considered worth while making an exhaustive investigation to establish it more accurately.

The effect of surface

The effect of increased surface was investigated with a cylindrical silica bulb of about 125 cc capacity. The packing consisted of short lengths of thin silica capillary tubing, and was rather loose, the top quarter of the bulb being empty. The results are given in Table V.

It is apparent that with increased surface:

(a) The rate is decreased at high pressures. At low pressures there is an apparent small increase in rate.

(b) The order of the reaction in the packed bulb is much lower than usual, being only about 1.4.

(c) There is a very marked decrease in the CO/CO_2 ratio in the packed bulb. In the unpacked bulb the CO/CO_2 ratio is independent of the pressure. In the packed bulb, however, the ratio decreases rapidly with decreasing pressure.

TABLE V. *The effect of increased surface.*

TEMPERATURE 320°C			$2O_2 : 1C_2H_2$ MIXTURE		
$P_{C_2H_2}$ (cm)	T_{25} (min.)	CO/CO_2 (products)	$P_{C_2H_2}$ (cm)	T_{25} (min.)	CO/CO_2 (products)
Packed bulb			*Unpacked bulb*		
22.8	25.0	1.56	22.5	16.0	2.52
19.9	27.3	1.21	19.8	18.2	2.32
17.4	30.8	1.08	17.0	25.9	2.37
12.7	34.8	0.71	14.6	29.2	2.48
12.3	34.0	0.65	12.5	34.0	2.49
10.1	36.1	0.58	11.3	38.8	2.57
9.4	36.8	0.47			

TABLE VI. *The effect of added glyoxal and formaldehyde.*

TEMPERATURE 320°C			$2O_2 : 1C_2H_2$ MIXTURE	
$P_{C_2H_2}$ (cm)	TIME (min.)	ADDED GAS	PARTIAL PRESSURE OF ADDED GAS (cm)	% OF ACETYLENE REACTED
12.4	17.7	none	—	23.0
12.4	17.7	glyoxal	1.1	23.6
9.6	26.5	none	—	22.6
9.6	26.5	glyoxal	2.6	25.8
12.3	27.0	none	—	24.3
12.3	27.0	formaldehyde	1.1	17.3
9.0	44.3	none	—	28.2
9.0	44.3	formaldehyde	5.3	9.8

These points will be discussed later.

The effect of additions of glyoxal and formaldehyde

Since glyoxal has often been assumed to play an important part in the oxidation of acetylene, it was of interest to determine the effect of its addition upon the rate of the reaction. A number of experiments were therefore made with and without added glyoxal, and the results are given in Table VI. In each case a known amount of nitrogen was present, so that the amount of acetylene which had reacted could be calculated from analyses of the gaseous products. It will be seen from Table VI that glyoxal has no influence on the rate when it is present in small quantities. At high glyoxal concentrations there is a very slight acceleration of the reaction, but this is probably merely due to the heat developed in the very rapid glyoxal oxidation causing a temporary interruption of isothermal conditions.

The data for similar experiments with formaldehyde are also given in Table VI. It will be seen that formaldehyde has a definite retarding action, which becomes very pronounced at high formaldehyde concentrations. It should be pointed out that an interval of about two weeks occurred between the experiments with glyoxal and those with formaldehyde. During this time considerable aging had occurred, and hence the times for the first 4 experiments in Table VI cannot be compared with those for the last 4 experiments.

Discussion

As we have seen, the over-all order of the reaction is 2.6, with a slight retardation by oxygen. The results can therefore be approximately expressed by

$$-(d/dt)(C_2H_2) = K(C_2H_2)^{2.7}/(O_2)^{0.1},$$

provided that oxygen is in excess. This is rather higher than the order of about 2 found in previous investigations. However, the order diminishes strongly in a packed bulb, and hence in the narrower vessels used in previous investigations by the flow method we would expect the order to be somewhat diminished.

Previous work has indicated the presence of an induction period. The form of the pressure-time curves obtained here (an initial small pressure decrease followed by an increase) suggests that the induction period is to be attributed to the building up of a stationary concentration of some intermediate substance. Curves of this form would be difficult to interpret merely on the conception of an initial time required for the development of branching chains.[6]

The main point is to account in a reasonable manner for the products of the reaction and their variation with changing surface-volume ratio. There seems to be no doubt that glyoxal is one of the most important products of the reaction, and in previous discussions of the mechanism of the reaction the fate of glyoxal has always played a prominent part. In view of the recent investigations of the oxidation and decomposition of glyoxal made in this laboratory,[7] it now seems possible to account for the products of the reaction without being obliged to assume that the intermediate substances react in a way which is contrary to their normal behavior.

We may assume, as has been done almost invariably in the past, that glyoxal is the first recognizable product of the acetylene oxidation. It has recently been shown that at the temperatures used here the glyoxal decomposition is negligibly slow and leads in part to the formation of tarry materials. It may therefore be concluded that none of the glyoxal formed disappears by decomposition. The oxidation of glyoxal is exceedingly rapid at 320°C, and we may assume that it follows its usual course, *viz.*,

$$CHO-CHO+O_2=CHO-COOOH,$$
$$CHO-CHO+CHO-COOOH = 2CHO-COOH.$$

At about 200°C a considerable amount of CO and CO_2 are formed in the glyoxal oxidation, but a large amount of glyoxylic acid survives. At the higher temperatures used here it is not surprising that glyoxylic acid is not detected as a product, especially since the usual tests do not distinguish between trimeric glyoxal and glyoxylic acid. The main fate of the glyoxylic acid will be

$$CHO-COOH \begin{cases} \nearrow CO+HCOOH \\ \searrow CO_2+HCHO \end{cases}$$

It may be remarked that under normal conditions glyoxylic acid does not oxidize to oxalic acid, although it is, of course, possible that some glyoxylic acid disappears by complete oxidation to the oxides of carbon and water. In the glyoxal oxidation the CO/CO_2 ratio of the products is about 3, and hence we may assume that the decomposition of glyoxylic acid to CO and HCOOH predominates. Formic acid can then disappear by decomposition in the usual way. At the temperatures used here, however, the decomposition and oxidation of formaldehyde are quite slow, and Spence has pointed out that in the acetylene oxidation formaldehyde must be oxidized at about 100 times its normal rate. It has recently been shown that various aldehydes oxidize by identical mechanisms,[8] and it therefore seems reasonable to assume that formaldehyde is oxidized by replacing glyoxal in the reaction with glyoxylic peracid, *viz.*,

$$HCHO+CHO-COOOH = HCOOH+CHO-COOH.$$

Hence as a complete scheme for the course of the reaction we have

[6] See Kontorovna and Neumann, Physik. Zeits. Sowjetunion **4**, 818 (1933).

[7] Hatcher, Horwood and Steacie, J. Chem. Phys. **3**, 291, 551 (1935).

[8] Hatcher, Steacie and Howland, Can. J. Research **5**, 648 (1931); **7**, 149 (1932). Steacie, Hatcher and Rosenberg, J. Phys. Chem. **38**, 1189 (1934). Hatcher, Horwood and Steacie, reference 7.

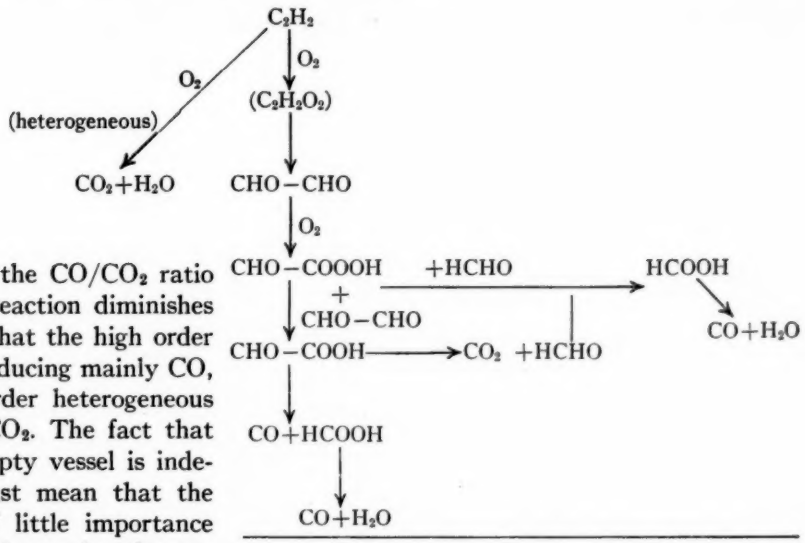

The effect of surface

On increasing the surface the CO/CO_2 ratio falls, and the order of the reaction diminishes to about 1.4. This suggests that the high order chain reaction in the gas, producing mainly CO, is accompanied by a low order heterogeneous reaction producing mainly CO_2. The fact that the CO/CO_2 ratio in the empty vessel is independent of the pressure must mean that the heterogeneous reaction is of little importance when the surface is small. On increasing the surface, however, the heterogeneous reaction is favored by a factor of about 6, while the homogeneous reaction is retarded by the chain-breaking effect of the surface, and hence in the packed bulb the surface reaction becomes prominent. Since the surface reaction has a low order, its influence will be greatest at low pressures, and hence in the packed bulb the CO/CO_2 ratio diminishes with decreasing pressure. The retarding effect of the increased surface also falls off at low pressures, since the increase in the heterogeneous process makes up for the decrease in the homogeneous reaction.

To the foregoing scheme for the course of the reaction, therefore, we must add a heterogeneous oxidation of acetylene to CO_2, which is not of much importance unless the surface-volume ratio is high.

The chain mechanism

The very great sensitivity of the rate of reaction to changes in the condition of the surface makes it apparent that the surface is important either for the initiation or for the breaking of reaction chains. The retarding effect of increased surface, however, is not great, and inert gases have little or no accelerating effect on the reaction. It seems certain, therefore, that the wall is of paramount importance in the initiation of the chains, and does not participate in their destruction to a very great extent.

As in most organic oxidation reactions, it is not possible to infer the carriers of the chains with any degree of certainty. The experiments with added glyoxal and formaldehyde show, however, that normal glyoxal and formaldehyde and their products of oxidation are not the chain carriers. We may therefore exclude glyoxal, glyoxylic acid, glyoxylic peracid, formaldehyde, and formic acid. We may of course assume that in an energy chain one of these products will act as a carrier when it is in an activated state. Since presumably such a substance must be activated before it oxidizes, this necessitates the assumption of different activated states for the same molecule in different, but equally exothermic, reactions. This does not appear very plausible, and it seems more reasonable to assume that the chain carrier is some product which precedes glyoxal. From this point of view a mechanism of the Bodenstein type appears the least objectionable.

Norrish has recently suggested[9] a general theory of hydrocarbon oxidation involving a free radical-oxygen atom chain. On the basis of this mechanism the initiation of the chains occurs by the reaction

$$RCHO+O_2=RCOOH+O.$$

The pertinent aldehydes in this case are glyoxal and formaldehyde, and since both have been shown to have no sensitizing effect on the reaction, it appears unlikely that such a mechanism can hold for the oxidation of acetylene.

[9] Norrish, Proc. Roy. Soc. **A150**, 36 (1935).

LETTERS TO THE EDITOR

The Raman Spectrum and Fundamental Vibration Frequencies of Silane (SiH_4)

We have found the Raman lines for silane, SiH_4, shown in Table I.

Two extremely faint lines were observed at 1195 ± 20 cm^{-1} and 1825 ± 20 cm^{-1}, but their presence is doubtful and they cannot safely be ascribed to SiH_4.

When the gas was exposed to the mercury arc in quartz, a slow decomposition occurred with the deposition of a yellow-white solid. This presumably consists of unsaturated polymerized hydrides. The lines from the gas were obtained without difficulty with Hg 3650, 4078 and 4358A as the exciting radiation.

The silane was prepared by the method of Stock.[1] The final product was purified by repeated fractionation and probably contained less than 0.1 percent impurity. It is of interest to note that our magnesium silicides, prepared by Stock's method, did not yield appreciable quantities of silicon hydrides when treated with NH_4Br in NH_3 (l). This procedure has been found satisfactory by Johnson and Isenberg[2] when the silicide is prepared by a different method.

Silane doubtless has a regular tetrahedral structure. Calling the completely symmetrical vibrational frequency ν_1, the symmetrical twofold degenerate frequency ν_2, and the high and low threefold degenerate frequencies ν_3 and ν_4, respectively, the selection rules[3] permit all four frequencies in the Raman effect, and only ν_3 and ν_4 in the infrared. Steward and Nielsen[4] have measured the infrared absorption bands of silane. The combined infrared and Raman data have led us to the following assignments of the fundamentals: $\nu_1 = 2187$ cm^{-1}, $\nu_2 = 978$ cm^{-1}, $\nu_3 = 2183$ cm^{-1}, $\nu_4 = 910$ cm^{-1}. The strong sharp Raman line 2187 is taken as ν_1. This choice is based on a characteristic of tetrahedral molecules XY_4,[5] namely, that the completely symmetric vibration appears sharp and most intense in the Raman effect.

$\nu_3 = 2183$ cm^{-1}, and ν_4 in the neighborhood of 910 to 980 cm^{-1}, must also be the correct assignments of the two strongest infrared bands. Steward and Nielsen chose $\nu_4 = 910$ cm^{-1}. The infrared band in that region[4] is very complex, and it is possible that the band center is not where they have chosen it. Judging from the appearance of the band the center is not as high as 978 cm^{-1}. Accordingly, with Steward and Nielsen, we have taken $\nu_4 = 910$ cm^{-1}, and have considered the Raman line at 978 cm^{-1} to be ν_2. However, there is the possible alternative that $\nu_4 = 978$ cm^{-1} and that ν_2 is yet to be found, although the above assignment seems more likely, with perhaps some uncertainty as to the numerical value for ν_4. Using the valence-force formulae (Eq. (36)) of Miss Rosenthal[6] which fits the frequencies of methane, CH_4[7] ($\nu_1 = 2915$ cm^{-1}, $\nu_2 = 1530$ cm^{-1}, $\nu_3 = 3020$ cm^{-1}, $\nu_4 = 1320$ cm^{-1}) with an error of about three percent, one calculates $\nu_2 \cong 1042$ cm^{-1} if $\nu_4 = 910$ cm^{-1} or $\nu_2 \cong 1121$ cm^{-1} if $\nu_4 = 978$ cm^{-1}.

TABLE I. *The Raman spectrum of silane.*

	$\Delta\nu$ cm^{-1}	
SiH_4(g), at 5 atmos.	2187	Strong, sharp
	978 ± 5	Very faint
SiH_4(l), at -120°C	2175	Very strong, sharp
	967 ± 10	Medium, diffuse

TABLE II. *Vibrational spectrum of silane.*

	Observed (cm^{-1})	Intensity	Calculated (cm^{-1})
ν_4	910	50	(910)
ν_2	978	Raman, medium	(978)
$\nu_3 - \nu_4$ or $\nu_1 - \nu_4$	1260	0.1	1273 or 1277
$\nu_2 + \nu_4$	1900	0.1	1888
ν_3	2183	20	(2183)
ν_1	2187	Raman, strong	(2187)
$\nu_1 + \nu_4$ or $\nu_3 + \nu_4$	3095	1.0	3093, 3097
$\nu_2 + \nu_3$	3153	1.0	3161
$2\nu_3$	4360	0.1	4366
?	1680	—	—

The complete assignment (compare reference 4) chosen for the vibrational spectrum of SiH_4 is shown in Table II.

The assignments here given to 3153 cm^{-1} and 1901 cm^{-1} differ from Steward and Nielsen's, but are justified by the appearance, with appreciable intensity, of the analogous bands in the methane spectrum.[7]

Fred B. Stitt
Don M. Yost

Gates Chemical Laboratory,
Pasadena, California,
December 5, 1935.

[1] Stock and Somieski, Ber. **49**, 111 (1916).
[2] Johnson and Isenberg, J. Am. Chem. Soc. **57**, 1349 (1935).
[3] E. Bright Wilson, Jr., J. Chem. Phys. **2**, 432 (1934); G. Placzek, *Rayleigh Streuung und Raman Effekt* (Leipzig, 1934).
[4] Steward and Nielsen, Phys. Rev. **47**, 828 (1935).
[5] See for example data in Kohlrausch, *Der Smekal-Raman-Effekt* (Berlin, 1931); also Placzek, reference 3.
[6] Rosenthal, Phys. Rev. **46**, 730 (1934).
[7] Vedder and Necke, Zeits. f. Physik **86**, 137 (1933).

Raman Spectrum of Benzene-d_6

In the Raman spectrum of benzene-d_6 as reported by Wood[1] appear two shifts, 3052 and 3108 cm^{-1}, of surprisingly high value. For a molecule containing no atoms lighter than deuterium, these frequencies imply force constants much larger than those customarily ascribed to the various bonds in benzene. Theoretical[2] and mechanical[3] investigations of the modes of vibration in benzene are in good agreement with each other and with experimentally determined frequencies, but the introduction of force constants needed to obtain frequencies of 3052 and 3108 in benzene-d_6 damages the agreement irreparably. This appears to be the stumbling block which has delayed the progress of theoretical investigations of the mechanics of the benzene molecule, and consequently some alternative source of these lines was sought.

In their note on the mode of preparation of the benzene-d_6 used by Wood, Bowman, Benedict and Taylor[4] state that the purity of the compound with respect to ordinary

TABLE I.

C_6H_6	C_6D_6	C_6H_6	C_6D_6
605	581	2947	2266
849	662	3042	2293
991	945	3062	
1178	873	3157	
1584 / 1606	1548	3176	

C_6D_6 or C_6D_5H: 1000, 2031, 2575, 2617(?), 2663(?).
C_6D_5H: 3052, 3108

hydrogen was determined by the ultraviolet absorption bands of the material, and they set the upper limit to the hydrogen present at one mole percent. If we assume that a negligible portion of this hydrogen is present in molecules containing two or more H atoms, then the amount of C_6D_5H in the C_6D_6 has an upper limit of roughly six mole percent. The high vibration frequencies in benzene and its derivatives are responsible for some of the strongest Raman lines, and accordingly if C_6D_5H were present in the C_6D_6, even to so slight an extent as one mole percent, there should unquestionably appear in the Raman spectrum of this solution traces of lines characteristic of the aromatic C—H linkage. It is therefore suggested that the faint lines 3052 and 3108 found by Wood are due to C_6D_5H and not to C_6D_6. In $C_6D_2H_4$ and C_6DH_5 the 3052 frequency has been found by Redlich and Stricks[5] and this appears almost certainly to be the strong 3062 line of C_6H_6 shifted to the slightly lower value by the lower symmetry and heavier mass of the deuterobenzenes.

One further question must be answered. The presence of the 3052 and 3108 lines in the C_6D_6 spectrum obtained by Wood led him to search for corresponding high lines in C_6H_6. He set a tentative and rough lower limit for the expected lines at 3500 cm^{-1}, although a closer figure would have been 4000 cm^{-1} or higher (i.e., approximately $3100\sqrt{2}$). In the paper on C_6D_6, Wood reported that by long exposure with a green sensitive plate, he was able to obtain a spectrum of C_6H_6 which showed shifts of 3573 and 3627 cm^{-1} from the exciting line, Hg-4358. Since these shifts did not seem very reasonable either on the basis of the customary force constants of C_6H_6 or on the basis of new force constants required to give shifts of 3052 and 3108 in C_6D_6, I obtained Professor Wood's consent to reanalyze his plate. The plate showed the lines in question quite definitely, but because of their very low intensity they were impossible to measure with the usual degree of accuracy. The wave numbers of the lines were found to be 19,341 and 19,296 cm^{-1}. Instead of assigning the lines to excitation by Hg-4358, however, I found that an alternative assignment could be made. If one assigns the line at 19,341 cm^{-1} to Hg-4916, there is observed shift of approximately 990 cm^{-1}, which is the frequency of the strongest line in C_6H_6. Hg-4916 appears on the plate with ample intensity to excite an intense Raman line. If one assigns the 19,296 cm^{-1} line to an anti-Stokes excitation by Hg-5461, again a shift of approximately 990 cm^{-1} is obtained. It is true that one would ordinarily scarcely expect to find an anti-Stokes line of so large a shift as 1000 cm^{-1}. However the 990 line is a very intense one, and Hg-5461 is of extreme intensity on the plate. As a corroboration of this assignment, the 990 anti-Stokes line excited by Hg-4358 was sought and found very definitely at 23,928 cm^{-1}. In consequence it is necessary to reject the 3573 and 3627 vibrations in benzene.

A table of frequencies for C_6H_6 and C_6D_6 revised in accordance with the above appears in Table I. At the foot of the table are included lines either assigned to C_6D_5H or of indefinite assignment. Further investigation of the Raman spectra of solutions containing higher percentages of C_6D_5H will be necessary to remove the ambiguity.

R. C. LORD, JR.

Department of Chemistry,
The Johns Hopkins University,
Baltimore, Maryland,
December 13, 1935.

[1] R. W. Wood, J. Chem. Phys. **3**, 444 (1935).
[2] E. B. Wilson, Jr., Phys. Rev. **45**, 706 (1934); Phys. Rev. **46**, 146 (1934).
[3] D. E. Teets and D. H. Andrews, J. Chem. Phys. **3**, 175 (1935).
[4] Bowman, Benedict and Taylor, J. Am. Chem. Soc. **57**, 960 (1935).
[5] Redlich and Stricks, J. Chem. Phys. **3**, 834 (1935); see also Kohlrausch, *Der Smekal-Raman Effekt*, p. 329 ff.

Raman Spectrum of Oxalic Acid

Recently we published preliminary results on an investigation of the Raman spectra of light and heavy acetic acids.[1] In an extension of this investigation we have examined the Raman spectra of oxalic acid, both in the hydrated crystalline state and as a saturated aqueous solution. The results which we have obtained are sufficiently different from those given by Hibben[2] in a recent paper in this journal as to prompt us to publish our values immediately.

In Table I our values are compared with those previously recorded.

The lack of agreement between the independent values of the different investigators arises doubtless from the difficulty of obtaining clear and distinct Raman spectra on account of a continuous background. This is a difficulty which we have experienced in agreement with the observations of previous workers. Thus an unusually large divergence in the values of a particular frequency is to be expected.

We have included in the table Rao's data for the solid as data on the hydrated crystals since he does not state specifically in his paper that they were anhydrous; and we have therefore inferred that they were the usual dihydrate crystals. On the other hand Hibben has cited Rao's values for the solid as data for anhydrous oxalic acid and finds that Rao's values are in good agreement with his own for the anhydrous acid.

The main point of dissimilarity between Hibben's results

TABLE I.

	Krishnamurti[4]	Rao[3]	Hibben[2]	Authors
$H_2C_2O_4 \cdot 2H_2O$ (Solid)		473		495
	855	851	847	854
			1365	
		1506	1470	1471
		1640±20		1661(Broad)
		1758		1759
Aqueous Solution		248(?)		
			395	
		480	453	493
		673(?)		
		845	842	
				1375
		1430±30	1460	
		1656	1645	1647
				1684
		1744	1740	1749

and ours is the fact that from microphotometer records we obtain definite proof that the frequencies 1661 and 1759 cm^{-1} in the spectrum of the crystals have real existence and are as strong as the corresponding frequencies in the aqueous solution. Hibben found that these frequencies were absent in the dihydrate crystals but present in the anhydrous solid. Our results, obtained from crystals which were definitely dihydrate crystals, agree with those of Rao and support our inference regarding the crystals examined by him.

Since Hibben's conclusions that the two carboxyl groups behave differently depend to a large extent on the difference in the spectra of the anhydrous and hydrated crystals we submit that such conclusions may be invalidated by his comparing the spectrum he obtained for his anhydrous crystals with Rao's spectrum for the solid.

To enter into a full discussion of the results is beyond the scope of this letter in which we merely wish to indicate our observations that the Raman spectra obtained from saturated aqueous solutions of oxalic acid and from dihydrated oxalic acid crystals are substantially the same.

W. Rogie Angus
Alan H. Leckie

University College,
London, W.C. 1,
December 5, 1935.

[1] Angus, Leckie and Wilson, Nature **135**, 913 (1935).
[2] Hibben, J. Chem. Phys. **3**, 675 (1935).
[3] Rao, Zeits. f. Physik **94**, 536 (1935).
[4] Krishnamurti, Ind. J. Phys. **6**, 309 (1931).

Infrared Evidence for the Existence of an Isomeric Form of HCN

Hydrogen cyanide has been shown by the experiments of Badger and Binder[1] and of Choi and Barker[2] to be a rectilinear molecule with a simple structure of the vibration-rotation lines. In their work on hydrocyanic gas these investigators found an absorption band with a maximum at 4.76μ.

In recent studies of the effects of isomerism on infrared absorption spectra the writer finds that all organic cyanides have an intense absorption band near 4.5μ, while the isomeric forms of these compounds in which the carbon is divalent give rise to more intense bands at slightly longer wave-lengths. The shift in band position due to isomerism is found to be approximately 0.2μ in every case studied.

The work of Nef[3] and his co-workers seems to indicate the existence of a small amount of the isomer HNC in all hydrocyanic gas. A study of the absorption of a saturated solution of hydrocyanic gas in the region between 4.5μ and 5μ reveals a strong band at 4.76μ and a much weaker band at 4.95μ. The absorption at 4.95μ is attributed to the presence of a small amount of the isomer HNC in the solution. From a comparison of intensities it would seem that the isomer HNC makes up about two percent of the gas in aqueous solution.

Dudley Williams

University of North Carolina,
Chapel Hill,
December 5, 1935.

[1] R. M. Badger and J. L. Binder, Phys. Rev. **37**, 800 (1931).
[2] K. N. Choi and E. F. Barker, Phys. Rev. **42**, 777 (1932).
[3] J. V. Nef, J. Am. Chem. Soc. **26**. 1549 (1904).

An X-Ray Study of Symmetrical Trinitrotoluene and Cyclo Trimethylenetrinitramine

An x-ray study of the above crystals was undertaken with the hope of finding the crystal structure of these powerful explosives and thus contribute toward an understanding of why they decompose violently to shocks of a definite frequency while being unaffected by much stronger shocks of a different frequency. Although the crystal structures proved to be too complicated to be readily found, the symmetries of the crystals and their unit cells were determined.

Professor Tenney L. Davis of the Massachusetts Institute of Technology kindly furnished the crystals.

The trinitrotoluene crystals had been obtained by precipitation in benzene. They were amber in color and flattened along the b axis with (210), (110), (011) and (010) prominent.

There are two reports* as to the crystallographic symmetry of symmetrical trinitrotoluene. Friedländer reports it to be orthorhombic with $a:b:c=0.7586:1:0.5970$. Artini later reported that he had detected a slight inclination of the c axis and that the crystals were therefore monoclinic.

Our Laue photographs clearly show two planes of symmetry parallel to the b axis. Since the intensity of Laue spots is very sensitive to the symmetry, it may be regarded as established that TNT is really orthorhombic. Complete rotation photographs give $a=14.85$A, $b=39.5$A, and $c=5.96$A in agreement with the crystallographic ratios. If there are 16 molecules in the unit cell, the calculated density is 1.710, compared with 1.654 given in the literature.

Reflections $hk0$ are missing for either h or k odd and $0kl$ for k odd. However, the latter is a special case of the non-space group vanishing hkl for h even and k odd, which occurs. This can be accounted for by special positions of the molecules, but the intensity calculations are very complicated and were not carried further.

The cyclo trimethylenetrinitramine crystals were transparent with beautifully developed faces and a brilliant luster. Mr. Harry Berman, mineralogist at Harvard, kindly examined them crystallographically for us. He reported them to be orthorhombic with $a:b:c=0.878:1:0.819$.

X-ray photographs confirm this. We obtain $a=11.5$A, $b=13.2$A, and $c=10.6$A. With eight molecules in the unit cell, the calculated density is 1.82. Reflections $0kl$ with l odd, $h0l$ with h odd and $hk0$ with k odd are missing. All space groups are eliminated except V_h', V_h^5, V_h^{11}, and V_h^{15} with the last most probable since it accounts for all the extinctions.

I am indebted to the Massachusetts Institute of Technology which furnished the facilities for this research and to the National Research Council for the National Research Fellowship under which this work was done.

Ralph Hultgren

Graduate School of Engineering,
Harvard University,
November 21, 1935.

* Groth, Chem. Krist. **4**, 364,766.